Copy 220
RM A55L09

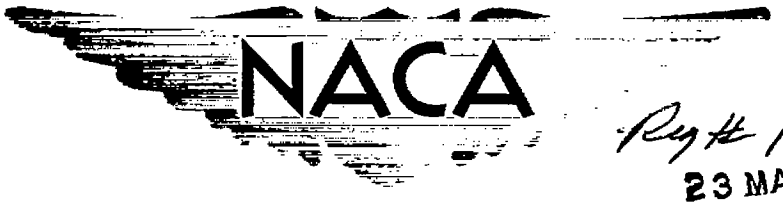

RESEARCH MEMORANDUM

INVESTIGATION OF THE POSSIBILITY OF SIMPLIFYING MISSILE GUIDANCE SYSTEMS BY THE USE OF FREE-FLOATING FLAPS AND SPRING-MOUNTED CONTROL SURFACES

By Katsumi Hikido, Paul H. Hayashi,
and Henry C. Lessing

Ames Aeronautical Laboratory
Moffett Field, Calif.

NATIONAL ADVISORY COMMITTEE
FOR AERONAUTICS

WASHINGTON
May 17, 1956

Classification canc[illegible] Unclassified

By Auth. NASA Tech Pub Announcement #4

By [illegible] 16 Mar 59

NK

GRADE OF OFFICER MAKING CHANGE)

14 May 61

DATE

NATIONAL ADVISORY COMMITTEE FOR AERONAUTICS

RESEARCH MEMORANDUM

INVESTIGATION OF THE POSSIBILITY OF SIMPLIFYING MISSILE GUIDANCE SYSTEMS BY THE USE OF FREE-FLOATING FLAPS AND SPRING-MOUNTED CONTROL SURFACES

By Katsumi Hikido, Paul H. Hayashi,
and Henry C. Lessing

SUMMARY

The use of aerodynamic and mechanical devices for improving the response of guided missiles is investigated. An analysis is made which shows that by the use of free-floating flaps and spring-mounted control surfaces it should be possible to improve the airframe longitudinal damping and to decrease the variation of the steady-state maneuverability with flight condition to an extent such that electronic automatic stabilization and gain-adjusting devices can be eliminated. An application of the analysis is presented in which the design of a free-floating flap damper is considered, and results of a wind-tunnel test are presented which show that a flap with the desired linear characteristics can be obtained.

INTRODUCTION

In the design of a guided missile, the fundamental problem consists of integrating the aerodynamic characteristics and guidance system in a manner such that the missile can be controlled accurately throughout its flight. For certain types of missiles, such as the boost-glide type, the flight conditions may vary over a fairly wide range, and it is necessary to design the missile so that adequate maneuverability is retained over the entire range. It is known that Mach number and altitude changes have a marked effect on missile performance and that some means must be provided to compensate for these changes if the performance is to be adequate for all flight conditions. In particular, the aerodynamic damping of missile airframes, especially at high altitudes, is so low that some means of automatic stabilization is necessary, and the wide variation with

dynamic pressure of the maximum available turning rate requires the use of a gain-adjusting mechanism. Until recently, electronic devices have been used to cope with these problems, but the growing complexity of guidance systems has made it desirable that the possibilities of a different approach be investigated.

Currently increased effort is being directed toward the investigation of mechanical and aerodynamic devices for improving the characteristics of missile airframes, and it is the purpose of this report to consider a few devices which appear to show some promise in this regard. In the past some investigations on the effect of free controls on the stability of airplanes have been made (see, e.g., refs. 1, 2, and 3) in which it is shown that the damping of the airplane can be altered appreciably by changes in the aerodynamic and mass characteristics of the free control. In the analysis presented herein consideration is given to methods of choosing combinations of these characteristics which will result in increased airframe damping and, in addition, to means of reducing the effect of Mach number and dynamic pressure changes on the steady-state maneuverability.

This report is concerned with a theoretical study based on linear aerodynamic parameters of methods for reducing the variation in the maximum available turning rate and a study of stability diagrams to determine the flap characteristics necessary to improve the missile damping over the specified range of flight conditions. In addition, the design of a flap with the desired linear characteristics is considered and wind-tunnel data are presented to demonstrate the feasibility of obtaining these characteristics.

SYMBOLS

a_o local speed of sound, ft/sec

A_o, A_1, A_2, A_3 coefficients of the characteristic equation

b wing span, ft

$\bar{c}$ mean aerodynamic chord of wing, M.A.C., ft

$\bar{c}_f$ mean aerodynamic chord of free-floating flap, ft

c.g. center of gravity

C_h hinge-moment coefficient of one flap or control surface (based on M.A.C. and area of wing unless otherwise noted), $\frac{\text{hinge moment}}{qS\bar{c}}$

C_D drag coefficient, $\frac{\text{drag force}}{qS}$

C_l rolling-moment coefficient, $\frac{\text{rolling moment}}{qSb}$

C_L lift coefficient, $\frac{\text{lifting force}}{qS}$

C_m pitching-moment coefficient, $\frac{\text{pitching moment}}{qS\bar{c}}$

C_{L_α} $\frac{\partial C_L}{\partial \alpha}$

C_{L_δ} $\frac{\partial C_L}{\partial \delta}$

C_{L_Δ} $\frac{\partial C_L}{\partial \Delta}$

$C_{L_{\dot{\alpha}}}$ $\frac{\partial C_L}{\partial (\dot{\alpha}\bar{c}/2V)}$

C_{L_q} $\frac{\partial C_L}{\partial (\dot{\theta}\bar{c}/2V)}$

C_{m_α} $\frac{\partial C_m}{\partial \alpha}$

$C_{m_{\dot{\alpha}}}$ $\frac{\partial C_m}{\partial (\dot{\alpha}\bar{c}/2V)}$

C_{m_δ} $\frac{\partial C_m}{\partial \delta}$

C_{m_Δ} $\frac{\partial C_m}{\partial \Delta}$

C_{m_q} $\frac{\partial C_m}{\partial (\dot{\theta}\bar{c}/2V)}$

C_{h_α} $\frac{\partial C_h}{\partial \alpha}$

$C_{h_{\alpha_c}}$ $\left(\frac{\partial C_h}{\partial \alpha}\right)_c$

C_{h_δ} $\frac{\partial C_h}{\partial \delta}$

$C_{h_{\dot{\delta}}}$ $\frac{\partial C_h}{\partial (\dot{\delta}\bar{c}/2V)}$

C_{h_Δ} $\frac{\partial C_h}{\partial \Delta}$

$C_{h_{\dot{\Delta}}}$ $\frac{\partial C_h}{\partial (\dot{\Delta}\bar{c}/2V)}$

$D,(\dot{})$ differentiation with respect to time, $\frac{d}{dt}$

$F(D)$ symbol for the characteristic equation

g acceleration due to gravity, ft/sec^2

h altitude, ft

H hinge moment, ft-lb

H_Δ $\frac{\partial H}{\partial \Delta}$

H_α $\frac{\partial H}{\partial \alpha}$

$H_{\dot{\Delta}}$ $\frac{\partial H}{\partial \dot{\Delta}}$

H_a value of flap mass-unbalance hinge moment for which the damping and frequency of the missile with flaps floating freely are equal to those of the missile with flaps fixed, ft-lb

H_D value of flap mass-unbalance hinge moment for the divergence boundary, ft-lb

H_e value of flap mass-unbalance hinge moment for which the gain of the missile with flaps floating freely is equal to that of the missile with flaps fixed, ft-lb

[redacted]

i	$\sqrt{-1}$
I_c	moment of inertia of canard control surface about its hinge line, slug-ft^2
I_f	moment of inertia of free-floating flap about its hinge line, slug-ft^2
I_y	longitudinal moment of inertia of missile about its center of gravity, slug-ft^2
K_T	spring constant for the torque spring on which the canard control surface is mounted, ft-lb/radian
l_c	distance from hinge line of canard control surface to missile center of gravity, ft
l_f	distance from hinge line of free-floating flap to missile center of gravity, ft
m	mass of missile, slugs
m_c	mass of one canard control surface, slugs
m_f	mass of one free-floating flap, slugs
M	free-stream Mach number
p	roll rate, radians/sec, or root of characteristic equation
q	free-stream dynamic pressure, lb/ft^2
r	damping factor
R	Reynolds number, based on M.A.C. of wing, or Routh's discriminant (see eq. (15))
S	total area of two coplanar wing panels, including the portion enclosed by the body, sq ft
S_f	area of one free-floating flap, sq ft
s_c	distance from center of gravity of canard control surface to its hinge line, positive for center of gravity behind the hinge line, ft
s_f	distance from center of gravity of free-floating flap to its hinge line, positive for center of gravity behind the hinge line, ft

[redacted]

$T_{1/2}$ time required for the envelope of an oscillation to damp to one-half of its amplitude, $-\frac{\ln 2}{r}$

V velocity, ft/sec

w_f weight of one free-floating flap, lb

$\bar{x}$ distance from center of pressure to missile center of gravity, positive for center of gravity forward of center of pressure, ft

α angle of attack, radians unless otherwise indicated (see fig. 1)

γ flight path angle, radians unless otherwise indicated (see fig. 1)

δ deflection angle of canard control surface, radians unless otherwise indicated

Δ deflection angle of free-floating flap, radians unless otherwise indicated

Δ_{nom} nominal value of deflection of flap, uncorrected for aerodynamic load, deg

ϵ deflection angle of control surface actuator, radians unless otherwise indicated

ζ damping ratio (see eq. (26))

θ angle of pitch, radians unless otherwise indicated (see fig. 1)

ξ_c mass-unbalance term for one canard control surface, $\frac{m_c s_c}{qS\bar{c}}$, sec^2/ft

ξ_f mass-unbalance term for one free-floating flap, $\frac{m_f s_f}{qS\bar{c}}$, sec^2/ft

ρ density of air, slugs/cu ft

σ_c $\frac{I_c}{qS\bar{c}}$, sec^2

σ_A $\frac{I_y}{qS\bar{c}}$, sec^2

σ_f $\frac{I_f}{qS\bar{c}}$, sec^2

2τ mass factor, $\frac{2m}{\rho VS}$, sec

μ ω^2, $1/sec^2$

ω frequency of oscillation, radians/sec

$\left(\frac{\Delta}{\epsilon}\right)_{ss}$ flap gain, steady-state deflection of free-floating flap per unit canard-control-actuator deflection

$\left(\frac{\dot{\gamma}}{\epsilon}\right)_{ss}$ turning-rate gain, steady-state turning rate of missile per unit canard-control-actuator deflection

$\left(\frac{\dot{\gamma}}{\delta}\right)_{ss}$ turning-rate gain, steady-state turning rate of missile per unit canard-control-surface deflection

Subscripts

c canard control surface

f free-floating flap

nom nominal value of flap deflection uncorrected for aerodynamic loads

ss steady-state condition

ANALYSIS

In the analysis which follows, the problems of reducing the variation with flight condition of the maximum turning rate and of increasing the damping of airframes will be considered. Throughout the analysis it has been assumed that the aerodynamic force and moment coefficients depend linearly on their respective variables and that the missile airframe is perfectly rigid. It is realized that linear aerodynamic coefficients are difficult to achieve; however, the insight and physical interpretation possible through the use of a "linear" analysis make it a valuable tool for the study of relatively complex systems. Consideration is given in a later section to means for obtaining linear hinge-moment coefficients.

The geometric characteristics of the missile to be analyzed are shown in figure 1. This configuration was chosen for purposes of illustration as representing a typical air-to-air missile, and estimated values of its mass and aerodynamic characteristics are given in tables I and II. The angles which define the inclination of the missile and deflections of surfaces with respect to their reference planes are positive as shown.

To avoid confusion, the term "flap" will always be used to refer to the free-floating surfaces attached to the wings, and the term "control surface" will refer to the canard control surfaces.

The Variation of Turning-Rate Gain With Altitude

Gain variation of the position-servo missile.- In this section and throughout the discussion which follows, the term "gain" is used in the conventional manner to refer to the steady-state value of the ratio of an output quantity to the input quantity causing the change in output. With a position-servo control, the details of which are shown sketched in figure 2(a), the missile responds to an error signal by specifying a control-surface deflection which is proportional to the signal.

The equation for lift for this case may be written in operator notation as

$$\left(2\tau D + C_{L_{\dot{\alpha}}} \frac{\bar{c}}{2V} D + C_{L_\alpha}\right)\gamma - \left[\left(C_{L_q} + C_{L_{\dot{\alpha}}}\right) \frac{\bar{c}}{2V} D + C_{L_\alpha}\right] \theta = C_{L_\delta}\delta \qquad (1)$$

The terms $C_{L_{\dot{\alpha}}}$ and C_{L_q} are small compared to the other terms and may be disregarded without introducing any significant errors. Equation (1) then becomes

$$\left(2\tau D + C_{L_\alpha}\right)\gamma - C_{L_\alpha}\theta = C_{L_\delta}\delta \qquad (2)$$

Similarly, the equation for pitching moment may be written

$$\left(C_{m_{\dot{\alpha}}} \frac{\bar{c}}{2V} D + C_{m_\alpha}\right)\gamma + \left[\sigma_A D^2 - \left(C_{m_q} + C_{m_{\dot{\alpha}}}\right) \frac{\bar{c}}{2V} D - C_{m_\alpha}\right]\theta = C_{m_\delta}\delta \qquad (3)$$

The turning-rate gain is obtained by solving for $(\dot{\gamma}/\delta)$ from equations (2) and (3) and then setting $D = 0$ in the resulting equation. If this is done, the expression for the gain is derived as

$$\left(\frac{\dot{\gamma}}{\delta}\right)_{ss} = \frac{C_{L_\delta} C_{m_\alpha} - C_{L_\alpha} C_{m_\delta}}{2\tau C_{m_\alpha} + C_{L_\alpha} C_{m_q} \frac{\bar{c}}{2V}} \tag{4}$$

It is indicated in Appendix A that the second term in the denominator is generally small compared to the first and may be disregarded, leaving

$$\left(\frac{\dot{\gamma}}{\delta}\right)_{ss} = \frac{S}{ma_o}\left(\frac{q}{M}\right)\left(C_{L_\delta} - \frac{C_{m_\delta}}{C_{m_\alpha}} C_{L_\alpha}\right) \tag{5}$$

Note that the dynamic pressure q appears explicitly in this expression; hence the gain will vary by a factor of approximately 10 for an altitude range of sea level to 60,000 feet. This variation, shown for the present missile by the dashed line in figure 3, is undesirable from the standpoint of autopilot design, and some means of reducing it to acceptable limits is needed. Several devices will be considered in the following sections.

Influence on the gain of free-floating flaps.- It is known that free-floating flaps can change appreciably the damping of airframes, but first it will be necessary to determine their influence on the steady-state turning rate of the missile. The problem is one involving the three degrees of freedom γ, θ, and Δ, and, in accordance with the assumptions made previously, the equations of motion may be written as

$$\left(2\tau D + C_{L_\alpha}\right)\gamma - \left(C_{L_\alpha}\right)\theta - \left(C_{L_\Delta}\right)\Delta = C_{L_\delta}\delta \tag{6}$$

$$\left(C_{m_{\dot{\alpha}}} \frac{\bar{c}}{2V} D + C_{m_\alpha}\right)\gamma + \left[\sigma_A D^2 - \left(C_{m_q} + C_{m_{\dot{\alpha}}}\right)\frac{\bar{c}}{2V} D - C_{m_\alpha}\right]\theta - \left(C_{m_\Delta}\right)\Delta = C_{m_\delta}\delta \tag{7}$$

$$\left(\xi_f V D - C_{h_\alpha}\right)\gamma - \left[\left(\sigma_f + \xi_f l_f\right)D^2 - C_{h_{\dot{\alpha}}} \frac{l_f}{V} D - C_{h_\alpha}\right]\theta - \left(\sigma_f D^2 - C_{h_{\dot{\alpha}}} \frac{\bar{c}}{2V} D - C_{h_\Delta}\right)\Delta = 0 \tag{8}$$

where the hinge-moment coefficients of equation (8) are based on the mean aerodynamic chord and area of the wing. Equation (8) is the equation of motion for one flap only, but since symmetry of motion is assumed and

two flaps will deflect as a unit, the lift and pitching-moment coefficients due to flap deflection $\left(C_{L_\Delta} \text{ and } C_{m_\Delta}\right)$ are for two flaps deflected together. It has been assumed here that the lift and pitching moments due to rate of change of flap deflection and the hinge moment of the flap due to control deflection are negligible. From these equations the expression for the gain is

$$\left(\frac{\dot{\gamma}}{\delta}\right)_{ss} = \left[C_{L_\delta}\left(C_{m_\Delta}C_{h_\alpha} - C_{m_\alpha}C_{h_\Delta}\right) + C_{m_\delta}\left(C_{L_\alpha}C_{h_\Delta} - C_{L_\Delta}C_{h_\alpha}\right)\right]\left[2\tau\left(C_{m_\Delta}C_{h_\alpha} - C_{m_\alpha}C_{h_\Delta}\right) + \left(C_{m_\Delta}C_{L_\alpha} - C_{m_\alpha}C_{L_\Delta}\right)\left(V\xi_f + \frac{l_f}{V}C_{h_\alpha}\right) + C_{m_q}\frac{\bar{c}}{2V}\left(C_{h_\alpha}C_{L_\Delta} - C_{h_\Delta}C_{L_\alpha}\right)\right]^{-1} \quad (9)$$

which reduces to equation (4), as it should, when the flap effectiveness $\left(C_{L_\Delta},\ C_{m_\Delta}\right)$ is set equal to zero. As for the previous case, some of these terms are small and may be disregarded (see Appendix A), and the gain is given with good accuracy by

$$\left(\frac{\dot{\gamma}}{\delta}\right)_{ss} = \left(\frac{S}{ma_o}\right)\left(\frac{q}{M}\right)\left[\frac{C_{L_\delta}\left(C_{m_\Delta}C_{h_\alpha} - C_{m_\alpha}C_{h_\Delta}\right) + C_{m_\delta}\left(C_{L_\alpha}C_{h_\Delta} - C_{L_\Delta}C_{h_\alpha}\right)}{\frac{m_f s_f}{m\bar{c}}\left(C_{L_\alpha}C_{m_\Delta} - C_{L_\Delta}C_{m_\alpha}\right) + \left(C_{m_\Delta}C_{h_\alpha} - C_{m_\alpha}C_{h_\Delta}\right)}\right] \quad (10)$$

Note that the form of equation (10) is similar to that of equation (5); thus it would be expected that the free-floating flap would not reduce the variation in gain with altitude. The variation for the missile with free-floating flaps for typical values of the aerodynamic parameters (table II) is shown by the solid line in figure 3 and is again approximately a factor of 10.

Influence on the gain of spring-mounted control surfaces.- Since the variations in gain obtained for the above cases are unacceptable, some other approach must be used. One solution to the problem is to mount the control surface on a torque spring so that its deflection will be influenced by the aerodynamic moments imposed upon it. The displacement of the servo is still proportional to the error signal as before. This device is illustrated by the sketch in figure 2(b), which compares the spring control with the usual position control.

To determine the influence of the torque spring on the gain variation, the following equation of motion is assumed for the canard control surface:

$$\left(\xi_c VD - C_{h_{\alpha_c}}\right)\gamma + \left[\left(\xi_c l_c - \sigma_c\right)D^2 - C_{h_{\alpha_c}}\left(\frac{l_c}{V}D - 1\right)\right]\theta - \left(\sigma_c D^2 - C_{h_{\dot{\delta}}}\frac{\bar{c}}{2V}D - C_{h_\delta} + \frac{K_T}{qS\bar{c}}\right)\delta = -\frac{K_T}{qS\bar{c}}\epsilon \quad (11)$$

where K_T is the spring constant of the torque spring, and all aerodynamic derivatives, including hinge-moment coefficients, are based on the mean aerodynamic chord and area of the wing. It is desired to find only the effect of the spring on the missile gain; hence the system is defined by equations (2), (3), and (11). If, for simplicity, the mass-unbalance term $m_c s_c$ is set equal to zero, there results the following expression for the turning-rate gain:

$$\left(\frac{\dot{\gamma}}{\epsilon}\right)_{ss} = \frac{K_T\left(C_{L_\alpha}C_{m_\delta} - C_{L_\delta}C_{m_\alpha}\right)}{\left(C_{h_\delta}qS\bar{c} - K_T\right)\left(2\tau C_{m_\alpha} + C_{L_\alpha}C_{m_q}\frac{\bar{c}}{2V}\right) - C_{h_{\alpha_c}}qS\bar{c}\left[2\tau C_{m_\delta} + C_{L_\delta}C_{m_q}\frac{\bar{c}}{2V} + \frac{l_c}{V}\left(C_{L_\delta}C_{m_\alpha} - C_{L_\alpha}C_{m_\delta}\right)\right]} \quad (12)$$

This expression can be simplified as for the other cases (see Appendix A) giving

$$\left(\frac{\dot{\gamma}}{\epsilon}\right)_{ss} = \frac{K_T}{m\bar{c}a_0 M}\left[\frac{C_{L_\alpha}C_{m_\delta} - C_{L_\delta}C_{m_\alpha}}{C_{m_\alpha}\left(C_{h_\delta} - \frac{K_T}{qS\bar{c}}\right) - C_{m_\delta}C_{h_{\alpha_c}}}\right] \quad (13)$$

Note that the dynamic pressure q appears only as a factor in one of the terms of the denominator; hence its effect has been suppressed. Physically it can be seen why the gain becomes less sensitive to changes in q. As the dynamic pressure increases, the effective spring constant $(C_{h_\delta} - (K_T/qS\bar{c}))$ becomes smaller; hence the deflection of the control surface for a given servo

displacement ϵ also decreases. The increasing effectiveness of the control surface is thus compensated for by smaller deflections. Mach number still appears explicitly but, since all the coefficients are affected by Mach number changes, it is not possible to see the influence of Mach number from equation (13). It will be seen later, however, that Mach number effects have also been reduced. It is evident from equation (13) that if the spring constant goes to zero, the gain will also go to zero. For very large values of spring constant, the term $K_T/qS\bar{c}$ becomes the dominant term in the denominator, and the expression (13) for the gain approaches that given by equation (5) for the gain of the missile with a position control. Therefore, if the beneficial effect of the spring is to be realized, some intermediate value of K_T is needed. For reasons which will be discussed in a later section, a value of K_T = 10.35 foot-pounds per radian was chosen. It can be seen from figure 3 that the gain variation has been reduced considerably, varying by a factor of only 2 over the indicated altitude range.

It should be mentioned here that the gain variation with altitude can be reduced also by using a torque servo to actuate the control surfaces. The principle of the torque servo is similar to that of the torque spring; the servo responds to an input signal by specifying a hinge moment on the control surface, whereupon the control surface deflects until the specified torque is balanced by the external aerodynamic hinge moment acting on the surface. It can readily be seen that the control-surface deflections are influenced by the dynamic pressure and will decrease with increasing q, thus compensating for the change of flight condition in exactly the same manner as for the torque spring. Since the principle involved in the use of these two devices is similar, it was decided to analyze only the effects of the torque spring in the present investigation. As a matter of interest, however, the equations for a missile equipped with a torque servo are given in Appendix A, and the variation in turning-rate gain with altitude and Mach number are given in figure 4.

Augmentation of Airframe Damping

In the preceding sections, it was found that the spring-mounted canard control surfaces provide satisfactory compensation for the gain variation with altitude. In the following section, the feasibility of increasing the damping of airframes through the use of free-floating surfaces will be investigated. It is possible to use the canard surfaces to provide added damping as well as to compensate for the gain variation; however, in the present case the flaps on the main lifting surfaces, as shown in figure 1, were utilized to provide damping. A similar investigation was carried out by Curfman, Strass, and Crane in reference 4. The analysis to follow is based on a study of contours of constant damping

and frequency constructed by the method of reference 5. For convenience in the discussion, the term "basic missile" will henceforth be used to refer to the configuration consisting of the missile with the spring-mounted canard controls and with flaps fixed.

Method of analysis.- The characteristic equation derived from equations (6), (7), (8), and (11) is of sixth order; however, it will be shown later that simplifying assumptions can be made which reduce the equation to one of fourth order having the form

$$F(D) = D^4 + A_3D^3 + A_2D^2 + A_1D + A_0 = 0 \qquad (14)$$

where the coefficients are functions of the flap and missile parameters. The solution of equation (14) determines the stability of all the degrees of freedom of the system, and the motion of each degree of freedom has the form

$$C_1e^{p_1t} + C_2e^{p_2t} + C_3e^{p_3t} + C_4e^{p_4t}$$

where p_1, p_2, p_3, and p_4 are the roots of equation (14) and the coefficients C_1, C_2, C_3, and C_4 are determined from initial conditions. Note that the motion of each degree of freedom is composed of the sum of four modes, and the magnitude of each mode making up the sum is determined by the size of its coefficient. If any of the roots are complex, they must appear in conjugate pairs, and the corresponding modes combine to form one oscillatory mode. Thus each degree of freedom may be represented by the sum of two oscillatory, one oscillatory and two aperiodic, or four aperiodic modes of motion. The complex roots have the form

$$p = r \pm i\omega$$

and the motion will be stable only when all the numbers r have negative values. To insure this condition, it is necessary to satisfy the well-known conditions for stability, which state that all the coefficients of equation (14) and the Routh discriminant given by

$$R = A_1A_2A_3 - A_1^2 - A_0A_3^2 \qquad (15)$$

must have the same sign if the motion is to be stable. If all but two of the parameters comprising the coefficients of equation (14) are fixed, stability diagrams which show the combination of parameters giving stable motion can be constructed in the plane of the two parameters. The

oscillatory boundary, which represents points where an oscillatory mode of motion has zero damping, is obtained by setting equation (15) to zero, and the divergence boundary, where an aperiodic mode is neutrally stable, by setting the coefficient A_0 equal to zero. The stable region will be that portion of the diagram lying on the positive side of both boundaries. Furthermore, as shown in reference 5, additional contours of constant damping and frequency can be constructed by assuming a solution $D = r + i\omega$ and substituting into equation (14). This results in a complex equation which can be written as two real equations by equating the real and imaginary parts to zero. Carrying out this procedure for the present case results in the two parametric equations

$$4r^3 + 3A_3r^2 + (2A_2 - 4\mu)r + A_1 - \mu A_3 = 0 \tag{16}$$

$$r^4 + A_3r^3 + (A_2 - 6\mu)r^2 + (A_1 - 3\mu A_3)r + A_0 - \mu A_2 + \mu^2 = 0 \tag{17}$$

where $\mu = \omega^2$. If r is set equal to zero and μ is eliminated from equations (16) and (17), it can be seen that the result is exactly the Routh discriminant R. To obtain curves of constant damping, a value is chosen for the damping r, and equations (16) and (17) are solved in terms of the variable parameter μ for the quantities whose effects are being investigated. The frequency of oscillation at each point along the contours thus obtained is given by $\sqrt{\mu}/2\pi$, and if the same sequence of values of μ is used for each value of r, curves of constant frequency can be obtained simultaneously with the constant-damping curves.

Substitution of the complex root, $D = r + i\omega$, into equation (14) presupposes the presence of oscillatory modes of motion, and the procedures outlined above will yield points only for those regions where at least one oscillatory mode occurs.

Application of the analysis.- The equations of motion defining the system consisting of the missile with spring-mounted control surfaces and free-floating flaps are given by equations (6), (7), (8), and (11). As stated in the preceding section, the characteristic equation derived from these equations of motion is of sixth order. It is not necessary, however, to use this sixth-order equation since some simplifying assumptions can be made which reduce considerably the complexity of the problem.

If the natural frequency of the canard control surface is much greater than that of the missile, the missile mode of motion will be relatively undisturbed by the high-frequency oscillations of the control surface. Conversely, the control surface will follow almost exactly the motion of the missile, and the only deflection of the surface with

respect to the missile axis will be due to the static aerodynamic moments imposed upon it. The inertial and damping terms can thus be dropped from equation (11) which can then be written as

$$C_{h_{\alpha_c}}\gamma + \left(\frac{l_c}{V}D - 1\right)C_{h_{\alpha_c}}\theta + \left(\frac{K_T}{q\bar{S}\bar{c}} - C_{h_\delta}\right)\delta = \frac{K_T}{q\bar{S}\bar{c}}\epsilon \qquad (18)$$

The use of equation (18) in the place of equation (11) for the canard control surface reduces the characteristic equation to one of fourth order.

In order for the use of equation (18) to be valid, the spring constant K_T must be made large enough so that the natural frequency of the control surface will be large relative to that of the missile. It must not be made too large, however, since, as shown previously, the variation in gain with altitude approaches that of the position-servo missile for very large values. Since the gain can be made independent of altitude only for the trivial case of zero spring constant, some variation in gain with altitude must be expected. It was decided that a gain variation by a factor of 2 in the altitude range of 5,000 to 60,000 feet was acceptable; the resulting value of $K_T = 10.35$ foot-pounds per radian gave a control-surface natural frequency approximately 23 times that of the basic missile airframe.

As a check on the validity of the foregoing assumptions, the roots of the exact sixth-order equation and the simplified fourth-order version were obtained for the missile at a flight condition of 30,000 feet altitude and a Mach number of 1.5. The roots of the sixth-order characteristic equation are

$$D_1 = -29.96$$

$$D_2 = -2156.23$$

$$D_{3,4} = -2.00 \pm i17.02$$

$$D_{5,6} = -0.01 \pm i247.71$$

and the roots of the fourth-order equation are

$$D_1 = -29.96$$

$$D_2 = -2156.23$$

$$D_{3,4} = -2.00 \pm i17.02$$

[redacted]

The last pair of roots of the sixth-order equation corresponds to the canard surface mode of motion, and it can be seen that its oscillations are of high frequency with a low amount of damping. This small amount of damping is due to the fact that C_{h_δ} was assumed to be zero in equation (11), and the value shown above is due only to interaction with the missile motion. A comparison of the other roots, which correspond to the missile and floating-flap modes of motion shows that, to the accuracy with which they were obtained, they are identical; therefore, for the purposes of this report wherein the missile responses and the characteristics of the floating flap are of primary concern, the equations of motion (6), (7), (8), and the simplified equation (18) are adequate to represent the system.

The characteristic equation derived from these equations of motion can be written in the form of equation (14). The coefficients A_0, A_1, A_2, and A_3 are functions of the missile and flap parameters and are given in complete form in Appendix B. Stability diagrams can now be constructed for the system represented by equation (14) by taking two of the quantities as coordinates as was discussed in the preceding section. The two quantities to be chosen were determined by the following considerations.

Since it is desired to find the effects of the floating-flap characteristics on the missile response, the choice of parameters is limited to those involving the flap, namely, H_α, H_Δ, $H_{\dot{\Delta}}$, and the mass-unbalance hinge moment. The hinge moments H_α and H_Δ are functions of Mach number and dynamic pressure and, in general, will not remain constant as flight conditions change. On the other hand, preliminary computations showed that, in general, values of $H_{\dot{\Delta}}$ much larger than can be obtained aerodynamically were desirable, and some auxiliary mechanical or viscous damping device is needed. The aerodynamic flap damping is thus only a small part of the total damping, and $H_{\dot{\Delta}}$ is essentially independent of flight conditions. Similarly, the mass-unbalance hinge moment is a function only of the mass characteristics of the flap and is, therefore, independent of flight conditions also. This independence of flight condition, and the fact that they may be varied completely independently of each other, serves to make stability diagrams having $H_{\dot{\Delta}}$ and mass-unbalance hinge moment as coordinates more useful from the standpoint of design.

Discussion of the stability diagram.- A typical stability diagram is shown in figure 5 for the flight condition of 30,000-feet altitude and a Mach number of 1.5. The ordinates represent values of $H_{\dot{\Delta}}$, negative upward, and the abscissas represent values of flap mass-unbalance hinge moment. Positive values of mass-unbalance moment correspond to the cases where the center of gravity of the flap lies behind its hinge line. Only the first two quadrants are shown in the figure since one branch of the oscillatory stability boundary ($R = 0$) is essentially coincident with the horizontal axis. The divergence boundary ($A_0 = 0$) is independent of

[redacted]

damping about the flap hinge line and appears in the figure as a vertical line extending above and below the horizontal axis. The oscillatory stability boundary first appears in figure 5 at the upper right-hand corner of the figure. It may be seen that as the damping about the flap hinge line is decreased, the mass-unbalance hinge moment necessary to cause a neutrally damped oscillatory mode first decreases and then increases. As $H_{\dot{\Delta}}$ is decreased further, the mass-unbalance hinge moment on the boundary increases to a value of approximately 0.75 foot-pounds after which the boundary reverses suddenly and becomes essentially coincident with the horizontal axis as indicated in sketch (a). In order to indicate the variation of oscillation frequency of the neutrally damped mode on the boundary, the frequencies are noted in figure 5 in cycles per second at points designated by the small open circles.

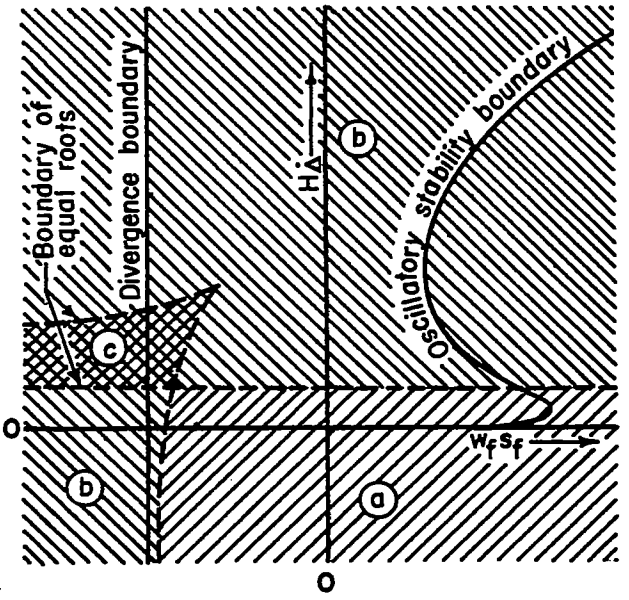

Sketch (a)

Each contour of constant damping originates on the boundary of equal roots, two branches of which are shown in figure 5. On this boundary the imaginary parts of two complex conjugate roots defining an oscillatory mode of motion become equal to zero; therefore, the oscillatory mode represented by the constant damping contour degenerates into two aperiodic modes, both of which damp to half amplitude in the indicated time. In figure 5 each of the constant damping curves originates on the upper branch of the boundary of equal roots and, as the damping is increased, the starting point of each curve moves out along the boundary. For very high values of damping, other constant damping curves not shown in the figure lie below and originate on the lower branch of the boundary.

The constant damping curve of greatest interest in figure 5 is that which has the same $T_{1/2}$ as the missile with the free-floating flaps fixed. The $T_{1/2}$ for this case was calculated to be 0.634 second. This curve is discontinuous at $f = 1.69$ cycles per second, which corresponds to the short period longitudinal mode of the basic airframe. Note that the curve is asymptotic to the vertical line designated H_a, which will be discussed in more detail later. As the frequency is increased beyond 1.69 cps, a new branch of this curve starts in the fourth quadrant and forms a small loop in the first quadrant lying between the boundary of equal roots and the lower branch of the oscillatory boundary. This branch of the curve has been omitted for purposes of clarity. The region of greatest interest is that area enclosed by the initial portion of the

constant damping curve designated by $T_{1/2}$ = 0.634 second and the divergence boundary. This region represents the values of flap damping and mass-unbalance hinge moment for which all modes of motion are stable and for which there are no oscillatory modes which have less damping than the basic missile.

In order to interpret properly the curves shown in figure 5, it is necessary to remember that each point in the figure represents the complementary solution of equation (14). It will be recalled that the four roots of this equation may be (a) all complex, corresponding to two oscillatory modes of motion, (b) two real and two complex, corresponding to two aperiodic modes and one oscillatory mode, or, (c) all real, corresponding to completely aperiodic motion. Since the boundary of equal roots represents the locus of points at which the frequency of oscillation goes to zero, these three types of motion correspond to the regions of figure 5 which are separated by the branches of this boundary. It was stated previously that curves of very high damping not shown in the figure lie below and originate on the lower branch of the boundary of equal roots. The constant damping curves which are shown originate on the upper branch. Then motion of the type (a) occurs in the semi-infinite region below and to the right of these two branches. The oscillatory modes represented by the constant damping curves which lie below and originate on the lower branch of the boundary of equal roots degenerate on this boundary to two aperiodic modes, and type (b) motion occurs in the semi-infinite region lying above the two branches of this boundary. Type (b) motion also occurs in the region which lies primarily in the unstable third quadrant lying to the left of and below the two branches. Type (c) motion occurs in the region lying to the left of the essentially vertical portion of the upper branch of the boundary of equal roots and between the two approximately horizontal portions of the two branches. These regions are indicated in sketch (a) by letters corresponding to the type of motion which occurs.

When either one or both modes of motion are of an oscillatory nature, an indication of the type of response to be expected may be obtained from examination of the frequencies which occur at the point under consideration. For instance, in the region of figure 5 where two oscillatory modes are present, every point in the region must be the intersection point of two constant damping curves in order to define completely the solution of equation (14). Generally, one of these modes may be associated with the airframe, and the other with the flap. The primary response of the airframe will have the damping and frequency of the constant-damping curve whose frequency most nearly corresponds to the airframe frequency at the point of intersection.

As an example of these remarks, consider point 1 in figure 5. Two oscillatory modes must occur, one of which should be almost neutrally damped since the point lies essentially on the neutral oscillatory boundary, and should have a frequency of between 36 and 39 cycles per second.

The undamped natural frequency of the control surface at this flight condition is 41.7 cycles per second, and it might therefore be expected that the high frequency undamped mode of point 1 would form the primary component of the flap motion. The point also lies close to the constant-damping curve which has the same $T_{1/2}$ as the airframe with flaps fixed, and the second oscillatory mode should, therefore, have a frequency of oscillation and time to damp to half amplitude of approximately 1.69 cycles per second and 0.634 second. This mode should form the primary component of the airframe motion. Time histories of the response due to a unit step control servo displacement for the basic missile and for the conditions of point 1 are presented in figure 6(a) and 6(b). The airframe motion with free-floating flaps has damping and frequency characteristics which are almost identical with those for the missile with flaps fixed as expected. The flap motion consists primarily of a small-amplitude, neutrally damped oscillation with a frequency of 38 cycles per second. The effect of the undamped oscillations of the flap on the airframe motion is negligible because of the relatively high frequency of the flap motion.

All the time histories presented in this report were obtained on the Reeves Electronic Analog Computer, and the points for which time histories were computed are designated by the filled circles in figure 5 and denoted by numbers from 1 through 7.

Points 2 and 3 of figure 5 lie in a region where type (b) motion occurs; that is, the motion should consist of one oscillatory and two aperiodic modes. Both points lie close to the constant-damping curve having the same $T_{1/2}$ as the missile with flaps fixed, and the airframe motion, which for point 1 was found to consist primarily of this mode, should be unchanged. The flap motion should now be well damped. These results are confirmed in figures 6(c) and 6(d).

The time histories of the missile response shown in figures 6(e), 6(f), and 6(g) correspond to points 4, 5, and 6 in figure 5. Points 4 and 5 lie in a region where the oscillatory mode has greater damping than that for the missile with flaps fixed, while point 6 lies on the oscillatory stability boundary. The aperiodic modes associated with these three points are well damped.

Figure 6(h) presents results for point 7 corresponding to $H_{\dot{\Delta}}$=-0.00275 foot-pound per radian per second and mass-unbalance hinge moment of 0.563 foot-pound. This point is outside the range of mass-unbalance hinge moments presented in figure 5, but lies in the region interior to the small loop mentioned previously which is formed by the constant-damping curve $T_{1/2}$ = 0.634. Each of the curves of constant damping greater than that for the missile with flaps fixed also forms loops in this region, and the conditions chosen for figure 6(h) correspond to the point where the $T_{1/2}$ = 0.346-second curve crosses itself. Both modes damp to half amplitude in this time, and the oscillation frequencies are 4.06 and 24.1 cycles per second.

Effect of flap damping and mass-unbalance hinge moment on missile gain and frequency.- It can be seen from the results just presented that the primary component of the airframe motion can be made to damp to half amplitude in a specified time through the use of two different combinations of flap damping and mass-unbalance hinge moment. The oscillatory modes of points 5 and 7 damp to half amplitude in 0.346 second. The airframe responses, however, for the two cases as shown in figures 6(f) and 6(h) have marked differences other than the presence of the second oscillatory mode for point 7. The frequency of the primary component of the airframe motion for point 7 is 2.4 times that of the basic missile, while that for point 5 is 0.66 times that of the basic missile. In addition, the steady-state turning rate per unit servo displacement for point 7 is approximately one-half that for the basic missile, while that for point 5 is almost twice that for the basic missile. Since a relatively high airframe frequency is generally desirable, it may appear that the combination of $H_\Delta^\cdot$ and mass-unbalance hinge moment corresponding to point 7 is preferable; however, it should be noted that this value of $H_\Delta^\cdot$ is of the order of that which may be obtained aerodynamically, and any small change in its value can cause drastic changes in the missile response. Because of this, the conditions corresponding to point 5 are more practical.

It is important to note this variation with mass-unbalance hinge moment and $H_\Delta^\cdot$ of the frequency and gain, since these quantities, as well as the damping, are essential factors governing the response of a missile. In figure 5, the curves of constant frequency are given by the broken lines which approach the boundary of equal roots as the frequency goes to zero. It can be seen that the region where the maximum damping can be obtained lies in the neighborhood of the cusp in the boundary of equal roots; however, in practice it is desirable to keep the frequency as high as possible, and it is evident that the frequency is very low in this region. If the small loop region mentioned above is excluded, the maximum frequency that can be obtained is that of the basic missile; hence, if the damping is to be increased by the use of the flaps, the frequency will always be somewhat less. However, though some decrease is unavoidable, the reduction in frequency can be kept to a minimum by considering the contours of constant frequency as well as those of constant damping in selecting the value of $H_\Delta^\cdot$ and unbalance hinge moment.

From equations of motion (6), (7), (8), and (18), the expression for the turning-rate gain for the missile-flap combination is given by

$$\left(\frac{\dot{\gamma}}{\epsilon}\right)_{ss} = \left\{K_T\left[Ch_\alpha\left(Cm_\delta CL_\Delta - Cm_\Delta CL_\delta\right) - Ch_\Delta\left(Cm_\delta CL_\alpha - Cm_\alpha CL_\delta\right)\right]\right\}\left\{\left(K_T - Ch_\delta qS\bar{c}\right)\right.$$
$$\left[Cm_q\frac{\bar{c}}{2V}\left(CL_\alpha Ch_\Delta - CL_\Delta Ch_\alpha\right) - \left(\xi_f V + \frac{l_f}{V}Ch_\alpha\right)\left(CL_\alpha Cm_\Delta - CL_\Delta Cm_\alpha\right) + \right.$$
$$\left.2\tau\left(Cm_\alpha Ch_\Delta - Cm_\Delta Ch_\alpha\right)\right] + Ch_{\alpha_c} qS\bar{c}\left(\xi_f V + Ch_\alpha\frac{l_f + l_c}{V}\right)\left(Cm_\delta CL_\Delta - CL_\delta Cm_\Delta\right) +$$
$$\left.Ch_\Delta Ch_{\alpha_c} qS\bar{c}\left[2\tau Cm_\delta + CL_\delta Cm_q\frac{\bar{c}}{2V} - \frac{l_c}{V}\left(Cm_\delta CL_\alpha - CL_\delta Cm_\alpha\right)\right]\right\}^{-1} \qquad (19)$$

This expression may be simplified by disregarding the small terms and may be written as

$$\left(\frac{\dot{\gamma}}{\epsilon}\right)_{ss} = \left(\frac{K_T}{m\bar{c}a_oM}\right)\left[C_{h_\alpha}\left(C_{m_\delta}C_{L_\Delta} - C_{m_\Delta}C_{L_\delta}\right) - C_{h_\Delta}\left(C_{m_\delta}C_{L_\alpha} - C_{m_\alpha}C_{L_\delta}\right)\right]\left\{\left(\frac{K_T}{qS\bar{c}} - C_{h_\delta}\right)\right.$$

$$\left[C_{h_\Delta}C_{m_\alpha} - C_{h_\alpha}C_{m_\Delta} - \frac{m_f s_f}{m\bar{c}}\left(C_{L_\alpha}C_{m_\Delta} - C_{L_\Delta}C_{m_\alpha}\right)\right] +$$

$$\left.C_{h_{\alpha_c}}\left[\frac{m_f s_f}{m\bar{c}}\left(C_{m_\delta}C_{L_\Delta} - C_{m_\Delta}C_{L_\delta}\right) + C_{m_\delta}C_{h_\Delta}\right]\right\}^{-1} \qquad (20)$$

The variation in turning-rate gain as a function of mass-unbalance hinge moment for the flight condition corresponding to figure 5 is given by the upper curve in figure 7. It can be seen that for very large positive values of mass-unbalance hinge moment, the gain tends toward zero, and that for values of mass-unbalance hinge moment approaching the divergence boundary, the gain tends to infinity. Thus there is a value of mass-unbalance hinge moment to the right of the divergence boundary for which the gain of the missile-flap combination is equal to that of the basic missile. This value of mass-unbalance hinge moment is shown by the line labeled "H_e" in figure 5. The exact expression for this boundary is derived in Appendix C, but for most purposes, it is sufficiently accurate to use the approximate expression

$$H_e = gm\bar{c}\left(\frac{C_{m_\delta}C_{h_\alpha}}{C_{L_\delta}C_{m_\alpha} - C_{L_\alpha}C_{m_\delta}}\right) \qquad (21)$$

It can be seen from figure 7 that for all values of mass-unbalance hinge moment between the divergence boundary and that given by H_e, the turning-rate gain for the missile-flap combination is always greater than that of the basic missile. This consideration of the gain variation with mass-unbalance hinge moment, as well as that of damping and frequency, is an important one in the design of the flap.

The lower curve in figure 7 gives the steady-state value of the flap deflection per unit servo deflection angle as a function of the unbalance hinge moment. The flight condition again corresponds to that of figure 5. From equations (6), (7), (8), and (18) the expression for the flap gain is

$$\left(\frac{\Delta}{\epsilon}\right)_{ss} = \frac{K_T\left\{\xi_f V\left(C_{L_\alpha}C_{m_\delta} - C_{L_\delta}C_{m_\alpha}\right) + C_{h_\alpha}\left[C_{m_\delta}\left(2\tau + \frac{l_f}{V}C_{L_\alpha}\right) + C_{L_\delta}\left(C_{m_q}\frac{\bar{c}}{2V} - \frac{l_f}{V}C_{m_\alpha}\right)\right]\right\}}{\text{(denominator of equation (19))}} \qquad (22)$$

[redacted]

which may be simplified to

$$\left(\frac{\Delta}{\epsilon}\right)_{ss} = \frac{K_T\left[C_{m_\delta}C_{h_\alpha} + \frac{m_f s_f}{m\bar{c}}\left(C_{L_\alpha}C_{m_\delta} - C_{L_\delta}C_{m_\alpha}\right)\right]}{(\text{denominator of equation (20)})} \tag{23}$$

Note in figure 7 that near the divergence boundary where the damping is the highest, as mentioned above, the flap gain tends to become very large. For the present analysis wherein it is assumed that the aerodynamic coefficients are linear functions of their variables, it is necessary to keep the deflections small in order to stay within the limitations of the theory, and care must be taken to avoid values of unbalance hinge moment near the divergence boundary.

Expressions for H_a and the divergence boundary.- It will be shown in this section that approximate expressions for H_a and H_D can be derived which will greatly simplify computations. The divergence boundary is independent of H_Δ, and the value of mass-unbalance hinge moment representing this boundary is obtained by setting the constant term of the characteristic equation (14) equal to zero. On the other hand, the constant-damping contour representing the damping of the basic missile is a function of H_Δ and is not as simple to obtain. It can be seen from figure 5, however, that the initial portion of the curve is almost horizontal and rapidly approaches the value of unbalance hinge moment given by H_a, becoming asymptotic to it as the frequency approaches that of the basic missile. The region where the flap adds damping is thus a roughly rectangular area. The transient solutions shown in figures 6(b), 6(c), and 6(d) for points 1, 2, and 3, respectively, on the line designated by H_a in figure 5 show that the damping and frequency of the primary mode of motion corresponding to the missile mode is very nearly that of the basic missile. Therefore the region of interest where the flaps add damping can be considered with little loss in accuracy to be bounded by the divergence boundary, the horizontal portion of the contour which has the same $T_{1/2}$ as the missile with flaps fixed, and the vertical line designated by H_a. This latter line will henceforth be referred to as the H_a boundary.

The derivation of the exact expressions for the divergence and H_a boundaries and the steps taken to simplify them are given in Appendix C. It is shown that the divergence boundary is given with good accuracy by

$$H_D = gm\bar{c}\left[\frac{\left(K_T - C_{h_\delta}qS\bar{c}\right)\left(C_{m_\alpha}C_{h_\Delta} - C_{m_\Delta}C_{h_\alpha}\right) + C_{h_{\alpha_c}}qS\bar{c}\ C_{h_\Delta}C_{m_\delta}}{\left(K_T - C_{h_\delta}qS\bar{c}\right)\left(C_{m_\Delta}C_{L_\alpha} - C_{m_\alpha}C_{L_\Delta}\right) + C_{h_{\alpha_c}}qS\bar{c}\left(C_{L_\delta}C_{m_\Delta} - C_{L_\Delta}C_{m_\delta}\right)}\right] \tag{24}$$

[redacted]

Similarly, the expression for the H_a boundary can be written as

$$H_a = gm\bar{c}\left[\frac{C_{h_\alpha}}{\frac{m\bar{c}l_f}{I_y}C_{m_\alpha} - C_{L_\alpha} - \frac{C_{h_{\alpha c}}qS\bar{c}}{K_T - C_{h_\delta}qS\bar{c}}\left(C_{L_\delta} - \frac{m\bar{c}l_f}{I_y}C_{m_\delta}\right)}\right] \tag{25}$$

Since both boundaries are independent of H_Δ, the region of interest is bounded by two vertical lines in the stability diagram. Equations (24) and (25) plotted as functions of altitude, Mach number, static margin, hinge moments, and missile mass will show the effect on the region of interest of each of these parameters. These effects are shown in figure 8. For each case only the parameter whose effect is being considered was varied, and all others were held at the values given in table I and those corresponding to a Mach number of 1.5 and an altitude of 30,000 feet. The effect of variation in Mach number included using the aerodynamic derivatives given in table II.

In all the cases illustrated by figure 8, the region of damping higher than the damping for the basic missile lies between the two boundaries. Thus if it is known how the boundaries are affected by each of the above variables, it can easily be determined whether the motion will be stable for all anticipated conditions. Any chosen value of mass-unbalance moment must lie in the region of interest for all conditions. For example, it can be seen from figure 8(a) that the boundaries are relatively independent of altitude, and there is a wide range of mass-unbalance hinge moments which fall within the stable region for an altitude variation of from sea level to 60,000 feet.

The effect of Mach number changes on the region of interest is shown in figure 8(b). If the Mach number is increased, the region of interest is shifted to the right, but it can be seen that at first the divergence boundary is shifted much more rapidly than the H_a boundary.

The effect of C_{h_α} can be seen from figure 8(c). Note that as C_{h_α} is increased negatively, the region of interest is shifted toward more positive values of the unbalance hinge moment. In order to stay within the stable region, therefore, it would be necessary to use larger positive values of mass unbalance. Since values of mass-unbalance moment near the divergence boundary give high damping, it can be seen that for a given amount of mass unbalance, increasing C_{h_α} negatively will have the effect of increasing the damping and decreasing the frequency.

Figures 8(c) and 8(d) show that if C_{h_α} and C_{h_Δ} are varied simultaneously in the same direction, the divergence boundary can be held constant. The H_a boundary, however, is affected by changes in C_{h_α} only, and large changes in this quantity may have a significant effect on the missile characteristics.

Application of the Analysis

Design considerations for a free-floating flap.- To design a free-floating flap suitable for augmentation of airframe damping, it is necessary to select values of mass unbalance and damping about the hinge such that the response of the missile is improved for all anticipated flight conditions. As was pointed out in the foregoing sections, improvement of the response involves considerations of the damping, frequency, and the turning-rate gain. In designing the flap, it is desired to increase the damping as much as possible without causing a large decrease in frequency and, furthermore, it is desirable to keep the flap gain as small as possible.

To begin, it is necessary to estimate the range of Mach numbers and altitudes for which the missile is expected to function and to compile the necessary aerodynamic and mass parameters to cover this range. For the present case the Mach number is varied through a range of from 1.3 to 1.9, and the altitude range is from 5,000 to 60,000 feet. The parameters for these conditions are listed in tables I and II.

The next step is to use graphs of the type shown in figure 8 to determine the combination of parameters which will give increased stability throughout the range of flight conditions. The variation of the H_a and divergence boundaries must be such that a value of mass unbalance can be chosen which will fall between them for all anticipated flight conditions. Once it is determined that this condition is satisfied, the combination of $H_{\dot{\Delta}}$ and mass-unbalance hinge moment giving the best response can be found in one of three ways.

The first approach consists of the superposition of constant-damping curves for the various flight conditions. For example, if it is desired that the time to damp to half amplitude be less than 0.5 second for all cases, the contours corresponding to this value of damping can be constructed for each of the anticipated conditions. Then since each constant-damping curve encloses an area in which the time to damp to half amplitude is less than that on the contour, that is, less than 0.5 second, the enclosed areas common to all the contours will represent those values of $H_{\dot{\Delta}}$ and mass-unbalance hinge moment for which the desired damping is obtained. This approach is straightforward, but it is somewhat laborious in that it involves the computation of a constant-damping curve for each flight condition.

The second approach is to choose a reasonable value of $H_{\dot{\Delta}}$ and a value of mass-unbalance hinge moment known to fall within the stable region from a study of the aforementioned graphs showing the variations of the H_a and divergence boundaries with flight conditions. These chosen values can then be substituted into the characteristic equation and the

solutions found by numerical methods for all flight conditions. This approach is based on trial and error and, though adequate, it may involve much computation before the desired response is obtained.

The third method involves the construction of a stability diagram for an intermediate flight condition and the use of plots similar to those shown in figure 8 to deduce values of $H_{\dot{\Delta}}$ and mass-unbalance hinge moment which will give approximately the desired damping for all conditions. The exact damping ratio and frequency for each condition can be obtained by substituting these values into the characteristic equation and solving for the roots by numerical methods. The third approach will be used here.

It is desired to find values of $H_{\dot{\Delta}}$ and mass-unbalance hinge moment for which the damping is greater than basic missile damping throughout the range of flight conditions previously selected. To minimize the possibility of flutter, it may be desirable to mass-balance the flap; an examination of the graphs of figures 8(a) and 8(b) shows that a value of zero mass-unbalance hinge moment always falls within the region between the two boundaries, indicating that the damping may be increased throughout the range of Mach numbers and altitudes being considered through a suitable choice of $H_{\dot{\Delta}}$ only.

The intermediate condition for the present case is the flight condition corresponding to a Mach number of 1.5 and an altitude of 30,000 feet. The stability diagram for this condition is that given in figure 5, and the frequency and $T_{1/2}$ for each value of $H_{\dot{\Delta}}$ can be obtained by an examination of the diagram. For purposes of illustration, the value of $H_{\dot{\Delta}}$ corresponding to point 5 will be tentatively chosen. The damping and frequency of the missile-flap configuration is obtained for each of the other flight conditions by substituting the values of $H_{\dot{\Delta}}$ and mass-unbalance hinge moment corresponding to point 5 and the quantities in tables I and II into equation (14) and solving for the roots.

The results of these computations are shown in figures 9 and 10. Also shown for comparison are results for the missile with position control and with spring-mounted control. In these figures the damping is given in terms of the damping ratio ζ, which can be obtained from the oscillation frequency and $T_{1/2}$ by using the equation

$$\zeta = \frac{\ln 2}{\sqrt{(\omega T_{1/2})^2 + (\ln 2)^2}} \tag{26}$$

Note that the effect on the damping and frequency of replacing the position control with the spring-mounted control is small, but that the effect of the free-floating flap can be considerable. For low supersonic Mach numbers the damping is not increased appreciably, but for Mach numbers greater than about 1.5, the damping ratio is increased by a factor of approximately 3. At sea level the damping ratio is increased by

approximately 80 percent. It remains essentially constant up to an altitude of about 30,000 feet, and then increases as the altitude is increased further.

It is evident from the above discussion that as far as damping is concerned, the combination of H_{Λ} and mass-unbalance moment corresponding to point 5 in figure 5 will result in an improvement of the missile response throughout the specified range of conditions. As mentioned previously, however, it is necessary to examine the flap gain $(\Lambda/\epsilon)_{ss}$ before it can be determined whether the results are practical. The variation in flap gain with altitude and Mach number is given in figure 11, and it can be seen that the ratio of free-floating flap deflection to servo deflection remains relatively small (less than -0.45) for all flight conditions.

The improvement in the variation of turning-rate gain of the missile due to the torque spring is evident from figure 12, where the gains for the missile with spring-mounted controls and free flaps are compared with those for the missile with position controls and with flaps fixed. Note that for both altitude and Mach number changes, the gain variation has been reduced considerably.

Transient solutions for the flight conditions presented in this section were obtained on the REAC and are shown in figure 13. In this figure, the time histories on the left give the response of the basic missile, and the time histories on the right give the response of the missile with the flaps floating. It can be seen that the responses with the flaps floating are generally improved as far as the damping is concerned, and that the frequencies are reduced in all cases as expected.

Experimental investigation of flap characteristics.- Throughout the theoretical analysis it was assumed that all the aerodynamic coefficients were linear functions of their respective variables, and the computations were carried out for flaps which were closely balanced aerodynamically. In reference 6, it is shown that the hinge moments for aerodynamically balanced trailing-edge control surfaces are highly nonlinear. However, it is known from other data that by placing a gap between the flap and the trailing edge of the wing, much of the nonlinearity can be removed. Furthermore, it is shown in reference 7 that blunting the trailing edges of the flaps also has the effect of linearizing the hinge moments.

From these considerations it was decided that an aerodynamically balanced flap with a blunt trailing edge mounted behind the wing with a gap between the flap and wing, as shown in figure 14, would give the desired linear characteristics. The use of aerodynamic balance was made in the analysis because it was anticipated that the flaps could be used to provide increased damping in roll as well as in pitch; hence, the leading and trailing edges were swept forward and the flap designed to be closely balanced in order to provide increased negative values of the

[redacted]

damping-in-roll derivative C_{l_p}. Subsequent wind-tunnel tests, however, showed that the effectiveness of the flap in providing increased roll damping was not significant; the damping in roll was increased by a maximum of only 15 percent.

It was estimated from the hinge-moment data of reference 6 that, for a biconvex airfoil section, placing the hinge line at a point approximately one-third of the chord from the leading edge would result in a closely balanced flap. Furthermore, since it is known from the results of reference 7 that blunting the trailing edge of the flap would shift the center of pressure rearward, the hinge line was placed at a point on the midspan of the flap a distance 40 percent of the chord from the leading edge. The airfoil section of the flap was a 5-percent-thick, biconvex section, blunted at the trailing edge so that the ratio of trailing-edge thickness to maximum thickness was 0.5. Preliminary tests with the same flap with sharp trailing edges showed that the hinge moments were slightly more linear with the blunt trailing edges, but the major effect of the blunting was to shift the center of pressure rearward about 7 percent of the chord as expected.

The wind-tunnel tests were conducted in the Ames 6- by 6-foot supersonic wind tunnel, which is described in reference 8. The testing procedures and corrections to data can be obtained from reference 6. The testing was done for a range of Mach numbers of 0.6 to 0.9 and 1.3 to 1.9 at a Reynolds number of 2.4 million. Hinge-moment measurements were made at constant flap deflections through a nominal angle-of-attack range of -17° to $+17^\circ$ with the flap settings varied in 4° increments through a range of deflections of -20° to $+20^\circ$. Representative results of the hinge moments obtained in the wind-tunnel tests are presented in graphical form in figure 15. Results for the complete range of tests variables are given in tabular form in table III.

The results presented in figure 15 show that at subsonic speeds, the flap is unstable and the hinge-moment variation is quite nonlinear. Although the magnitudes of the moments are relatively small, the fact that they are unstable precludes the use of this flap at subsonic speeds. The results for the supersonic Mach numbers shown in figures 15(c) and 15(d) show the hinge moments to be generally linear and closely balanced for the relatively large range of angles tested, and these flaps should be satisfactory in this speed range for use as a free-floating damper.

The change in hinge-moment characteristics obtained for these flaps as the speed range is varied from subsonic to supersonic is characteristic of most aerodynamic surfaces, and illustrates the problems of designing a free-floating flap which will function satisfactorily throughout the operating Mach number range of present-day missiles.

CONCLUDING REMARKS

The use of mechanical and aerodynamic devices intended to improve missile response over a specified range of flight conditions appears to be feasible on the basis of the results presented in this paper. The use of these relatively simple devices appears particularly advantageous if the operational speed range lies wholly in either the subsonic or supersonic regime; their use on a missile which operates in both speed ranges would present considerable difficulties from the standpoint of obtaining the desired hinge-moment characteristics, and extensive experimental investigations would be required.

The analysis made in this paper was relatively simplified from the standpoint that only symmetrical motions were considered; that is, the results apply only to an airframe performing motions in the pitch or yaw plane. In any specific application of such devices, the coupling which may be present due to rolling will have an effect and must be investigated. A further simplification was made when it was assumed that the flight speed was invariant during the motions investigated. It should be noted that if use is made of mass-unbalance hinge moment to obtain the desired missile response, an effective hinge moment due to control deflection will be present for any longitudinal accelerations of the missile airframe. Although this effect will generally be small over most of the missile trajectory, it can be appreciable during the launch phase and must be taken into account.

Ames Aeronautical Laboratory
National Advisory Committee for Aeronautics
Moffett Field, Calif., Dec. 9, 1955

APPENDIX A

DERIVATION OF APPROXIMATE EXPRESSIONS FOR GAIN

Position Control; Floating Flaps Fixed

From equation (4) the gain for this case is

$$\left(\frac{\dot{\gamma}}{\delta}\right)_{ss} = \frac{C_{L_\delta} C_{m_\alpha} - C_{L_\alpha} C_{m_\delta}}{2\tau C_{m_\alpha} + C_{L_\alpha} C_{m_q} \frac{\bar{c}}{2V}} \tag{A1}$$

since $\tau = \frac{m}{\rho V S}$, this becomes

$$\left(\frac{\dot{\gamma}}{\delta}\right)_{ss} = \frac{\rho V\left(C_{L_\delta} C_{m_\alpha} - C_{L_\alpha} C_{m_\delta}\right)}{\frac{2m}{S} C_{m_\alpha} + \rho C_{L_\alpha} C_{m_q} \frac{\bar{c}}{2}}$$

where ρ is the density of air and is of the order of 10^{-3} slugs per cubic foot. The second term in the denominator is generally much smaller than the first and can be ignored leaving just

$$\left(\frac{\dot{\gamma}}{\delta}\right)_{ss} = \left(\frac{S}{ma_o}\right)\left(\frac{q}{M}\right)\left(C_{L_\delta} - \frac{C_{m_\delta}}{C_{m_\alpha}} C_{L_\alpha}\right) \tag{A2}$$

Position Control; Floating Flaps Operative

Equation (9) gives the exact expression for the turning-rate gain. If the expressions for τ, q, and ξ_f are introduced, the denominator becomes

$$\frac{1}{\rho V}\left[\left(C_{L_\alpha} C_{m_\Delta} - C_{L_\Delta} C_{m_\alpha}\right)\left(\frac{2m_f s_f}{S\bar{c}} + \rho l_f C_{h_\alpha}\right) + C_{h_\alpha}\left(\frac{2m}{S} C_{m_\Delta} + \rho C_{L_\Delta} C_{m_q} \frac{\bar{c}}{2}\right) - C_{h_\Delta}\left(\frac{2m}{S} C_{m_\alpha} + \rho C_{L_\alpha} C_{m_q} \frac{\bar{c}}{2}\right)\right] \tag{A3}$$

and if the terms within the brackets containing ρ are disregarded there results

$$\frac{2mV}{qS}\left[\left(C_{L_\alpha}C_{m_\Delta} - C_{L_\Delta}C_{m_\alpha}\right)\frac{m_f s_f}{m\bar{c}} + \left(C_{m_\Delta}C_{h_\alpha} - C_{m_\alpha}C_{h_\Delta}\right)\right]$$

Substituting $V = a_o M$ and the above expression into equation (9) gives

$$\left(\frac{\dot{\gamma}}{\delta}\right)_{ss} = \left(\frac{S}{ma_o}\right)\left(\frac{q}{M}\right)\left[\frac{C_{L_\delta}\left(C_{m_\Delta}C_{h_\alpha} - C_{m_\alpha}C_{h_\Delta}\right) + C_{m_\delta}\left(C_{L_\alpha}C_{h_\Delta} - C_{L_\Delta}C_{h_\alpha}\right)}{\frac{m_f s_f}{m\bar{c}}\left(C_{L_\alpha}C_{m_\Delta} - C_{L_\Delta}C_{m_\alpha}\right) + \left(C_{m_\Delta}C_{h_\alpha} - C_{m_\alpha}C_{h_\Delta}\right)}\right] \quad (A4)$$

Spring-Position Control

If, in the denominator of equation (12), the expression for τ is substituted, there results

$$\frac{1}{\rho V}\left\{\left(C_{h_\delta}qS\bar{c} - K_T\right)\left(\frac{2m}{S}C_{m_\alpha} + \rho C_{L_\alpha}C_{m_q}\frac{\bar{c}}{2}\right) - C_{h_{\alpha_c}}qS\bar{c}\left[\frac{2m}{S}C_{m_\delta} + \right.\right.$$

$$\left.\left.\rho C_{L_\delta}C_{m_q}\frac{\bar{c}}{2} + \rho l_c\left(C_{L_\delta}C_{m_\alpha} - C_{L_\alpha}C_{m_\delta}\right)\right]\right\} \quad (A5)$$

Disregarding the terms within the braces containing ρ and simplifying gives

$$\left(\frac{\dot{\gamma}}{\epsilon}\right)_{ss} = \frac{K_T}{m\bar{c}a_o M}\left[\frac{C_{L_\alpha}C_{m_\delta} - C_{L_\delta}C_{m_\alpha}}{C_{m_\alpha}\left(C_{h_\delta} - \frac{K_T}{qS\bar{c}}\right) - C_{m_\delta}C_{h_{\alpha_c}}}\right] \quad (A6)$$

Controls Actuated by a Torque Servo

The equations of motion used in the analysis of the torque-servo missile are very similar to those for the spring-position missile. The

equations for lift and pitching are, of course, identical, but in the place of equation (11), the equation for the control surface is

$$\left(\xi_c VD - Ch_{\alpha_c}\right)\gamma + \left[\left(\xi_c l_c - \sigma_c\right)D^2 - \left(\frac{l_c}{V}D - 1\right)Ch_{\alpha_c}\right]\theta - \left(\sigma_c D^2 - Ch_{\dot{\delta}}\frac{\bar{c}}{2V}D - Ch_{\delta}\right)\delta = -\frac{H}{qS\bar{c}} \qquad (A7)$$

where H is the hinge moment specified by the torque servo in response to an input signal.

The missile turning-rate gain is obtained by solving for $(\dot{\gamma}/H)$ from equations (2), (3), and (A7) and letting D go to zero. If this is done, there results the expression

$$\left(\frac{\dot{\gamma}}{H}\right)_{ss} = \frac{C_{L_\alpha}C_{m_\delta} - C_{L_\delta}C_{m_\alpha}}{mV\bar{c}\left\{Ch_\delta\left(C_{m_\alpha} + \frac{\rho S}{2m}C_{L_\alpha}C_{m_q}\frac{\bar{c}}{2}\right) - Ch_{\alpha_c}\left(C_{m_\delta} + \frac{\rho S}{2m}C_{L_\delta}C_{m_q}\frac{\bar{c}}{2}\right) + \left(C_{L_\alpha}C_{m_\delta} - C_{L_\delta}C_{m_\alpha}\right)\left(Ch_{\alpha_c}\frac{\rho S}{2m}l_c - \frac{m_c s_c}{m\bar{c}}\right)\right\}} \qquad (A8)$$

The terms containing a factor of ρ are generally small compared to the remaining terms and may be disregarded, leaving

$$\left(\frac{\dot{\gamma}}{H}\right)_{ss} = \frac{1}{m\bar{c}V\left(\frac{Ch_\delta C_{m_\alpha} - Ch_{\alpha_c}C_{m_\delta}}{C_{L_\alpha}C_{m_\delta} - C_{L_\delta}C_{m_\alpha}}\right) - m_c s_c V} \qquad (A9)$$

APPENDIX B

COEFFICIENTS OF THE CHARACTERISTIC EQUATION

From the equations of motion (6), (7), (8), and (18) it can be shown that the characteristic equation may be put into the form

$$F(D) = D^4 + A_3D^3 + A_2D^2 + A_1D + A_0 = 0 \tag{B1}$$

where

$$A_3 = \frac{C_{L_\alpha}}{2\tau} - \frac{C_{m_q} + C_{m_{\dot{\alpha}}}}{\sigma_A}\frac{\bar{c}}{2V} + \frac{C_{h_{\alpha_c}} qS\bar{c}}{K_T - C_{h_\delta} qS\bar{c}}\left[\frac{C_{L_\delta}}{2\tau} + \frac{l_c}{V\sigma_A}\left(C_{m_\delta} - \frac{C_{L_\delta}}{2\tau}\frac{C_{m_{\dot{\alpha}}}}{\sigma_A}\frac{\bar{c}}{2V}\right)\right] - C_{h_{\dot{\Delta}}}\frac{qS\bar{c}^2}{2VI_f} \tag{B2}$$

$$A_2 = \frac{m_f s_f}{I_f}\left[\frac{l_f}{\sigma_A}\left(C_{m_\Delta} - \frac{C_{L_\Delta}}{2\tau}C_{m_{\dot{\alpha}}}\frac{\bar{c}}{2V}\right) - \frac{C_{L_\Delta}}{2\tau}V\right] - C_{h_{\dot{\Delta}}}\frac{qS\bar{c}^2}{2VI_f}\left(\frac{C_{L_q}}{2\tau} - \frac{C_{m_q} + C_{m_{\dot{\alpha}}}}{\sigma_A}\frac{\bar{c}}{2V}\right) + \frac{C_{m_\Delta} - C_{m_\alpha}}{\sigma_A} -$$

$$\frac{1}{2\tau\sigma_A}\frac{\bar{c}}{2V}\left(C_{L_\alpha}C_{m_q} + C_{L_\Delta}C_{m_{\dot{\alpha}}}\right) - \frac{C_{h_\Delta}}{\sigma_f} + \frac{C_{h_{\alpha_c}} qS\bar{c}}{K_T - C_{h_\delta} qS\bar{c}}\left\{\frac{l_c}{2\tau\sigma_A V}\left(C_{L_\alpha}C_{m_\delta} - C_{L_\delta}C_{m_\alpha}\right) - \frac{1}{\sigma_A}\left(C_{m_\delta} + \frac{C_{L_\delta}}{2\tau}C_{m_q}\frac{\bar{c}}{2V}\right) - \right.$$

$$\left. C_{h_{\dot{\Delta}}}\frac{qS\bar{c}^2}{2VI_f}\left[\frac{C_{L_\delta}}{2\tau} + \frac{l_c}{V\sigma_A}\left(C_{m_\delta} - \frac{C_{L_\delta}}{2\tau}C_{m_{\dot{\alpha}}}\frac{\bar{c}}{2V}\right)\right]\right\} \tag{B3}$$

$$A_1 = C_{h_{\dot{\Delta}}} \frac{qS\bar{c}^2}{2VI_f\sigma_A}\left(C_{m_\alpha} + C_{L_\alpha}C_{m_q}\frac{\bar{c}}{4\tau V}\right) + \frac{1}{2\tau\sigma_A}\left(\frac{m_f s_f l_f}{I_f} + 1\right)\left(C_{L_\alpha}C_{m_\Delta} - C_{L_\Delta}C_{m_\alpha}\right) + \left(\frac{m_f s_f \bar{c}}{4\tau I_f \sigma_A}\right)C_{L_\Delta}\left(C_{m_q} + C_{m_{\dot{\alpha}}}\right) -$$

$$\frac{C_{h_\Delta}}{\sigma_f}\left(\frac{C_{L_\alpha}}{2\tau} - \frac{C_{m_q} + C_{m_{\dot{\alpha}}}}{\sigma_A}\frac{\bar{c}}{2V}\right) + \frac{C_{h_\alpha}}{\sigma_f}\left[\frac{C_{L_\Delta}}{2\tau} - \frac{l_f}{V\sigma_A}\left(C_{m_\Delta} + \frac{C_{L_\Delta}}{2\tau}C_{m_{\dot{\alpha}}}\frac{\bar{c}}{2V}\right)\right] + \frac{C_{h_{\alpha_c}}qS\bar{c}}{K_T - C_{h_\delta}qS\bar{c}}\left\{C_{h_{\dot{\Delta}}}\frac{qS\bar{c}^2}{2VI_f}\left[\left(\frac{C_{m_\delta}}{\sigma_A} +\right.\right.\right.$$

$$\left.\left.\left.\frac{C_{L_\delta}}{2\tau}\frac{C_{m_q}}{\sigma_A}\frac{\bar{c}}{2V}\right) - \frac{l_c}{2\tau\sigma_A V}\left(C_{m_\delta}C_{L_\alpha} - C_{L_\delta}C_{m_\alpha}\right)\right] - \frac{m_f s_f}{2\tau\sigma_A I_f}\left(l_c + l_f\right)\left(C_{m_\delta}C_{L_\Delta} - C_{L_\delta}C_{m_\Delta}\right) - \frac{1}{2\tau\sigma_A}\left(C_{m_\delta}C_{L_\Delta} -\right.\right.$$

$$\left.\left.C_{L_\delta}C_{m_\Delta}\right) - \left(\frac{l_c}{V}\right)\left(\frac{C_{h_\Delta}}{\sigma_f}\right)\left(\frac{C_{m_\delta}}{\sigma_A} - \frac{C_{L_\delta}}{2\tau}\frac{C_{m_{\dot{\alpha}}}}{\sigma_A}\frac{\bar{c}}{2V}\right) - \frac{C_{L_\delta}}{2\tau}\frac{C_{h_\Delta}}{\sigma_f}\right\} \tag{B4}$$

$$A_0 = \frac{1}{\sigma_A\sigma_f}\left\{C_{h_\Delta}\left(C_{m_\alpha} + \frac{C_{L_\alpha}}{2\tau}C_{m_q}\frac{\bar{c}}{2V}\right) - C_{h_\alpha}\left[C_{m_\Delta} + \frac{C_{L_\Delta}}{2\tau}C_{m_q}\frac{\bar{c}}{2V} - \frac{l_f}{2\tau V}\left(C_{L_\Delta}C_{m_\alpha} - C_{L_\alpha}C_{m_\Delta}\right)\right] -\right.$$

$$\sigma_f\frac{m_f s_f}{I_f}\frac{V}{2\tau}\left(C_{L_\alpha}C_{m_\Delta} - C_{L_\Delta}C_{m_\alpha}\right) + \frac{C_{h_{\alpha_c}}qS\bar{c}}{K_T - C_{h_\delta}qS\bar{c}}\left[C_{h_\alpha}\left(\frac{l_c + l_f}{2\tau V}\right)\left(C_{m_\delta}C_{L_\Delta} - C_{L_\delta}C_{m_\Delta}\right) -\right.$$

$$\left.\left.C_{h_\Delta}\left(\frac{l_c}{2\tau V}\right)\left(C_{m_\delta}C_{L_\alpha} - C_{L_\delta}C_{m_\alpha}\right) + C_{h_\Delta}\left(C_{m_\delta} + \frac{C_{L_\delta}}{2\tau}C_{m_q}\frac{\bar{c}}{2V}\right) + \sigma_f\left(\frac{m_f s_f V}{2\tau I_f}\right)\left(C_{m_\delta}C_{L_\Delta} - C_{L_\delta}C_{m_\Delta}\right)\right]\right\} \tag{B5}$$

If the spring constant K_T is made very large, equation (B1) reduces to the characteristic equation for a position-control missile where motion is governed by equations (6), (7), and (8).

APPENDIX C

DERIVATION AND SIMPLIFICATION OF EXPRESSIONS FOR BOUNDARIES

NOTATION

The expressions to be derived in this section are rather lengthy, so to simplify the writing the following notations are introduced:

$$Q_o = \left(\frac{C_{L_\alpha}}{2\tau} - \frac{C_{m_q} + C_{m_{\dot{\alpha}}}}{\sigma_A}\frac{\bar{c}}{2V}\right) + \frac{C_{h_{\alpha_c}} qS\bar{c}}{K_T - C_{h_\delta} qS\bar{c}}\left[\frac{C_{L_\delta}}{2\tau} + \frac{l_c}{V\sigma_A}\left(C_{m_\delta} - \frac{C_{L_\delta}}{2\tau} C_{m_{\dot{\alpha}}}\frac{\bar{c}}{2V}\right)\right] \tag{C1}$$

$$P_o = \frac{1}{\sigma_A}\left\{-\left(C_{m_\alpha} + \frac{C_{L_\alpha}}{2\tau} C_{m_q}\frac{\bar{c}}{2V}\right) + \frac{C_{h_{\alpha_c}} qS\bar{c}}{K_T - C_{h_\delta} qS\bar{c}}\left[-\left(C_{m_\delta} + \frac{C_{L_\delta}}{2\tau} C_{m_q}\frac{c}{2V}\right) + \frac{l_c}{2\tau V}\left(C_{m_\delta} C_{L_\alpha} - C_{L_\delta} C_{m_\alpha}\right)\right]\right\} \tag{C2}$$

$$B_1 = -\frac{1}{\sigma_A}\left(C_{m_\alpha} + \frac{C_{L_\alpha}}{2\tau} C_{m_q}\frac{\bar{c}}{2V}\right) - \frac{C_{h_\Delta}}{\sigma_f} + \frac{1}{\sigma_A}\left(C_{m_\Delta} - \frac{C_{L_\Delta}}{2\tau} C_{m_{\dot{\alpha}}}\frac{\bar{c}}{2V}\right) + \frac{C_{h_{\alpha_c}} qS\bar{c}}{K_T - C_{h_\delta} qS\bar{c}}\left\{\frac{1}{2\tau\sigma_A}\left[\frac{l_c}{V}\left(C_{m_\delta} C_{L_\alpha} - C_{L_\delta} C_{m_\alpha}\right) - 2\tau C_{m_\delta} - C_{L_\delta} C_{m_q}\frac{\bar{c}}{2V}\right]\right\} \tag{C3}$$

$$B_2 = \frac{1}{2\tau\sigma_A\sigma_f}\left\{C_{h_\Delta}\left(2\tau C_{m_\alpha} + C_{L_\alpha} C_{m_q}\frac{\bar{c}}{2V}\right) + C_{h_\alpha}\left[-\left(2\tau C_{m_\Delta} + C_{L_\Delta} C_{m_q}\frac{\bar{c}}{2V}\right) + \frac{l_f}{V}\left(C_{L_\Delta} C_{m_\alpha} - C_{L_\alpha} C_{m_\Delta}\right)\right] + \frac{C_{h_{\alpha_c}} qS\bar{c}}{K_T - C_{h_\delta} qS\bar{c}}\left[\left(\frac{l_c + l_f}{V}\right)\left(C_{m_\delta} C_{L_\Delta} - C_{L_\delta} C_{m_\Delta}\right) C_{h_\alpha} - \frac{l_c}{V}\left(C_{m_\delta} C_{L_\alpha} - C_{L_\delta} C_{m_\alpha}\right) C_{h_\Delta} + \left(2\tau C_{m_\delta} + C_{L_\delta} C_{m_q}\frac{\bar{c}}{2V}\right) C_{h_\Delta}\right]\right\} \tag{C4}$$

$$a = \frac{l_f}{\sigma_A}\left(C_{m_\Delta} - \frac{C_{L_\Delta}}{2\tau} C_{m_{\dot{\alpha}}} \frac{\bar{c}}{2V}\right) - \frac{C_{L_\Delta}}{2\tau} V \tag{C5}$$

$$f = \frac{V}{2\tau\sigma_A}\left[\left(C_{L_\alpha}C_{m_\Delta} - C_{L_\Delta}C_{m_\alpha}\right) - \frac{C_{h_{\alpha_c}} qS\bar{c}}{K_T - C_{h_\delta} qS\bar{c}}\left(C_{m_\delta}C_{L_\Delta} - C_{L_\delta}C_{m_\Delta}\right)\right] \tag{C6}$$

THE DIVERGENCE BOUNDARY

The divergence boundary is obtained by setting the coefficient A_o of the characteristic equation to zero. If equation (B5) is written in the foregoing notation, the expression for A_o is

$$A_o = B_2 - f\left(\frac{m_f s_f}{I_f}\right) \tag{C7}$$

Equating to zero and solving for mass-unbalance hinge moment gives

$$H_D = \frac{gI_f B_2}{f} \tag{C8}$$

Consider the term B_2 in the numerator. If the expressions for q and τ are substituted, there results

$$B_2 = \frac{1}{2\tau\sigma_A}\frac{VS\bar{c}}{2I_f}\left\{C_{h_\Delta}\left(\frac{2m}{S} C_{m_\alpha} + \rho C_{L_\alpha} C_{m_q} \frac{\bar{c}}{2}\right) + C_{h_\alpha}\left[-\left(\frac{2m}{S} C_{m_\Delta} + \rho C_{L_\Delta} C_{m_q} \frac{\bar{c}}{2}\right) + \rho l_f \left(C_{L_\Delta}C_{m_\alpha} - C_{L_\alpha}C_{m_\Delta}\right)\right] +\right.$$

$$\left.\frac{C_{h_{\alpha_c}} qS\bar{c}}{K_T - C_{h_\delta} qS\bar{c}}\left[\rho\left(l_f + l_c\right)\left(C_{m_\delta}C_{L_\Delta} - C_{L_\delta}C_{m_\Delta}\right)C_{h_\alpha} - \rho l_c\left(C_{m_\delta}C_{L_\alpha} - C_{L_\delta}C_{m_\alpha}\right)C_{h_\Delta} + \left(\frac{2m}{S} C_{m_\delta} + \rho C_{L_\delta} C_{m_q}\frac{\bar{c}}{2}\right)C_{h_\Delta}\right]\right\}$$

The terms multiplied by the factor ρ are small compared to the remaining terms and may be disregarded, so that the expression for B_2 may be written

$$B_2 = \frac{V}{2\tau\sigma_A}\frac{m\bar{c}}{I_f}\left[\left(C_{m_\alpha}C_{h_\Delta} - C_{h_\alpha}C_{m_\Delta}\right) + \frac{C_{h_{\alpha_c}}qS\bar{c}}{K_T - C_{h_\delta}qS\bar{c}}\left(C_{h_\Delta}C_{m_\delta}\right)\right] \tag{C9}$$

Substitution of equations (C6) and (C9) into equation (C8) gives

$$H_D = gm\bar{c}\left[\frac{\left(K_T - C_{h_\delta}qS\bar{c}\right)\left(C_{m_\alpha}C_{h_\Delta} - C_{m_\Delta}C_{h_\alpha}\right) + C_{h_\Delta}C_{m_\delta}C_{h_{\alpha_c}}qS\bar{c}}{\left(K_T - C_{h_\delta}qS\bar{c}\right)\left(C_{L_\alpha}C_{m_\Delta} - C_{L_\Delta}C_{m_\alpha}\right) + \left(C_{L_\delta}C_{m_\Delta} - C_{L_\Delta}C_{m_\delta}\right)C_{h_{\alpha_c}}qS\bar{c}}\right] \tag{C10}$$

THE H_a BOUNDARY

From equations of motion (2), (3), and (18) the characteristic equation for the spring-position missile with floating flaps fixed is

$$D^2 + Q_oD + P_o = 0 \tag{C11}$$

which represents a simple second-order system of the form

$$D^2 + 2\zeta\omega_nD + \omega_n^2 = 0$$

The roots of equation (C11) are

$$D = -\frac{Q_o}{2} \pm i\sqrt{P_o - \frac{Q_o^2}{4}}$$

so that the damping is given by $r = -(Q_o/2)$ and the frequency by

$$\omega = \sqrt{P_o - \frac{Q_o^2}{4}}$$

[redacted]

Since the H_a boundary represents the mass unbalance for which the damping and frequency of the missile with floating flaps are equal to that for the missile with flaps fixed, the expression for H_a can be obtained by substituting these values of r and μ and the coefficients from Appendix B into equations (16) and (17). Solving for the unbalance hinge moment from the resulting equations gives

$$H_a = \frac{gI_f(B_2 + P_o^2 - B_1P_o)}{f + aP_o} \tag{C12}$$

As for the divergence boundary, if $\tau = m/\rho VS$ and $q = (1/2)\rho V^2$ are substituted and the terms of the order of ρ or smaller are disregarded, the following expressions result:

$$B_2 = \frac{(\rho V^2)^2(S\bar{c})^2}{4I_yI_f}\left[C_{m_\alpha}C_{h_\Delta} - C_{m_\Delta}C_{h_\alpha} + \frac{C_{h_{\alpha_c}}qS\bar{c}}{K_T - C_{h_\delta}qS\bar{c}}\left(C_{m_\delta}C_{h_\Delta}\right)\right] \tag{C13}$$

$$P_o = -\frac{(\rho V^2)S\bar{c}}{2I_y}\left(C_{m_\alpha} + \frac{C_{h_{\alpha_c}}qS\bar{c}}{K_T - C_{h_\delta}qS\bar{c}}C_{m_\delta}\right) \tag{C14}$$

$$B_1 = \frac{\rho V^2S\bar{c}}{2}\left[-\frac{C_{h_\Delta}}{I_f} + \frac{1}{I_y}\left(C_{m_\Delta} - C_{m_\alpha} - \frac{C_{h_{\alpha_c}}qS\bar{c}}{K_T - C_{h_\delta}qS\bar{c}}C_{m_\delta}\right)\right] \tag{C15}$$

$$f = \frac{(\rho V^2S\bar{c})^2}{4I_ym\bar{c}}\left[\left(C_{L_\alpha}C_{m_\Delta} - C_{L_\Delta}C_{m_\alpha}\right) - \frac{C_{h_{\alpha_c}}qS\bar{c}}{K_T - C_{h_\delta}qS\bar{c}}\left(C_{m_\delta}C_{L_\Delta} - C_{L_\delta}C_{m_\Delta}\right)\right] \tag{C16}$$

$$a = \frac{\rho V^2S\bar{c}}{2}\left(l_f\frac{C_{m_\Delta}}{I_y} - \frac{C_{L_\Delta}}{m\bar{c}}\right) \tag{C17}$$

Substitution of equations (C13) through (C17) into equation (C12) results in the simplified expression

$$H_a = \frac{gm\bar{c}\left[C_{h_\alpha} - \frac{I_f}{I_y}\left(\frac{C_{m_\delta}C_{h_{\alpha_c}}qS\bar{c}}{K_T - C_{h_\delta}qS\bar{c}} + C_{m_\alpha}\right)\right]}{\frac{m\bar{c}l_f}{I_y}C_{m_\alpha} - C_{L_\alpha} - \frac{C_{h_{\alpha_c}}qS\bar{c}}{K_T - C_{h_\delta}qS\bar{c}}\left(C_{L_\delta} - \frac{m\bar{c}l_f}{I_y}C_{m_\delta}\right)} \tag{C18}$$

Since, in general, $I_f << I_y$, this expression can be further simplified to

$$H_a = \frac{gm\bar{c}\,C_{h_\alpha}}{\frac{m\bar{c}\,l_f}{I_y}C_{m_\alpha} - C_{L_\alpha} - \frac{C_{h_{\alpha_c}}qS\bar{c}}{K_T - C_{h_\delta}qS\bar{c}}\left(C_{L_\delta} - \frac{m\bar{c}\,l_f}{I_y}C_{m_\delta}\right)} \tag{C19}$$

THE H_e BOUNDARY

The turning-rate gain is the steady-state value of the rate of change of flight-path angle $\dot{\gamma}$ per unit canard-control-actuator deflection ϵ. Equation (13) may be written

$$\left(\frac{\dot{\gamma}}{\epsilon}\right)_{ss} = \frac{K_T\left(C_{m_\delta}C_{L_\alpha} - C_{L_\delta}C_{m_\alpha}\right)}{2\tau\sigma_A P_o\left(K_T - C_{h_\delta}qS\bar{c}\right)} \tag{C20}$$

as the gain for the spring-control missile with flaps fixed.

Similarly, from equations (6), (7), (8), and (11) the gain for the missile with canard surfaces mass-balanced and with flaps floating is

$$\left(\frac{\dot{\gamma}}{\epsilon}\right)_{ss} = \frac{K_T\left[\left(C_{m_\delta}C_{L_\Delta} - C_{L_\delta}C_{m_\Delta}\right)C_{h_\alpha} - \left(C_{m_\delta}C_{L_\alpha} - C_{L_\delta}C_{m_\alpha}\right)C_{h_\Delta}\right]}{\left(2\tau\sigma_A\sigma_f\right)\left(K_T - C_{h_\delta}qS\bar{c}\right)\left(B_2 - \frac{m_f s_f}{I_f}f\right)} \tag{C21}$$

The H_e boundary represents the flap mass unbalance for which the gains are equal; therefore, if we equate the right-hand sides of equations (C20) and (C21) and solve for the unbalance hinge moment, there results

$$H_e = \frac{I_f g}{f}\left\{B_2 + \frac{P_o}{\sigma_f}\left[\left(\frac{C_{m_\delta}C_{L_\Delta} - C_{L_\delta}C_{m_\Delta}}{C_{m_\delta}C_{L_\alpha} - C_{L_\delta}C_{m_\alpha}}\right)C_{h_\alpha} + C_{h_\Delta}\right]\right\} \tag{C22}$$

If the expressions for B_2, P_o, and f from equations (C13), (C14), and (C16) are used, there results the simplified expression

$$H_e = \frac{gm\bar{c}\;C_{m_\delta}C_{h_\alpha}}{C_{L_\delta}C_{m_\alpha} - C_{L_\alpha}C_{m_\delta}} \tag{C23}$$

REFERENCES

1. Cohen, Doris: Theoretical Investigation of the Rolling Oscillations of an Airplane with Ailerons Free. NACA Rep. 787, 1944.

2. Greenberg, Harry, and Sternfield, Leonard: Theoretical Investigation of the Lateral Oscillations of an Airplane with Free Rudder with Special Reference to the Effect of Friction. NACA Rep. 762, 1943.

3. Greenberg, Harry, and Sternfield, Leonard: A Theoretical Investigation of Longitudinal Stability of Airplanes with Free Controls Including Effect of Friction in the Control System. NACA Rep. 791, 1944.

4. Curfman, Howard J., Jr., Strass, Kurt H., and Crane, Harold L.: Investigations Toward Simplification of Missile Control Systems. NACA RM L53I21a, 1953.

5. Brown, W. S.: A Simple Method of Constructing Stability Diagrams. Ministry of Aircraft Production, R. & M. No. 1905, British A.R.C., 1942.

6. Boyd, John W., and Pfyl, Frank A.: Experimental Investigations of Aerodynamically Balanced Trailing-Edge Control Surfaces on an Aspect Ratio 2 Triangular Wing at Subsonic and Supersonic Speeds. NACA RM A52L04, 1953.

7. Boyd, John W.: Aerodynamic Characteristics of Two 25-Percent-Area Trailing-Edge Flaps on an Aspect Ratio 2 Triangular Wing at Subsonic and Supersonic Speeds. NACA RM A52D01c, 1952.

8. Frick, Charles W., and Olson, Robert N.: Flow Studies in the Asymmetric Adjustable Nozzle of the Ames 6- by 6-Foot Supersonic Wind Tunnel. NACA RM A9E24, 1949.

[redacted]

TABLE I.- MASS AND GEOMETRIC PARAMETERS OF THE MISSILE

m, missile mass, slugs	3.33
m_f, mass of one floating flap, slugs	0.0675
c, M.A.C. of wing, ft	1.475
S, wing plan-form area, sq ft	2.262
$\bar{c}_f$, M.A.C. of floating flap, ft	0.416
S_f, plan-form area of one flap, sq ft	0.248
l_f, (see "symbols"), ft	2.184
l_c, (see "symbols"), ft	2.776
I_y, longitudinal moment of inertia, slug-ft^2	23.28
I_f, moment of inertia of flap, slug-ft^2	0.000457
I_c, moment of inertia of control surface, slug-ft^2	0.000600

TABLE II.- AERODYNAMIC PARAMETERS OF THE MISSILE

Parameter	M = 1.3	M = 1.5	M = 1.9
C_{L_α}	4.047	3.740	3.156
C_{L_δ}	0	0	0
C_{L_Δ}	1.26	1.20	1.03
C_{m_α}	-0.6199	-0.695	-0.586
$C_{m_{\dot{\alpha}}}$	-1.74	-1.67	-1.63
C_{m_δ}	0.746	0.600	0.500
C_{m_Δ}	-1.021	-1.183	-0.850
C_{m_q}	-5.86	-5.80	-5.77
C_{h_α}	-0.0020	-0.0035	-0.0043
$C_{h_{\alpha_c}}$	-0.0040	-0.0017	-0.0020
C_{h_δ}	-0.0100	-0.0080	-0.0070
C_{h_Δ}	-0.0120	-0.0095	-0.0080
$\bar{x}/\bar{c}$	-0.153	-0.186	-0.189

TABLE III.- HINGE-MOMENT CHARACTERISTICS OF THE FREE-FLOATING FLAP

[Based on the area and M.A.C. of one free-floating flap]

(a) Nominal $\Delta = 0^\circ$

M = 0.60			M = 0.80			M = 0.90			M = 1.30			M = 1.50			M = 1.70			M = 1.90		
α	Δ	C_h	α	Δ	C_h	α	Δ	C_h	α	Δ	C_h	α	Δ	C_h	α	Δ	C_h	α	Δ	C_h
-17.71	-0.08	-0.0599	-17.82	-0.11	-0.0642	-17.71	-0.11	-0.0599	-17.43	0.02	0.0079	-17.41	0.05	0.0211	-17.42	0.08	0.0319	-17.40	0.09	0.0387
-16.65	-.07	-.0540	-16.77	-.10	-.0583	-16.66	-.10	-.0540	-16.39	.01	.0030	-16.37	.04	.0185	-16.36	.07	.0293	-16.35	.08	.0365
-14.56	-.06	-.0443	-14.66	-.08	-.0474	-14.71	-.08	-.0452	-14.32	0	-.0010	-14.29	.03	.0130	-14.27	.05	.0227	-14.25	.07	.0299
-12.47	-.04	-.0313	-12.55	-.06	-.0357	-12.59	-.07	-.0391	-12.25	0	-.0007	-12.22	.02	.0095	-12.20	.05	.0210	-12.17	.05	.0288
-10.39	-.03	-.0227	-10.45	-.05	-.0278	-10.49	-.05	-.0303	-10.18	-.01	-.0023	-10.16	.02	.0070	-10.14	.04	.0178	-10.11	.04	.0192
-8.31	-.02	-.0152	-8.36	-.03	-.0200	-8.38	-.04	-.0243	-8.12	-.01	-.0045	-8.10	.01	.0040	-8.08	.03	.0118	-8.06	.03	.0145
-6.23	-.01	-.0086	-6.27	-.02	-.0126	-6.29	-.03	-.0172	-6.06	-.02	-.0084	-6.04	0	.0011	-6.02	.01	.0052	-6.01	.02	.0083
-4.14	-.01	-.0049	-4.17	-.01	-.0082	-4.19	-.02	-.0124	-3.99	-.02	-.0081	-3.98	0	-.0009	-3.97	0	.0011	-3.96	.01	.0038
-2.07	0	-.0005	-2.08	-.01	-.0039	-2.09	-.01	-.0080	-2.08	-.01	-.0055	-1.91	0	-.0012	-1.91	0	0	-1.90	0	.0018
-1.04	0	.0025	-1.04	0	-.0013	-1.05	-.01	-.0052	-1.04	-.01	-.0038	-.87	0	-.0006	-.87	0	-.0006	-.87	0	.0015
-.52	0	.0030	-.52	0	-.0004	-.53	-.01	-.0040	-.52	-.01	-.0029	-.52	0	-.0009	-.52	0	-.0009	-.51	0	.0012
.50	.01	.0045	.50	0	.0020	.35	0	-.0024	.35	0	-.0016	.51	0	-.0009	.35	0	-.0012	.35	0	.0009
1.02	.01	.0051	1.03	.01	.0033	1.03	0	.0008	1.03	0	-.0007	1.03	0	-.0009	.86	0	-.0012	.86	0	.0003
2.05	.01	.0065	2.06	.01	.0049	2.07	0	.0021	2.06	0	.0018	1.90	0	-.0009	1.90	0	-.0019	1.89	0	0
4.12	.01	.0101	4.15	.01	.0090	4.16	.01	.0057	4.14	.01	.0039	3.98	0	-.0006	3.97	-.01	-.0030	3.95	0	-.0016
6.21	.02	.0132	6.25	.02	.0122	6.27	.02	.0097	6.04	.01	.0048	6.03	-.01	-.0022	6.02	-.02	-.0068	6.00	-.01	-.0054
8.29	.02	.0182	8.34	.03	.0183	8.37	.03	.0169	8.11	.01	.0030	8.09	-.01	-.0049	8.07	-.03	-.0123	8.05	-.03	-.0110
10.37	.03	.0253	10.44	.04	.0268	10.47	.04	.0235	10.17	0	.0018	10.15	-.02	-.0071	10.13	-.04	-.0178	10.10	-.04	-.0154
12.46	.04	.0334	12.54	.06	.0350	12.58	.06	.0321	12.24	0	.0012	12.22	-.02	-.0084	12.19	-.05	-.0203	12.16	-.04	-.0193
14.55	.06	.0465	14.64	.08	.0471	14.69	.08	.0416	14.30	0	-.0007	14.29	-.02	-.0099	14.26	-.05	-.0193	14.23	-.05	-.0240
16.65	.08	.0571	16.75	.09	.0569	16.65	.09	.0507	16.37	-.01	-.0023	16.36	-.03	-.0133	16.35	-.06	-.0236	16.34	-.07	-.0293
17.70	.08	-.0632	17.82	.11	.0634	17.70	.10	.0569	17.41	-.02	-.0087	17.40	-.04	-.0160	17.40	-.06	-.0255	17.39	-.07	-.0322

(b) Nominal $\Delta = -4^\circ$

-17.55	-4.11	-0.0853	-17.67	-4.13	-0.0784	-16.65	-4.08	-0.0457	-17.40	-3.94	0.0275	-17.39	-3.92	0.0343	-17.39	-3.91	0.0392	-17.39	-3.90	0.0436
-16.50	-4.11	-.0827	-16.61	-4.13	-.0780	-14.54	-4.10	-.0571	-16.36	-3.93	.0217	-16.35	-3.93	.0290	-16.34	-3.92	.0360	-16.34	-3.90	.0424
-14.41	-4.10	-.0773	-14.50	-4.12	-.0750	-12.42	-4.11	-.0614	-14.29	-3.97	.0150	-14.27	-3.95	.0197	-14.24	-3.94	.0271	-14.23	-3.91	.0376
-12.31	-4.09	-.0677	-12.39	-4.11	-.0669	-10.32	-4.10	-.0559	-12.22	-3.97	.0132	-12.20	-3.97	.0132	-12.17	-3.94	.0262	-12.15	-3.92	.0337
-10.23	-4.08	-.0613	-10.29	-4.10	-.0613	-8.21	-4.10	-.0540	-9.91	-3.97	.0132	-10.13	-3.97	.0117	-10.11	-3.94	.0250	-10.09	-3.93	.0304
-8.15	-4.07	-.0544	-8.19	-4.09	-.0548	-6.11	-4.09	-.0481	-8.09	-3.97	.0117	-8.07	-3.97	.0132	-8.05	-3.95	.0215	-8.04	-3.94	.0250
-6.07	-4.06	-.0480	-6.10	-4.08	-.0480	-4.02	-4.08	-.0423	-6.02	-3.98	.0104	-6.01	-3.97	.0112	-6.00	-3.96	.0162	-5.99	-3.95	.0197
-3.99	-4.06	-.0432	-4.01	-4.07	-.0432	-1.93	-4.07	-.0372	-3.96	-3.98	.0091	-3.95	-3.98	.0100	-3.95	-3.97	.0130	-3.94	-3.96	.0158
-1.91	-4.05	-.0384	-1.92	-4.06	-.0386	-.88	-4.06	-.0352	-1.89	-3.97	.0113	-1.89	-3.98	.0094	-1.89	-3.97	.0118	-1.89	-3.97	.0143
-.88	-4.05	-.0363	-.88	-4.06	-.0364	-.36	-4.06	-.0340	-.85	-3.97	.0126	-.85	-3.98	.0094	-.85	-3.97	.0115	-.85	-3.97	.0132
-.37	-4.05	-.0358	-.37	-4.06	-.0360	.51	-4.06	-.0329	-.34	-3.97	.0128	-.34	-3.98	.0091	-.34	-3.97	.0109	-.34	-3.97	.0128
.50	-4.05	-.0347	.51	-4.06	-.0347	1.03	-4.06	-.0321	.54	-3.97	.0138	.54	-3.98	.0091	.53	-3.98	.0103	.53	-3.97	.0116
1.02	-4.05	-.0341	1.02	-4.06	-.0343	2.07	-4.05	-.0293	1.05	-3.97	.0141	1.05	-3.98	.0088	1.05	-3.98	.0097	1.04	-3.97	.0110
2.05	-4.04	-.0325	2.06	-4.05	-.0322	4.17	-4.04	-.0238	2.09	-3.97	.0156	2.09	-3.98	.0091	2.08	-3.98	.0091	2.07	-3.98	.0098
4.12	-4.04	-.0282	4.15	-4.05	-.0274	6.28	-4.03	-.0188	4.17	-3.96	.0162	4.16	-3.98	.0085	4.15	-3.98	.0068	4.13	-3.98	.0072
6.20	-4.03	-.0256	6.25	-4.04	-.0244	8.38	-4.02	-.0117	6.24	-3.97	.0153	6.23	-3.99	.0047	6.21	-4.00	.0021	6.19	-3.99	.0024
8.29	-4.03	-.0213	8.35	-4.03	-.0176	10.49	-4.01	-.0055	8.30	-3.98	.0070	8.29	-4.00	-.0009	8.26	-4.01	-.0046	8.23	-4.00	-.0015
10.37	-4.02	-.0139	10.44	-4.02	-.0094	12.60	-3.99	.0034	10.37	-4.00	.0018	10.35	-4.01	-.0061	10.16	-4.02	-.0092	10.13	-4.01	-.0050
12.46	-4.01	-.0069	12.55	-4.00	.0008	14.71	-3.97	.0151	12.44	-4.01	-.0032	12.25	-4.02	-.0082	12.22	-4.03	-.0123	12.19	-4.02	-.0093
14.55	-3.99	-.0072	14.65	-3.98	.0136	16.82	-3.95	.0293	14.33	-4.01	-.0032	14.32	-4.03	-.0082	14.28	-4.03	-.0132	14.26	-4.04	-.0155
16.64	-3.98	-.0184	16.77	-3.96	.0243				16.41	-4.00	.0009	16.39	-4.03	-.0113	16.37	-4.05	-.0199	16.33	-4.05	-.0230
17.70	-3.97	-.0256	17.82	-3.95	.0313				17.45	-4.00	-.0007	17.43	-4.03	-.0134	17.43	-4.06	-.0242	17.58	-4.06	-.0276

TABLE III.- HINGE-MOMENT CHARACTERISTICS OF THE FREE-FLOATING FLAP - Continued

(c) Nominal $\Delta = 4^\circ$

M = 0.60			M = 0.80			M = 0.90			M = 1.30			M = 1.50			M = 1.70			M = 1.90		
α	Δ	C_h	α	Δ	C_h	α	Δ	C_h	α	Δ	C_h	α	Δ	C_h	α	Δ	C_h	α	Δ	C_h
-17.71	3.94	-0.0450	-17.83	3.91	-0.0511	-14.73	3.94	-0.0303	-17.47	3.98	-0.0104	-17.45	4.03	0.0113	-17.61	4.06	0.0234	-17.60	4.07	0.0295
-16.66	3.95	-.0378	-16.78	3.93	-.0423	-12.61	3.96	-.0193	-16.43	3.97	-.0118	-16.41	4.02	.0092	-16.39	4.04	.0181	-16.54	4.06	.0252
-14.56	3.96	-.0269	-14.67	3.95	-.0291	-10.50	3.98	-.0093	-14.36	3.98	-.0091	-14.33	4.01	.0038	-14.29	4.02	.0086	-14.44	4.04	.0159
-12.47	3.98	-.0137	-12.56	3.98	-.0145	-8.40	4.00	-.0016	-12.45	3.99	-.0049	-12.26	4.00	.0009	-12.23	4.02	.0068	-12.20	4.02	.0087
-10.39	3.99	-.0049	-10.46	3.99	-.0066	-6.30	4.01	.0076	-10.38	3.98	-.0091	-10.36	4.00	-.0019	-10.15	4.01	.0026	-10.30	4.01	.0051
-8.30	4.00	.0020	-8.37	4.00	.0012	-4.19	4.02	.0133	-8.32	3.97	-.0137	-8.29	3.99	-.0063	-8.27	4.00	-.0022	-8.24	4.00	.0009
-6.22	4.01	.0081	-6.27	4.01	.0088	-2.09	4.03	.0186	-6.25	3.95	-.0216	-6.23	3.97	-.0016	-6.21	3.98	-.0088	-6.19	3.99	-.0032
-4.14	4.01	.0112	-4.17	4.02	.0129	-1.05	4.04	.0220	-4.18	3.94	-.0255	-4.17	3.96	-.0154	-4.16	3.97	-.0141	-4.14	3.98	-.0086
-2.06	4.02	.0147	-2.08	4.03	.0175	-.53	4.04	.0232	-2.10	3.94	-.0255	-2.10	3.96	-.0157	-2.09	3.96	-.0152	-2.08	3.97	-.0118
-1.03	4.02	.0167	-1.04	4.03	.0200	.35	4.04	.0244	-1.07	3.95	-.0242	-1.06	3.96	-.0154	-1.06	3.96	-.0178	-1.05	3.97	-.0130
-.52	4.02	.0177	-.52	4.03	.0209	.87	4.05	.0251	-.55	3.95	-.0235	-.54	3.96	-.0154	-.54	3.96	-.0185	-.54	3.97	-.0137
.35	4.03	.0187	.35	4.04	.0221	1.91	4.05	.0266	.32	3.95	-.0222	.33	3.97	-.0150	.33	3.96	-.0191	.33	3.97	-.0149
.86	4.03	.0192	.87	4.04	.0225	4.00	4.06	.0315	.84	3.95	-.0212	.84	3.96	-.0154	.84	3.95	-.0194	.85	3.97	-.0147
1.90	4.03	.0202	1.90	4.04	.0241	6.09	4.07	.0369	1.88	3.95	-.0206	1.88	3.97	-.0147	1.88	3.95	-.0201	1.88	3.96	-.0165
3.97	4.03	.0248	3.99	4.05	.0284	8.19	4.08	.0433	3.95	3.96	-.0183	3.95	3.96	-.0160	3.94	3.95	-.0210	3.93	3.96	-.0184
6.05	4.04	.0283	6.08	4.05	.0321	10.30	4.08	.0460	6.01	3.96	-.0170	6.01	3.96	-.0166	5.99	3.95	-.0222	5.98	3.95	-.0207
8.13	4.05	.0338	8.17	4.06	.0387	12.41	4.09	.0490	8.08	3.97	-.0150	8.06	3.96	-.0178	8.05	3.94	-.0263	8.03	3.94	-.0245
10.21	4.05	.0405	10.27	4.08	.0467	14.52	4.09	.0506	10.14	3.96	-.0170	10.12	3.96	-.0163	10.10	3.93	-.0285	10.08	3.93	-.0292
12.30	4.06	.0470	12.37	4.09	.0521	16.63	4.08	.0441	12.21	3.96	-.0179	12.19	3.97	-.0132	12.16	3.93	-.0294	12.14	3.92	-.0327
14.39	4.08	.0571	14.48	4.10	.0600				14.27	3.96	-.0199	14.26	3.95	-.0204	14.23	3.93	-.0282	14.21	3.92	-.0356
16.49	4.09	.0682	16.59	4.11	.0675				16.35	3.94	-.0261	16.34	3.93	-.0295	16.32	3.92	-.0348	16.32	3.91	-.0407
17.54	4.09	.0672	17.65	4.11	.0688				17.39	3.93	-.0330	17.38	3.92	-.0345	17.38	3.91	-.0382	17.37	3.90	-.0423

(d) Nominal $\Delta = -8^\circ$

-17.54	-8.09	-0.0679	-17.66	-7.98	0.0118	-17.67	-8.06	-0.0321	-16.33	-7.91	0.0420	-17.36	-7.89	0.0497	-17.38	-7.89	0.0484	-17.36	-7.78	0.0479
-16.50	-8.09	-.0701	-16.60	-8.00	.0026	-16.63	-8.06	-.0350	-14.26	-7.92	.0370	-16.31	-7.90	.0430	-16.32	-7.90	.0437	-16.31	-7.79	.0451
-14.41	-8.10	-.0744	-14.49	-8.02	-.0119	-14.52	-8.08	-.0440	-12.19	-7.92	.0357	-14.24	-7.93	.0324	-14.23	-7.92	.0319	-14.20	-7.82	.0380
-12.32	-8.10	-.0728	-12.39	-8.05	-.0290	-12.41	-8.08	-.0468	-10.12	-7.93	.0329	-12.17	-7.95	.0233	-12.15	-7.93	.0280	-12.13	-7.84	.0285
-10.23	-8.09	-.0712	-10.29	-8.07	-.0409	-10.30	-8.09	-.0481	-8.06	-7.94	.0288	-10.11	-7.94	.0267	-10.09	-7.92	.0321	-10.07	-7.82	.0374
	-8.09	-.0679	-8.19	-8.08	-.0501	-8.20	-8.09	-.0497	-6.00	-7.94	.0282	-8.05	-7.94	.0267	-8.03	-7.92	.0324	-8.01	-7.83	.0353
-6.07	-8.09	-.0651	-6.10	-8.09	-.0569	-6.10	-8.10	-.0546	-3.93	-7.94	.0260	-5.99	-7.95	.0227	-5.98	-7.94	.0265	-5.97	-7.86	.0301
-4.00	-8.08	-.0606	-4.01	-8.10	-.0594	-4.01	-8.10	-.0578	-1.87	-7.94	.0263	-3.93	-7.95	.0206	-3.93	-7.95	.0230	-3.92	-7.88	.0264
-1.92	-8.07	-.0562	-1.93	-8.10	-.0615	-1.93	-8.10	-.0578	-.84	-7.94	.0263	-1.87	-7.96	.0194	-1.87	-7.95	.0212	-1.87	-7.89	.0233
-.89	-8.07	-.0541	-.88	-8.10	-.0620	-.89	-8.10	-.0566	-.32	-7.94	.0263	-.84	-7.96	.0185	-.84	-7.95	.0197	-.84	-7.90	.0215
-.38	-8.07	-.0535	-.37	-8.10	-.0611	-.37	-8.10	-.0566	.55	-7.94	.0266	-.32	-7.96	.0175	-.32	-7.96	.0186	-.32	-7.91	.0206
.49	-8.07	-.0541	.50	-8.10	-.0594	.51	-8.10	-.0570	1.07	-7.94	.0269	.55	-7.96	.0175	.55	-7.96	.0177	.54	-7.92	.0187
1.01	-8.07	-.0535	1.02	-8.10	-.0594	1.03	-8.10	-.0570	2.11	-7.94	.0276	1.07	-7.96	.0173	1.07	-7.96	.0168	1.06	-7.92	.0178
2.04	-8.07	-.0530	2.06	-8.10	-.0602	2.07	-8.10	-.0574	4.19	-7.94	.0276	2.11	-7.96	.0173	2.10	-7.96	.0154	2.08	-7.92	.0160
4.11	-8.07	-.0497	4.15	-8.11	-.0637	4.16	-8.10	-.0574	6.27	-7.94	.0260	4.18	-7.96	.0160	4.17	-7.97	.0118	4.15	-7.94	.0123
6.19	-8.06	-.0464	6.20	-8.11	-.0660	6.28	-8.09	-.0505	8.34	-7.97	.0150	6.26	-7.98	.0106	6.24	-7.99	.0065	6.21	-7.96	.0080
8.28	-8.06	-.0419	8.36	-8.11	-.0651	8.39	-8.08	-.0436	10.41	-7.99	.0056	8.31	-7.99	.0039	8.29	-8.00	.0009	8.26	-7.98	.0046
10.37	-8.05	-.0353	10.46	-8.10	-.0624	10.50	-8.07	-.0371	12.47	-8.01	-.0036	10.38	-8.01	-.0022	10.35	-8.01	-.0033	10.31	-7.98	.0031
12.45	-8.04	-.0270	12.55	-8.11	-.0664	12.60	-8.05	-.0265	14.54	-8.02	-.0101	12.44	-8.01	-.0031	12.41	-8.01	-.0047	12.37	-8.00	-.0003
14.54	-8.02	-.0133	14.66	-8.11	-.0646	14.71	-8.01	-.0049	16.61	-7.99	.0025	14.51	-8.01	-.0022	14.48	-8.01	-.0041	14.44	-8.02	-.0061
16.64	-8.00	-.0005	16.77	-8.09	-.0537	16.82	-7.96	.0230	17.65	-7.99	.0050	16.58	-8.01	-.0054	16.57	-8.03	-.0112	16.55	-8.06	-.0144
17.69	-7.99	.0069	17.82	-8.08	-.0501	17.88	-7.94	.0336				17.62	-8.02	-.0079	17.63	-8.04	-.0159	17.60	-8.08	-.0192

TABLE III.- HINGE-MOMENT CHARACTERISTICS OF THE FREE-FLOATING FLAP - Continued

(e) Nominal $\Delta = 8^\circ$

M = 0.60			M = 0.80			M = 0.90			M = 1.30			M = 1.50			M = 1.70			M = 1.90		
α	Δ	C_h	α	Δ	C_h	α	Δ	C_h	α	Δ	C_h	α	Δ	C_h	α	Δ	C_h	α	Δ	C_h
-17.70	8.00	0.0011	-17.84	8.10	0.0601	-17.90	7.95	-0.0269	-17.66	7.97	-0.0260	-17.63	8.02	0.0090	-17.63	8.10	0.0234	-17.62	8.04	0.0181
-16.65	8.01	.0071	-16.78	8.11	.0654		7.97	-.0182	-16.62	7.98	-.0224	-16.59	8.01	.0060	-16.57	8.08	.0171	-16.56	8.03	.0112
-14.56	8.02	.0173	-14.67	8.12	.0702	-14.73	8.01	.0068	-14.55	8.00	.0022	-14.52	8.00	.0003	-14.48	8.02	.0063	-14.46	8.00	.0013
-12.47	8.04	.0299	-12.57	8.11	.0689	-12.62	8.04	.0219	-12.48	8.00	-.0043	-12.45	8.00	-.0031	-12.41	8.00	-.0006	-12.38	8.00	.0006
-8.25	8.06	.0451	-10.47	8.11	.0663	-10.52	8.07	.0372	-10.41	7.98	-.0231	-10.39	8.00	-.0034	-10.35	7.98	-.0025	-10.32	7.99	-.0031
-2.06	8.08	.0581	-8.37	8.11	.0689	-8.41	8.08	.0435	-8.35	7.96	-.0398	-8.32	7.98	-.0087	-8.29	7.98	-.0047	-8.27	7.99	-.0056
-1.02	8.08	.0597	-6.27	8.11	.0690	-6.30	8.09	.0511	-6.28	7.94	-.0622	-6.26	7.97	-.0149	-6.23	7.96	-.0074	-6.22	7.97	-.0115
-.51	8.08	.0603	-4.16	8.11	.0666	-4.19	8.10	.0550	-4.20	7.93	-.0745	-4.19	7.95	-.0196	-4.17	7.94	-.0132	-4.16	7.96	-.0168
.36	8.08	.0603	-2.08	8.10	.0625	-2.09	8.10	.0570	-2.12	7.92	-.0759	-2.12	7.95	-.0215	-2.11	7.92	-.0167	-2.10	7.95	-.0203
.87	8.08	.0603	-1.03	8.10	.0619	-1.05	8.11	.0590	-1.09	7.93	-.0738	-1.08	7.95	-.0208	-1.07	7.92	-.0182	-1.06	7.95	-.0218
1.91	8.08	.0608	-.52	8.11	.0637	-.52	8.11	.0594	-.57	7.93	-.0731	-.56	7.95	-.0215	-.56	7.92	-.0192	-.55	7.95	-.0227
3.98	8.09	.0611	.36	8.11	.0645	.35	8.11	.0590	.30	7.93	-.0723	.31	7.95	-.0215	.31	7.90	-.0211	.32	7.94	-.0245
6.05	8.09	.0690	.87	8.11	.0644	.87	8.11	.0586	.82	7.93	-.0709	.83	7.95	-.0227	.83	7.90	-.0220	.83	7.94	-.0258
8.13	8.10	.0739	1.91	8.10	.0631	1.91	8.11	.0586	1.86	7.93	-.0702	1.86	7.95	-.0233	1.86	7.88	-.0242	1.86	7.94	-.0273
10.21	8.10	.0776	3.99	8.10	.0602	3.99	8.11	.0606	3.92	7.93	-.0702	3.92	7.94	-.0252	3.92	7.88	-.0270	3.91	7.93	-.0292
12.30	8.11	.0792	6.07	8.09	.0570	6.08	8.11	.0602	5.98	7.93	-.0723	5.98	7.94	-.0264	5.97	7.86	-.0296	5.96	7.93	-.0317
14.39	8.11	.0814	8.17	8.08	.0477	8.18	8.10	.0539	8.05	7.93	-.0680	8.04	7.93	-.0296	8.02	7.84	-.0336	8.01	7.92	-.0361
16.49	8.11	.0819	10.27	8.07	.0397	10.29	8.08	.0460	10.11	7.92	-.0774	10.10	7.93	-.0301	10.08	7.84	-.0352	10.06	7.92	-.0345
17.54	8.11	.0798	12.37	8.05	.0280	12.40	8.09	.0465	12.18	7.92	-.0839	12.16	7.94	-.0258	12.13	7.84	-.0330	12.12	7.93	-.0289
			14.48	8.02	.0135	14.63	8.09	.0511	14.24	7.92	-.0846	14.23	7.93	-.0311	14.20	7.84	-.0333	14.16	7.93	-.0298
			16.59	8.00	-.0004	16.52	8.08	.0462	16.31	7.90	-.0969	16.31	7.90	-.0429	16.29	7.82	-.0409	16.30	7.91	-.0398
			17.64	7.99	-.0070				17.35	7.90	-.1020	17.35	7.89	-.0489	17.35	7.80	-.0443	17.35	7.89	-.0460

(f) Nominal $\Delta = -12^\circ$

-17.55	-12.04	-0.0300	-17.65	-12.02	-0.0127	-16.63	-12.02	-0.0096	-17.35	-11.84	0.0720	-17.34	-11.85	0.0657	-17.36	-11.85	0.0633	-17.35	-11.87	0.0589
-16.50	-12.05	-.0348	-16.60	-12.03	-.0170	-14.51	-12.03	-.0174	-16.31	-11.84	.0720	-16.30	-11.86	.0614	-16.30	-11.86	.0585	-16.30	-11.87	.0567
-14.40	-12.05	-.0407	-14.48	-12.05	-.0271	-12.40	-12.03	-.0182	-14.24	-11.86	.0640	-14.23	-11.88	.0496	-14.20	-11.90	.0429	-14.19	-11.89	.0474
-12.32	-12.06	-.0454	-12.38	-12.05	-.0309	-10.30	-12.04	-.0201	-12.16	-11.87	.0563	-12.15	-11.90	.0423	-12.13	-11.90	.0429	-12.11	-11.90	.0439
-10.23	-12.06	-.0523	-10.28	-12.05	-.0309	-8.19	-12.06	-.0333	-10.10	-11.89	.0509	-10.09	-11.89	.0469	-10.07	-11.89	.0466	-10.05	-11.88	.0524
-8.15	-12.08	-.0575	-8.18	-12.07	-.0416	-6.10	-12.08	-.0418	-8.03	-11.90	.0461	-8.02	-11.90	.0428	-8.01	-11.90	.0447	-8.00	-11.89	.0474
-6.07	-12.08	-.0602	-6.09	-12.08	-.0470	-4.00	-12.09	-.0472	-5.97	-11.90	.0461	-5.97	-11.92	.0364	-5.96	-11.91	.0384	-5.95	-11.91	.0414
-4.00	-12.08	-.0612	-4.00	-12.08	-.0492	-1.92	-12.10	-.0561	-3.91	-11.91	.0406	-3.91	-11.92	.0334	-3.90	-11.92	.0347	-3.90	-11.91	.0377
-1.93	-12.08	-.0607	-1.93	-12.09	-.0521	-.89	-12.11	-.0584	-1.85	-11.91	.0403	-1.85	-11.93	.0306	-1.85	-11.93	.0304	-1.85	-11.93	.0324
-.90	-12.08	-.0623	-.89	-12.09	-.0543	-.37	-12.11	-.0586	-.82	-11.91	.0396	-.82	-11.93	.0291	-.82	-11.94	.0277	-.83	-11.93	.0286
-.38	-12.08	-.0628	-.37	-12.09	-.0559	.51	-12.11	-.0615	-.30	-11.91	.0394	-.30	-11.94	.0273	-.31	-11.94	.0255	-.31	-11.94	.0268
.49	-12.09	-.0654	.50	-12.10	-.0602	1.03	-12.11	-.0627	.57	-11.91	.0394	.57	-11.94	.0266	.56	-11.94	.0240	.55	-11.94	.0243
1.00	-12.09	-.0670	1.02	-12.10	-.0619	2.07	-12.12	-.0631	1.09	-11.91	.0390	1.08	-11.94	.0260	1.08	-11.95	.0231	1.07	-11.95	.0231
2.03	-12.09	-.0675	2.05	-12.11	-.0640	4.16	-12.11	-.0627	2.13	-11.91	.0390	2.12	-11.94	.0266	2.11	-11.95	.0210	2.10	-11.95	.0206
4.10	-12.09	-.0681	4.14	-12.11	-.0666	6.28	-12.11	-.0584	4.20	-11.91	.0384	4.20	-11.95	.0236	4.18	-11.96	.0161	4.16	-11.96	.0165
6.18	-12.09	-.0692	6.24	-12.12	-.0704	8.40	-12.10	-.0530	6.29	-11.92	.0362	6.28	-11.96	.0165	6.26	-11.97	.0109	6.23	-11.97	.0125
8.27	-12.09	-.0675	8.36	-12.12	-.0738	10.51	-12.08	-.0449	8.37	-11.95	.0234	8.34	-11.98	.0089	8.31	-11.99	.0052	8.28	-11.98	.0090
10.37	-12.09	-.0643	10.46	-12.12	-.0721	12.63	-12.05	-.0279	10.44	-11.97	.0138	10.41	-12.00	.0012	10.37	-12.00	.0021	10.33	-11.97	.0112
12.45	-12.08	-.0575	12.56	-12.10	-.0615	14.74	-12.00	.0015	12.50	-11.99	.0038	12.48	-11.99	.0031	12.44	-11.99	.0027	12.39	-11.98	.0100
14.54	-12.06	-.0438	14.67	-12.07	-.0449	16.84	-11.94	.0328	14.58	-12.01	-.0060	14.55	-11.99	.0040	14.50	-11.98	.0070	14.47	-11.99	.0065
16.64	-12.04	-.0290	16.78	-12.04	-.0267				16.65	-12.00	-.0007	16.62	-12.00	.0021	16.59	-12.00	0	16.57	-12.00	-.0012
17.69	-12.03	-.0232	17.83	-12.03	-.0178				17.69	-11.97	.0121	17.66	-12.00	-.0003	17.65	-12.01	-.0045	17.62	-12.02	-.0068

TABLE III.- HINGE-MOMENT CHARACTERISTICS OF THE FREE-FLOATING FLAP - Continued

(g) Nominal $\Delta = 12^0$

M = 0.60			M = 0.80			M = 0.90			M = 1.30			M = 1.50			M = 1.70			M = 1.90		
α	Δ	C_h	α	Δ	C_h	α	Δ	C_h	α	Δ	C_h	α	Δ	C_h	α	Δ	C_h	α	Δ	C_h
-17.70	12.01	0.0073	-17.82	12.01	0.0072	-14.75	11.98	-0.0095	-17.71	11.93	-0.0258	-17.67	11.98	-0.0105	-17.66	12.00	-0.0014	-17.64	12.02	0.0079
-16.65	12.02	.0113	-16.78	12.00	.0013	-12.63	12.04	.0231	-16.67	11.96	-.0191	-16.63	11.97	-.0126	-16.61	11.98	-.0073	-16.59	12.00	.0016
-14.56	12.04	.0270	-14.67	12.05	.0302	-10.53	12.07	.0371	-14.60	11.97	-.0143	-14.56	11.96	-.0158	-14.51	11.96	-.0158	-14.48	11.98	-.0078
-12.46	12.05	.0399	-12.57	12.08	.0463	-8.42	12.08	.0445	-12.52	11.95	-.0237	-12.49	11.95	-.0211	-12.44	11.96	-.0153	-12.40	11.97	-.0133
-10.38	12.06	.0472	-10.47	12.09	.0564	-6.30	12.09	.0499	-10.45	11.93	-.0325	-10.42	11.96	-.0193	-10.38	11.96	-.0158	-10.34	11.97	-.0142
-8.30	12.07	.0512	-8.37	12.10	.0608	-4.19	12.10	.0532	-8.39	11.91	-.0398	-8.36	11.94	-.0249	-8.32	11.96	-.0179	-8.19	11.97	-.0133
-6.21	12.07	.0528	-6.26	12.10	.0597	-2.09	12.10	.0544	-6.32	11.89	-.0495	-6.29	11.93	-.0319	-6.27	11.94	-.0237	-6.24	11.96	-.0156
-4.12	12.07	.0528	-4.16	12.09	.0568	-1.04	12.10	.0561	-4.23	11.88	-.0547	-4.21	11.91	-.0366	-4.19	11.93	-.0287	-4.17	11.95	-.0205
-2.05	12.07	.0528	-2.07	12.09	.0519	-.52	12.10	.0565	-2.16	11.87	-.0561	-2.13	11.91	-.0376	-2.12	11.92	-.0334	-2.11	11.94	-.0241
-1.02	12.07	.0535	-1.04	12.09	.0519	.35	12.10	.0548	-1.10	11.87	-.0567	-1.10	11.91	-.0376	-1.09	11.92	-.0349	-1.08	11.94	-.0259
-.50	12.07	.0523	-.52	12.09	.0511	.87	12.10	.0536	-.58	11.87	-.0565	-.58	11.91	-.0398	-.57	11.92	-.0358	-.56	11.94	-.0271
.36	12.07	.0500	.35	12.08	.0479	1.91	12.09	.0520	.29	11.87	-.0567	.29	11.91	-.0376	.30	11.91	-.0372	.27	11.93	-.0295
.88	12.06	.0478	.87	12.08	.0461	3.98	12.08	.0485	.81	11.87	-.0571	.81	11.90	-.0410	.81	11.91	-.0387	.82	11.93	-.0307
1.91	12.06	.0466	1.91	12.07	.0434	6.08	12.07	.0367	1.84	11.87	-.0574	1.84	11.90	-.0433	1.84	11.90	-.0414	1.85	11.92	-.0343
3.98	12.06	.0444	3.98	12.07	.0397	8.17	12.05	.0293	3.90	11.87	-.0586	3.90	11.89	-.0474	3.90	11.89	-.0460	3.90	11.91	-.0406
6.05	12.06	.0461	6.07	12.06	.0375	10.28	12.02	.0120	5.96	11.86	-.0613	5.96	11.88	-.0492	5.95	11.88	-.0504	5.94	11.90	-.0454
8.12	12.06	.0450	8.16	12.06	.0334	12.38	12.01	.0037	8.02	11.86	-.0604	8.02	11.87	-.0542	8.00	11.87	-.0548	7.99	11.89	-.0490
10.21	12.05	.0388	10.26	12.03	.0203	14.49	12.01	.0066	10.09	11.85	-.0647	10.08	11.86	-.0594	10.06	11.87	-.0546	10.04	11.88	
12.29	12.04	.0304	12.36	12.03	.0163				12.16	11.85	-.0671	12.14	11.86	-.0606	12.12	11.87	-.0537	12.10	11.89	-.0475
14.38	12.03	.0259	14.46	12.03	.0167				14.23	11.84	-.0707	14.22	11.86	-.0580	14.19	11.89	-.0478	14.17	11.89	-.0490
16.48	12.03	.0236	16.57	12.02	.0104				16.30	11.82	-.0805	16.29	11.84	-.0685	16.28	11.86	-.0613	16.28	11.87	-.0581
17.53	12.02	.0185	17.63	12.01	.0054				17.34	11.81	-.0838	17.34	11.83	-.0732	17.34	11.84	-.0683	17.34	11.86	-.0605

(h) Nominal $\Delta = -16^0$

-17.54	-16.01	-0.0064	-17.65	-15.98	0.0097	-16.62	-15.97	0.0172	-17.33	-15.78	0.0978	-17.32	-15.82	0.0769	-17.34	-15.83	0.0727	-17.34	-15.85	0.0662
-16.49	-16.01	-.0090	-16.59	-15.99	.0057	-14.51	-15.98	.0112	-16.29	-15.79	.0964	-16.28	-15.83	.0741	-16.29	-15.84	.0700	-16.29	-15.85	.0659
-14.40	-16.02	-.0148	-14.48	-16.00	-.0012	-12.39	-15.98	.0108	-14.22	-15.81	.0882	-14.20	-15.85	.0661	-14.19	-15.86	.0585	-14.18	-15.86	.0609
-12.31	-16.03	-.0190	-12.37	-16.01	-.0059	-10.29	-15.99	.0044	-12.14	-15.82	.0799	-12.13	-15.85	.0648	-12.12	-15.85	.0625	-12.10	-15.87	.0583
-10.22	-16.03	-.0242	-10.27	-16.02	-.0106	-8.19	-16.01	-.0050	-10.08	-15.84	.0712	-10.06	-15.84	.0683	-10.06	-15.86	.0594	-10.04	-15.86	.0618
-8.14	-16.04	-.0316	-8.18	-16.03	-.0169	-6.09	-16.03	-.0154	-8.01	-15.86	.0643	-8.01	-15.85	.0636	-8.00	-15.86	.0581	-7.98	-15.87	.0548
-6.07	-16.05	-.0379	-6.09	-16.04	-.0246	-4.00	-16.04	-.0205	-5.95	-15.87	.0613	-5.95	-15.88	.0540	-5.94	-15.88	.0504	-5.93	-15.89	.0488
-3.99	-16.05	-.0395	-4.00	-16.05	-.0288	-1.92	-16.05	-.0286	-3.89	-15.88	.0553	-3.89	-15.89	.0486	-3.89	-15.90	.0445	-3.89	-15.90	.0421
-1.93	-16.05	-.0406	-1.93	-16.06	-.0330	-.88	-16.06	-.0321	-1.83	-15.88	.0540	-1.83	-15.90	.0426	-1.83	-15.91	.0379	-1.84	-15.92	.0339
-.90	-16.06	-.0427	-.89	-16.06	-.0356	-.37	-16.06	-.0340	-.80	-15.88	.0534	-.80	-15.91	.0410	-.81	-15.92	.0342	-.82	-15.93	.0291
-.38	-16.06	-.0437	-.37	-16.06	-.0364	.51	-16.07	-.0367	-.28	-15.88	.0530	-.29	-15.92	.0369	-.29	-15.92	.0323	-.30	-15.94	.0276
.49	-16.06	-.0453	.50	-16.06	-.0385	1.03	-16.07	-.0375	.58	-15.88	.0527	.58	-15.92	.0369	.58	-15.93	.0304	.56	-15.94	.0241
1.00	-16.06	-.0469	1.02	-16.07	-.0398	2.07	-16.07	-.0387	1.10	-15.88	.0527	1.10	-15.92	.0366	1.09	-15.93	.0292	1.08	-15.95	.0225
2.03	-16.06	-.0485	2.05	-16.07	-.0406	4.17	-16.08	-.0433	2.14	-15.88	.0527	2.13	-15.92	.0369	2.13	-15.94	.0273	2.11	-15.95	.0197
4.10	-16.07	-.0495	4.14	-16.07	-.0427	6.28	-16.11	-.0626	4.22	-15.88	.0524	4.21	-15.93	.0328	4.20	-15.95	.0202	4.17	-15.97	.0139
6.18	-16.07	-.0554	6.25	-16.08	-.0478	8.40	-16.11	-.0584	6.31	-15.89	.0497	6.29	-15.94	.0245	6.27	-15.96	.0143	6.24	-15.98	.0095
8.27	-16.08	-.0601	8.36	-16.08	-.0508	10.51	-16.10	-.0541	8.39	-15.92	.0371	8.36	-15.96	.0163	8.34	-15.98	.0075	8.30	-15.98	.0083
10.36	-16.09	-.0643	10.45	-16.09	-.0534	12.62	-16.08	-.0464	10.45	-15.94	.0278	10.43	-15.99	.0060	10.40	-15.99	.0062	10.36	-15.98	.0105
12.45	-16.09	-.0669	12.56	-16.09	-.0542	14.74	-16.04	-.0220	12.53	-15.96	.0179	12.50	-15.98	.0102	12.47	-15.98	.0090	12.41	-15.97	.0117
14.54	-16.08	-.0616	14.67	-16.10	-.0572	16.85	-15.96	-.0197	14.59	-15.99	.0070	14.56	-15.97	.0143	14.53	-15.98	.0090	14.49	-15.98	.0083
16.63	-16.07	-.0558	16.77	-16.09	-.0509				16.67	-16.00	-.0003	16.64	-15.97	.0051	16.62	-15.99	.0037	16.60	-16.00	.0003
17.68	-16.07	-.0522	17.83	-16.08	-.0466				17.71	-15.99	.0050	17.68	-15.99	.0035	17.68	-16.00	.0009	17.65	-16.01	-.0031

TABLE III.- HINGE-MOMENT CHARACTERISTICS OF THE FREE-FLOATING FLAP - Continued

(i) Nominal $\Delta = 16^\circ$

M = 0.60			M = 0.80			M = 0.90			M = 1.30			M = 1.50			M = 1.70			M = 1.90		
α	Δ	C_h	α	Δ	C_h	α	Δ	C_h	α	Δ	C_h	α	Δ	C_h	α	Δ	C_h	α	Δ	C_h
-17.70	16.07	0.0495	-17.84	16.08	0.0462	-14.76	16.04	0.0242	-17.74	15.92	-0.0211	-17.72	15.97	-0.0136	-17.71	15.98	-0.0092	-17.67	16.00	-0.0023
-16.64	16.07	.0527	-16.79	16.09	.0522	-12.64	16.06	.0328	-16.70	15.94	-.0162	-16.67	15.96	-.0147	-16.65	15.97	-.0139	-16.62	15.98	-.0077
-14.55	16.07	.0548	-14.69	16.08	.0470	-10.53	16.08	.0453	-14.62	15.91	-.0226	-14.60	15.94	-.0234	-14.54	15.95	-.0195	-14.51	15.96	-.0169
-12.46	16.07	.0554	-12.58	16.07	.0419	-8.42	16.09	.0515	-12.55	15.89	-.0296	-12.53	15.95	-.0209	-12.48	15.95	-.0212	-12.43	15.95	-.0218
-10.38	16.07	.0559	-10.48	16.07	.0436	-6.30	16.08	.0414	-10.48	15.86	-.0376	-10.46	15.95	-.0228	-10.41	15.96	-.0181	-10.37	15.95	-.0206
-8.29	16.07	.0533	-8.38	16.07	.0428	-4.19	16.07	.0359	-8.41	15.83	-.0450	-8.39	15.93	-.0278	-8.35	15.96	-.0176	-8.31	15.96	-.0192
-6.20	16.07	.0490	-6.27	16.07	.0411	-2.09	16.06	.0332	-6.33	15.80	-.0531	-6.32	15.91	-.0359	-6.29	15.94	-.0245	-6.25	15.95	-.0201
-4.12	16.06	.0453	-4.16	16.06	.0381	-1.05	16.06	.0332	-4.24	15.77	-.0588	-4.23	15.90	-.0401	-4.21	15.93	-.0301	-4.18	15.94	-.0249
-2.05	16.06	.0431	-2.08	16.06	.0360	-.53	16.06	.0328	-2.16	15.77	-.0594	-2.15	15.89	-.0439	-2.14	15.91	-.0357	-2.12	15.93	-.0298
-1.02	16.06	.0431	-1.04	16.06	.0364	.35	16.05	.0301	-1.12	15.77	-.0596	-1.11	15.91	-.0434	-1.10	15.91	-.0376	-1.09	15.92	-.0324
-.50	16.06	.0431	-.52	16.06	.0364	.87	16.05	.0289	-.60	15.77	-.0590	-.59	15.90	-.0437	-.58	15.91	-.0380	-.57	15.92	-.0338
.37	16.05	.0405	.36	16.06	.0346	1.90	16.05	.0262	.27	15.77	-.0594	.27	15.90	-.0431	.28	15.90	-.0399	.29	15.92	-.0361
.85	16.05	.0399	.87	16.06	.0338	3.98	16.04	.0195	.78	15.77	-.0594	.79	15.89	-.0451	.80	15.90	-.0416	.81	15.91	-.0369
1.91	16.05	.0383	1.91	16.05	.0317	6.07	16.02	.0125	1.81	15.77	-.0594	1.82	15.88	-.0481	1.82	15.89	-.0447	1.83	15.91	-.0407
3.98	16.05	.0340	3.98	16.04	.0270	8.16	16.00	.0023	3.88	15.76	-.0614	3.88	15.87	-.0540	3.88	15.88	-.0513	3.88	15.88	-.0493
6.05	16.05	.0346	6.06	16.04	.0231	10.27	15.98	-.0103	5.94	15.75	-.0658	5.94	15.86	-.0570	5.93	15.86	-.0583	5.93	15.87	-.0561
8.12	16.04	.0298	8.15	16.03	.0167	12.37	15.97	-.0173	8.00	15.74	-.0683	8.00	15.84	-.0645	7.99	15.85	-.0644	7.98	15.86	-.0613
10.20	16.03	.0213	10.25	16.01	.0077	14.48	15.97	-.0188	10.07	15.71	-.0765	10.07	15.82	-.0729	10.05	15.84	-.0671	10.03	15.85	-.0630
12.29	16.02	.0165	12.35	16.00	.0026				12.14	15.68	-.0842	12.13	15.82	-.0737	12.11	15.83	-.0718	12.09	15.83	-.0710
14.38	16.02	.0133	14.45	16.00	.0009				14.21	15.66	-.0875	14.21	15.83	-.0726	14.18	15.84	-.0661	14.16	15.84	-.0696
16.48	16.01	.0096	16.56	15.99	-.0048				16.29	15.64	-.0921	16.28	15.82	-.0759	16.28	15.83	-.0722	16.27	15.83	-.0719
17.52	16.01	.0069	17.62	15.98	-.0097				17.33	15.62	-.0989	17.33	15.81	-.0807	17.33	15.82	-.0770	17.33	15.83	-.0716

(j) Nominal $\Delta = -20^\circ$

-17.54	-19.98	0.0168	-16.58	-19.95	0.0292	-14.50	-19.93	0.0405	-16.29	-19.75	0.112	-17.38	-19.80	0.0881	-17.33	-19.80	0.0877	-17.33	-19.79	0.0890
-16.49	-19.98	.0151	-14.47	-19.96	.0242	-12.38	-19.93	.0373	-14.21	-19.79	.095	-16.28	-19.76	.1026	-16.27	-19.77	.0999	-16.28	-19.79	.0926
-14.40	-19.99	.0095	-12.37	-19.97	.0175	-10.28	-19.94	.0340	-12.13	-19.80	.091	-14.20	-19.79	.0897	-14.18	-19.80	.0874	-14.17	-19.79	.0906
-12.31	-20.00	.0005	-10.27	-19.98	.0144	-8.18	-19.95	.0254	-10.06	-19.80	.089	-12.12	-19.78	.0945	-12.10	-19.79	.0905	-12.09	-19.79	.0909
-10.22	-20.00	-.0032	-8.17	-19.98	.0094	-6.08	-19.97	.0176	-8.00	-19.83	.077	-10.06	-19.77	.0974	-10.05	-19.78	.0931	-10.03	-19.81	.0825
-8.14	-20.01	-.0064	-1.92	-20.01	-.0063	-3.99	-19.97	.0139	-5.94	-19.85	.066	-8.00	-19.79	.0923	-7.99	-19.80	.0854	-7.97	-19.82	.0796
-6.07	-20.01	-.0105	-.89	-20.01	-.0085	-1.92	-19.99	.0053	-3.88	-19.87	.060	-5.94	-19.83	.0733	-5.93	-19.82	.0755	-5.92	-19.84	.0705
-3.99	-20.02	-.0137	-.37	-20.02	-.0093	-.88	-20.00	.0008	-1.81	-19.87	.059	-3.88	-19.84	.0675	-3.87	-19.85	.0639	-3.87	-19.87	.0573
-1.93	-20.02	-.0163	.50	-20.02	-.0101	-.36	-20.00	-.0011	-.78	-19.87	.059	-1.81	-19.85	.0636	-1.82	-19.87	.0568	-1.82	-19.89	.0485
-.90	-20.02	-.0201	1.02	-20.02	-.0123	.51	-20.01	-.0031	-.27	-19.87	.059	-.79	-19.86	.0614	-.79	-19.88	.0527	-.80	-19.90	.0437
-.38	-20.03	-.0205	2.05	-20.02	-.0140	1.03	-20.01	-.0062	.60	-19.87	.058	-.27	-19.86	.0585	-.28	-19.88	.0498	-.29	-19.90	.0421
.48	-20.03	-.0201	4.14	-20.03	-.0165	2.07	-20.02	-.0100	1.11	-19.87	.059	.59	-19.87	.0575	.58	-19.89	.0482	.57	-19.91	.0388
1.00	-20.03	-.0221	6.24	-20.03	-.0182	4.16	-20.02	-.0124	2.15	-19.87	.058	1.11	-19.87	.0575	1.10	-19.89	.0475	1.09	-19.91	.0369
2.03	-20.03	-.0248	8.35	-20.03	-.0190	6.27	-20.03	-.0150	4.23	-19.86	.062	2.14	-19.87	.0569	2.13	-19.90	.0446	2.12	-19.92	.0340
4.10	-20.03	-.0259	10.45	-20.03	-.0182	8.39	-20.03	-.0154	6.32	-19.86	.061	4.22	-19.88	.0508	4.20	-19.92	.0360	4.18	-19.94	.0259
6.18	-20.03	-.0269	12.56	-20.03	-.0169	10.50	-20.03	-.0158	8.41	-19.89	.050	6.30	-19.90	.0412	6.28	-19.93	.0282	6.25	-19.95	.0197
8.27	-20.04	-.0274	14.66	-20.02	-.0140	12.62	-20.03	-.0158	10.48	-19.91	.041	8.38	-19.93	.0315	8.35	-19.95	.0202	8.32	-19.96	.0178
10.36	-20.04	-.0285	16.77	-20.03	-.0152	14.73	-20.01	-.0081	12.55	-19.93	.032	10.45	-19.95	.0209	10.42	-19.96	.0154	10.37	-19.96	.0194
12.45	-20.04	-.0285	17.83	-20.03	-.0182	16.84	-20.01	-.0081	14.62	-19.95	.023	12.52	-19.96	.0173	12.48	-19.98	.0070	12.43	-19.96	.0188
14.54	-20.04	-.0280				17.88	-20.00	-.0015	16.70	-19.97	.014	14.59	-19.95	.0203	14.54	-19.95	.0222	14.51	-19.96	.0191
16.63	-20.04	-.0327							17.74	-19.97	.012	16.67	-19.95	.0225	16.63	-19.96	.0161	16.61	-19.97	.0139
17.68	-20.05	-.0374										17.71	-19.95	.0228	17.70	-19.97	.0141	17.67	-19.98	.0094

TABLE III.- HINGE-MOMENT CHARACTERISTICS OF THE FREE-FLOATING FLAP - Concluded

(k) Nominal $\Delta = 20^0$

M = 0.60			M = 0.80			M = 0.90			M = 1.30			M = 1.50			M = 1.70			M = 1.90		
α	Δ	C_h	α	Δ	C_h	α	Δ	C_h	α	Δ	C_h	α	Δ	C_h	α	Δ	C_h	α	Δ	C_h
-17.69	20.06	0.0412	-17.83	20.05	0.0271	-16.85	20.03	0.0143	-17.76	19.94	-0.0271	-17.74	19.94	-0.0268	-17.73	19.96	-0.0181	-17.71	19.97	-0.0133
-16.64	20.05	.0369	-16.79	20.04	.0246	-14.75	20.01	.0077	-16.72	19.93	-.0892	-16.69	19.93	-.0315	-16.67	19.95	-.0219	-16.65	19.96	-.0188
-14.55	20.04	.0296	-14.68	20.03	.0187	-12.63	20.02	.0093	-14.64	19.92	-.0353	-14.61	19.93	-.0280	-14.56	19.93	-.0300	-14.55	19.93	-.0286
-12.47	20.04	.0264	-12.58	20.03	.0157	-10.52	20.02	.0100	-12.57	19.91	-.0410	-12.54	19.94	-.0265	-12.49	19.96	-.0176	-12.45	19.93	-.0303
-10.38	20.03	.0259	-10.47	20.03	.0137	-8.42	20.02	.0104		19.89	-.0484	-10.46	19.92	-.0342	-10.43	19.94	-.0248	-10.39	19.93	-.0309
-8.26	20.04	.0264	-8.37	20.03	.0174	-6.30	20.02	.0096	-8.42	19.88	-.0553	-8.39	19.90	-.0418	-8.37	19.94	-.0271	-8.34	19.93	-.0297
-6.20	20.03	.0248	-6.27	20.03	.0152	-4.19	20.01	.0077	-6.34	19.86	-.0633	-6.32	19.89	-.0491	-6.29	19.92	-.0355	-6.26	19.93	-.0309
-4.12	20.03	.0242	-4.16	20.02	.0168	-2.09	20.01	.0047	-4.25	19.85	-.0678	-4.23	19.87	-.0549	-4.21	19.90	-.0424	-4.20	19.92	-.0355
-2.04	20.03	.0216	-2.07	20.02	.0119	-1.05	20.00	.0019	-1.93	19.85	-.0645	-2.16	19.86	-.0607	-2.14	19.88	-.0505	-2.13	19.90	-.0427
-1.01	20.03	.0206	-1.04	20.02	.0098	-.53	20.00	-.0007	-.89	19.86	-.0638	-1.12	19.86	-.0607	-1.11	19.88	-.0525	-1.16	19.89	-.0456
-.50	20.02	.0185	-.52	20.01	.0085	.35	19.99	-.0060	-.37	19.86	-.0638	-.60	19.86	-.0607	-.59	19.88	-.0528	-.59	19.89	-.0459
.37	20.02	.0142	.36	20.01	.0047	.87	19.99	-.0064	.49	19.86	-.0638	.26	19.86	-.0593	.78	19.87	-.0545	.28	19.88	-.0491
.88	20.02	.0142	.87	20.01	.0047	1.90	19.98	-.0109	.77	19.86	-.0636	.77	19.86	-.0613	1.81	19.87	-.0565	.79	19.88	-.0505
1.91	20.02	.0132	1.91	20.00	.0021	3.98	19.97	-.0188	1.80	19.86	-.0627	1.81	19.85	-.0654	3.87	19.86	-.0605	1.82	19.87	-.0546
3.98	20.01	.0105	3.98	20.00	-.0017	6.06	19.96	-.0233	3.86	19.85	-.0645	4.01	19.84	-.0683	4.77	19.84	-.0684	3.87	19.85	-.0644
6.05	20.01	.0095	6.06	19.99	-.0074	8.16	19.95	-.0297	5.93	19.85	-.0669	5.93	19.83	-.0733	5.93	19.81	-.0781	5.92	19.82	-.0742
8.12	20.01	.0053	8.15	19.98	-.0120	10.26	19.93	-.0387	7.99	19.83	-.0733	7.99	19.79	-.0876	7.99	19.79	-.0868	7.97	19.80	-.0843
10.20	20.00	.0011	10.25	19.97	-.0189	12.36	19.92	-.0421	10.05	19.81	-.0855	10.06	19.77	-.0992	10.05	19.77	-.0955	10.02	19.80	-.0834
12.29	20.00	-.0035	12.35	19.96	-.0218	14.48	19.93	-.0387	12.13	19.80	-.0888	12.12	19.77	-.0978	12.11	19.77	-.0969	12.08	19.77	-.0982
14.39	19.99	-.0066	14.46	19.96	-.0218				14.20	19.80	-.0894	14.19	19.79	-.0884	14.17	19.79	-.0905	14.16	19.76	-.1005
16.49	19.98	-.0113	16.57	19.95	-.0276				16.28	19.77	-.1031	16.27	19.79	-.0899	16.27	19.77	-.0974	16.27	19.77	-.0979
17.53	19.98	-.0128	17.63	19.95	-.0292				17.32	19.75	-.1122	17.31	19.79	-.0913	17.33	19.80	-.0845	17.33	19.78	-.0941

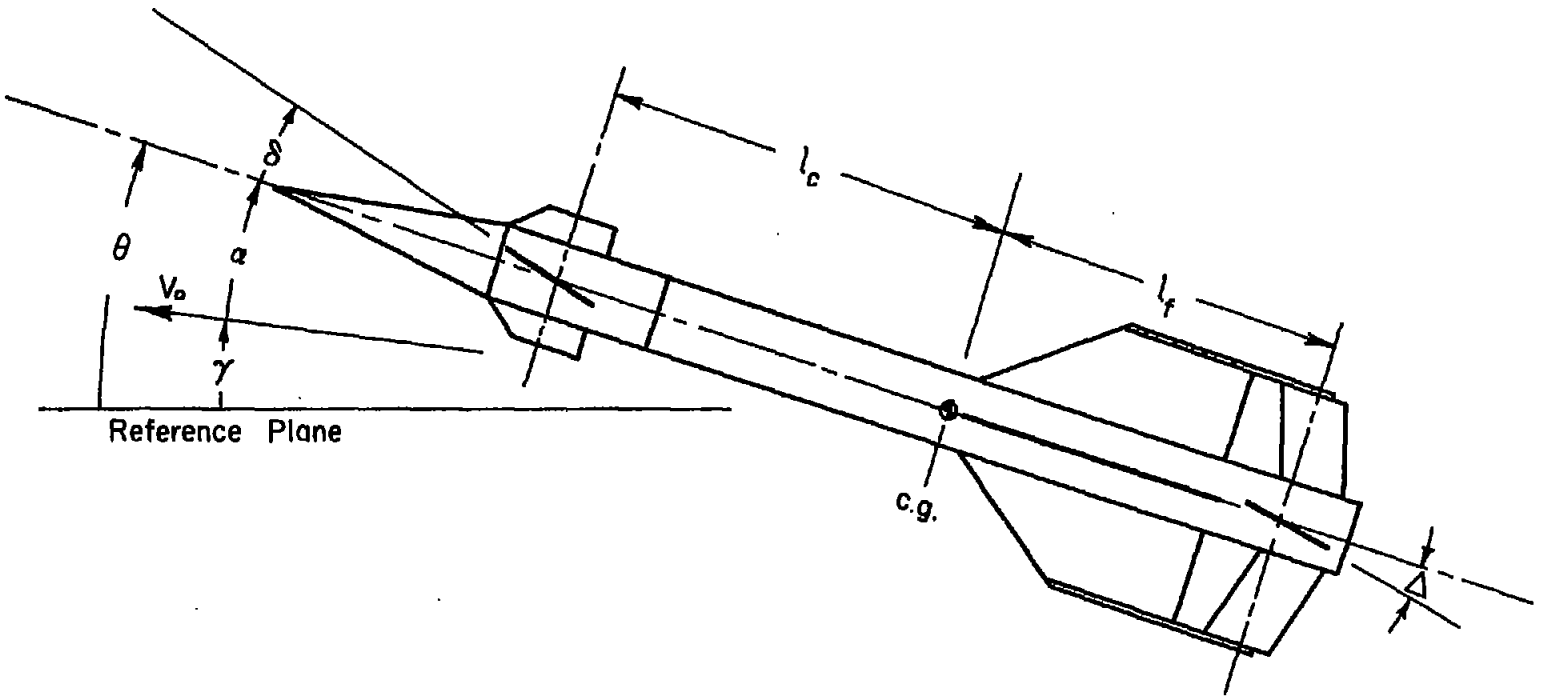

Figure 1.- Dimensional and angular relationships.

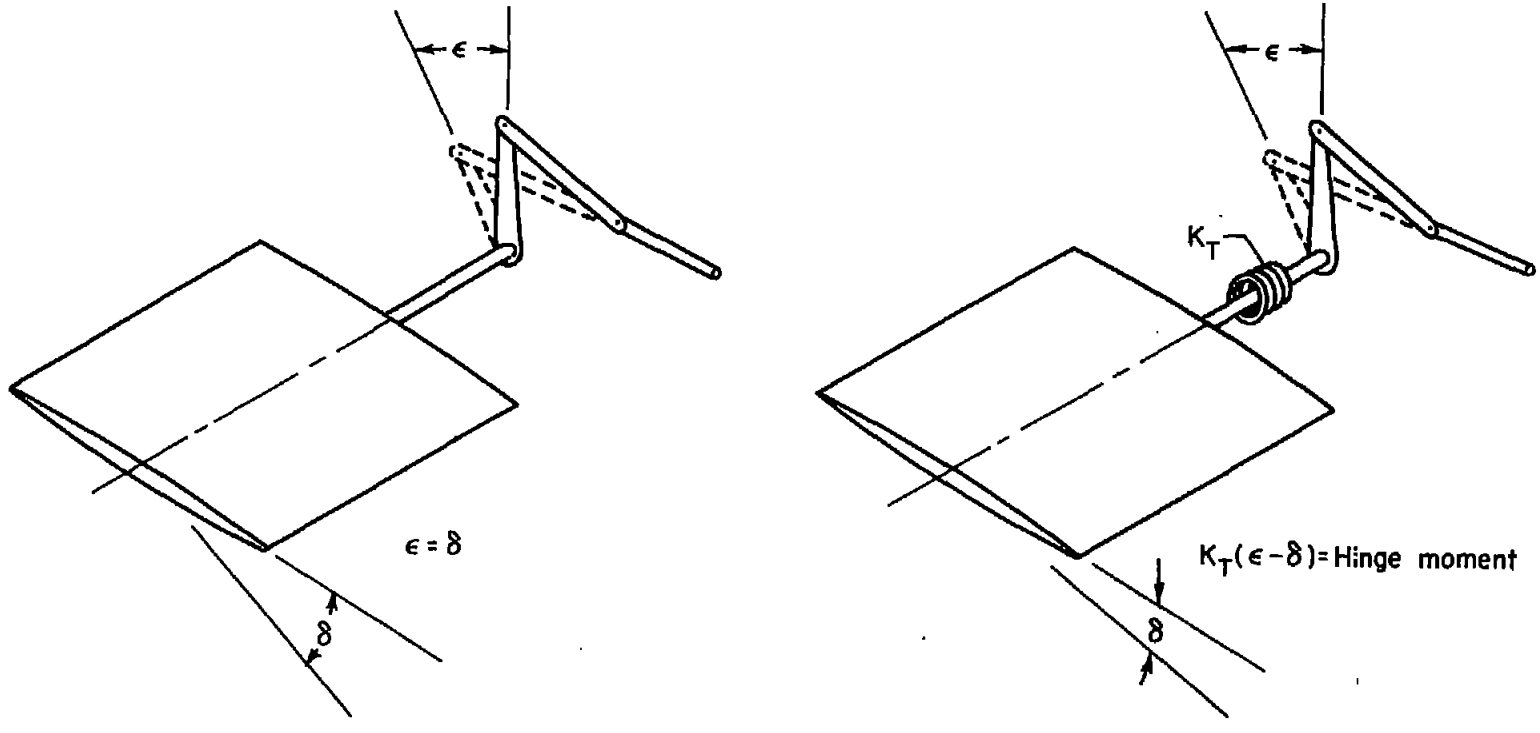

(a) Position control.

(b) Spring-mounted control.

Figure 2.- Schematic drawing of position and spring-mounted controls.

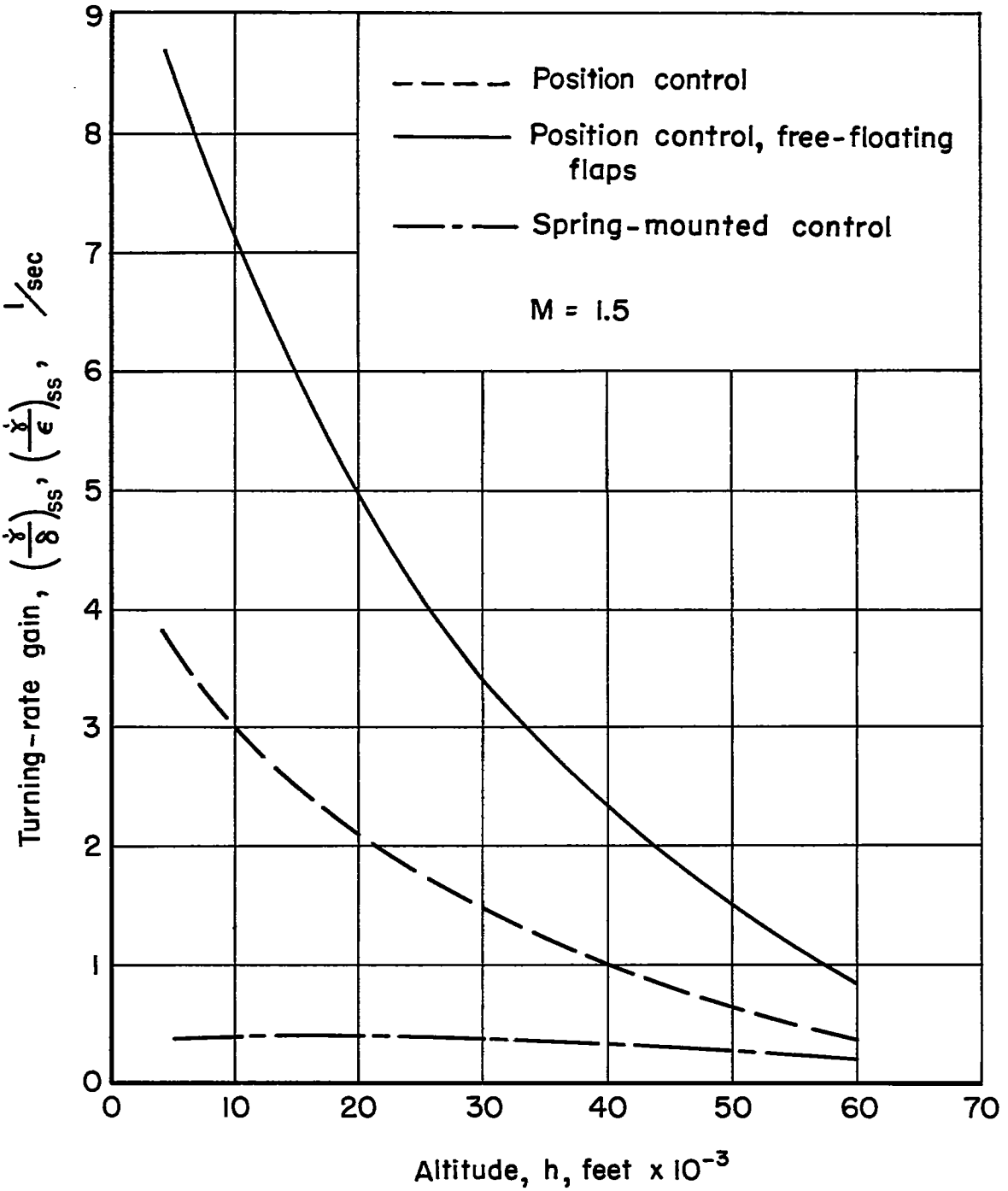

Figure 3.- Variation in the turning-rate gain with altitude.

[redacted]

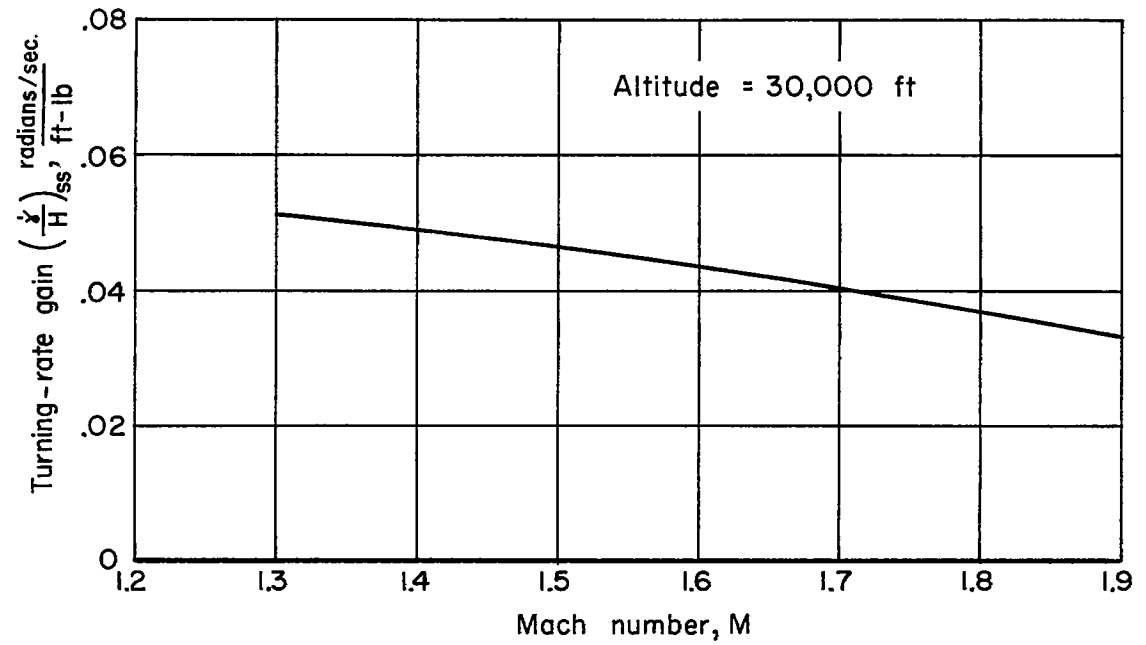

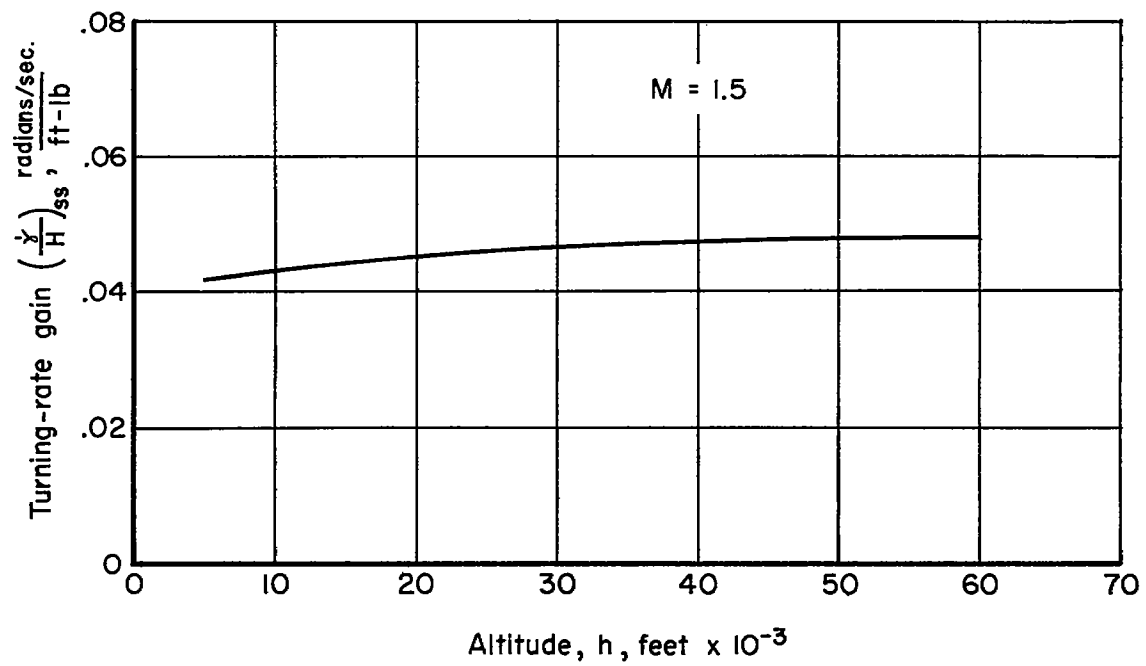

Figure 4.- Variation in the turning-rate gain for a missile equipped with torque-servo actuated control surfaces.

[redacted]

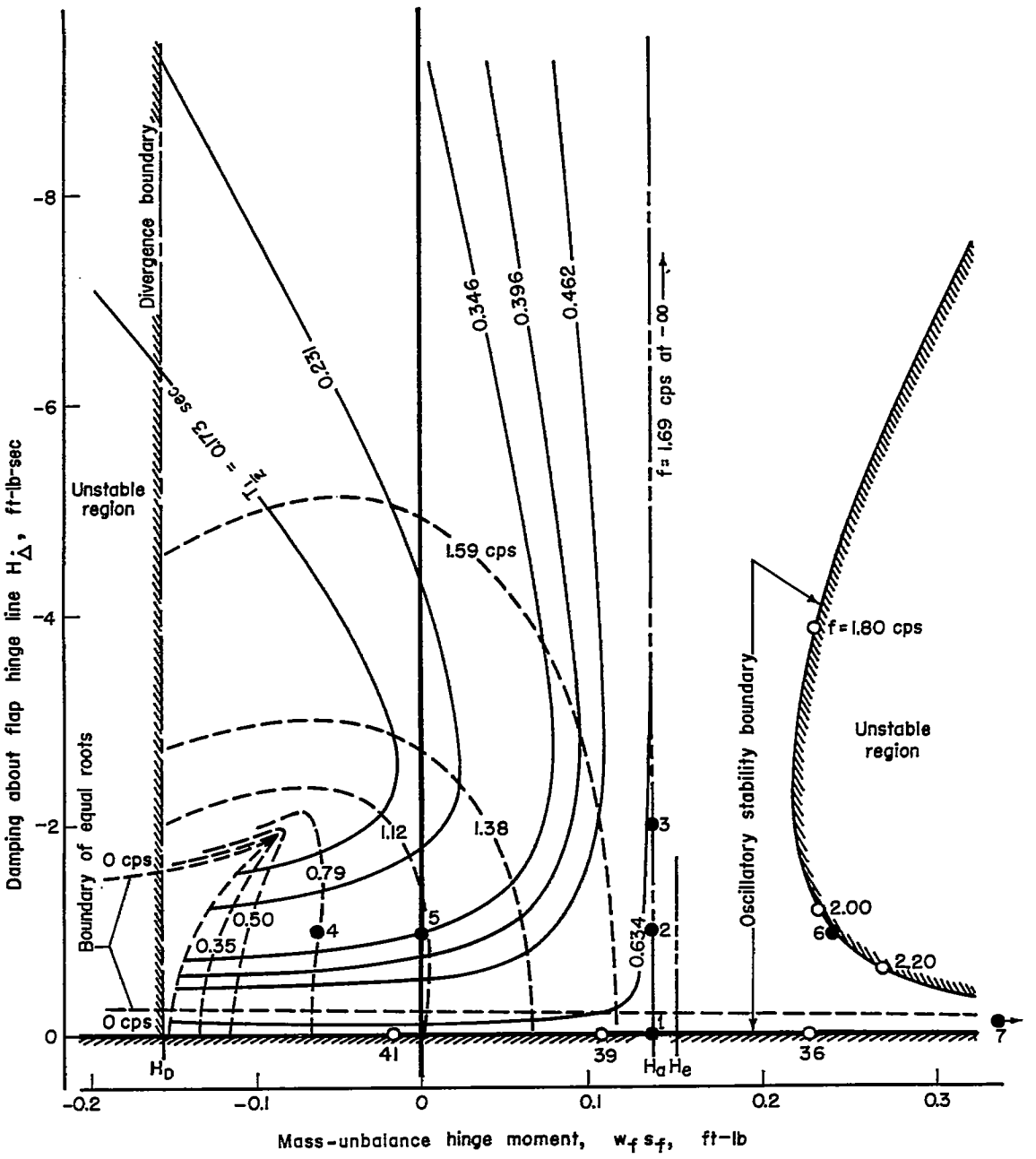

Figure 5.- Stability diagram for missile with spring-mounted controls and free-floating flaps showing values of flap damping and mass unbalance which give constant damping and frequency; M = 1.5, altitude = 30,000 feet.

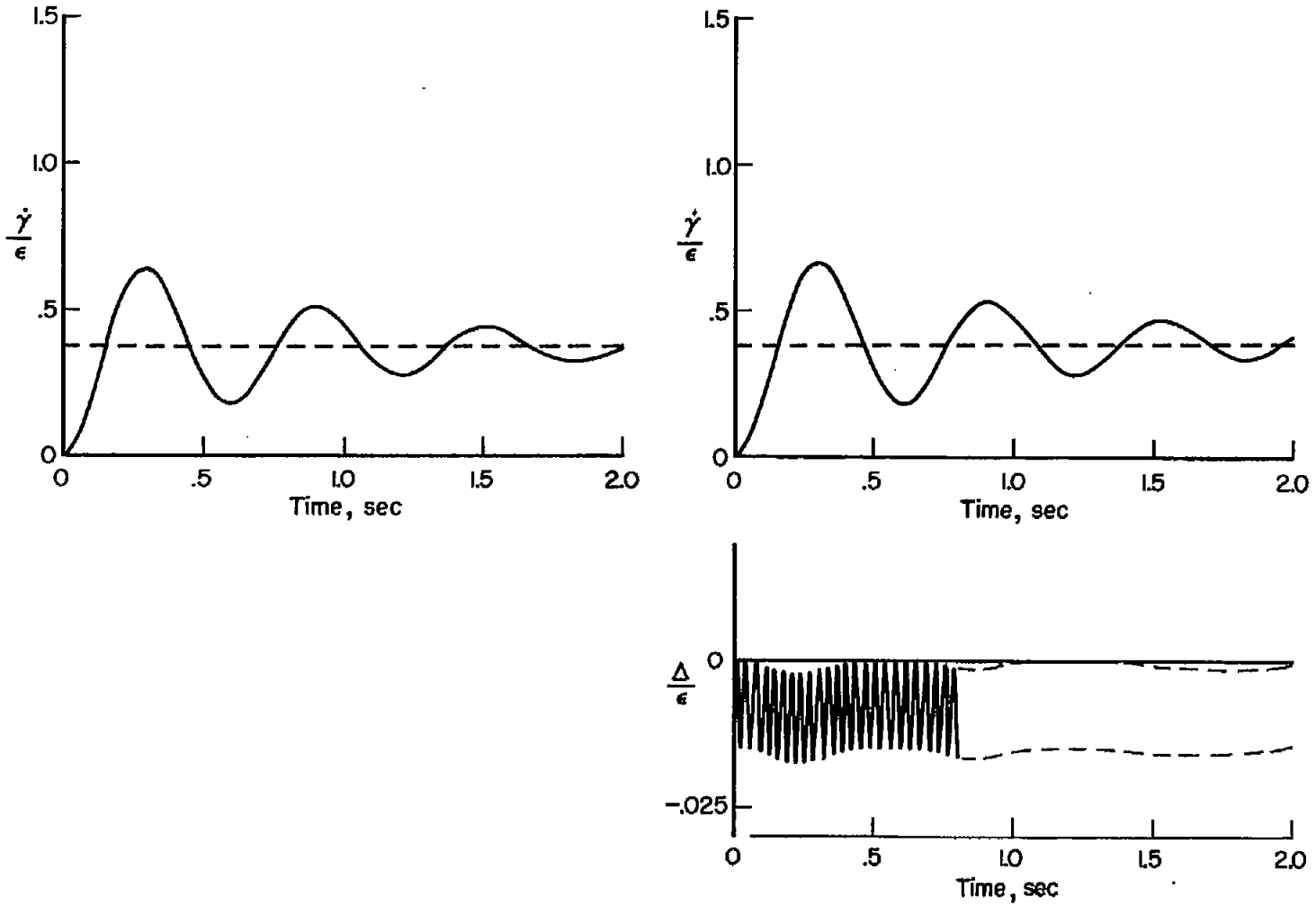

(a) Basic missile.

(b) Point 1.

Figure 6.- Time histories of turning rate and flap deflection for the basic missile and for the conditions of mass-unbalance hinge moment and flap damping shown in figure 5.

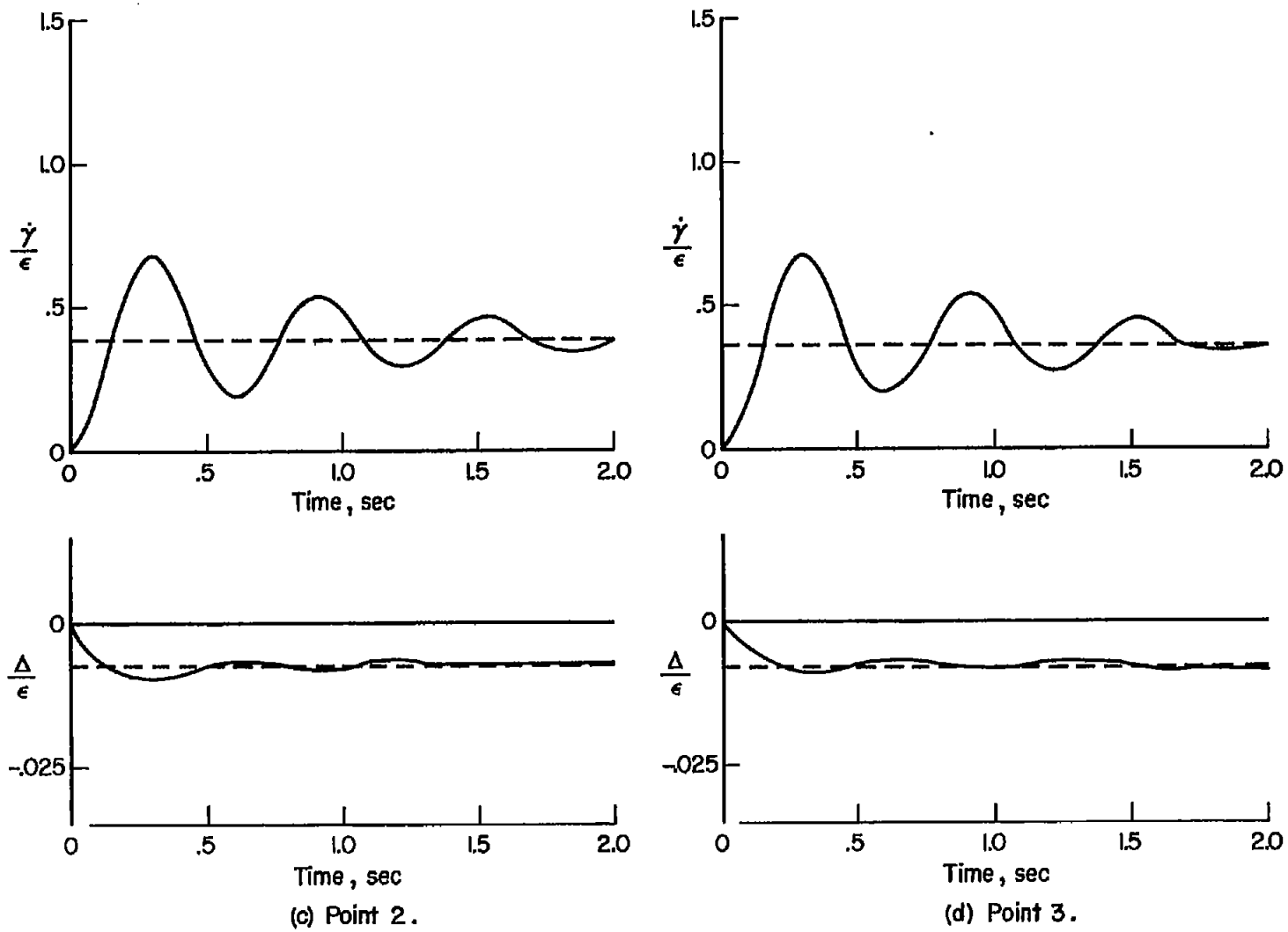

Figure 6.- Continued.

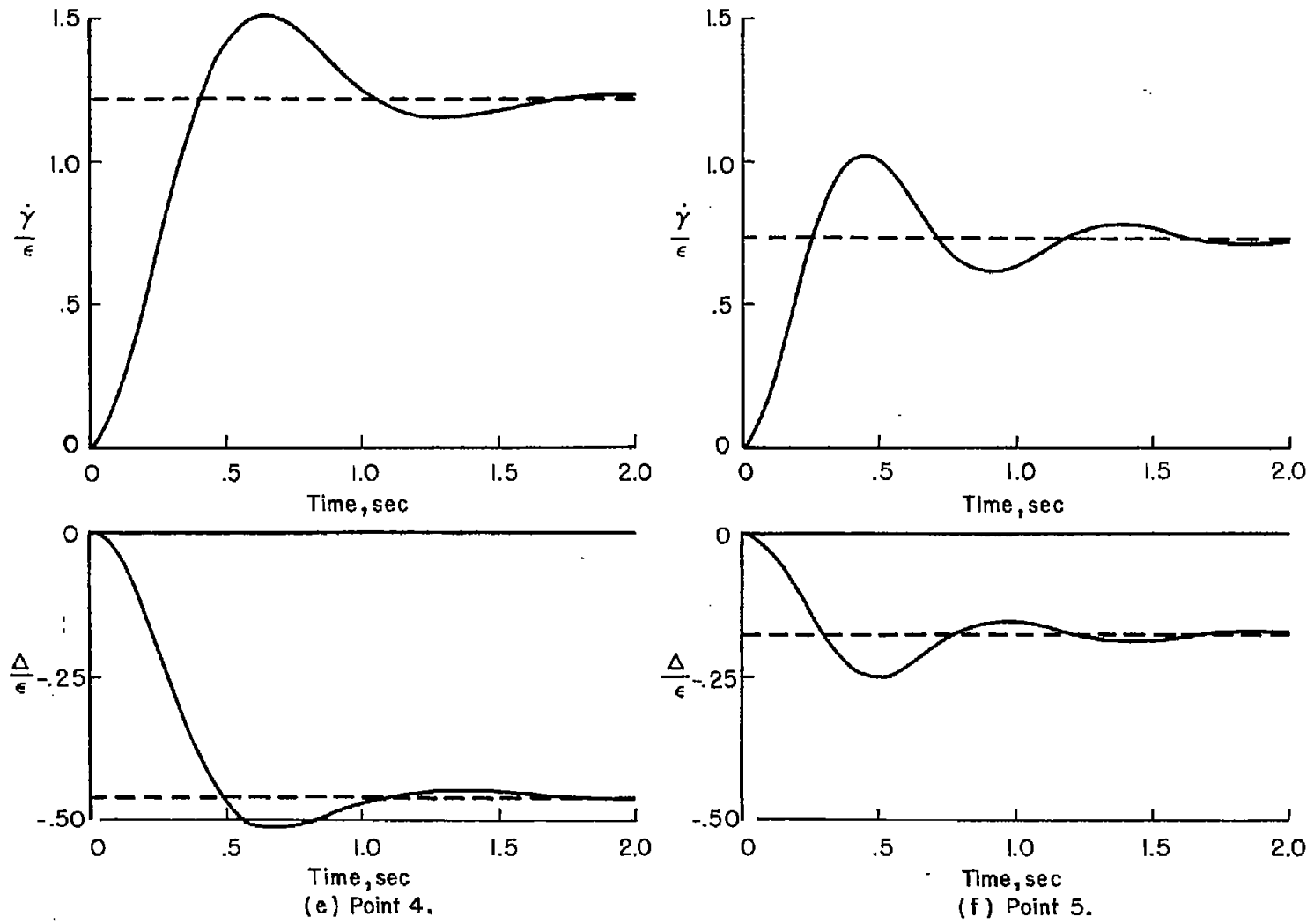

Figure 6.- Continued.

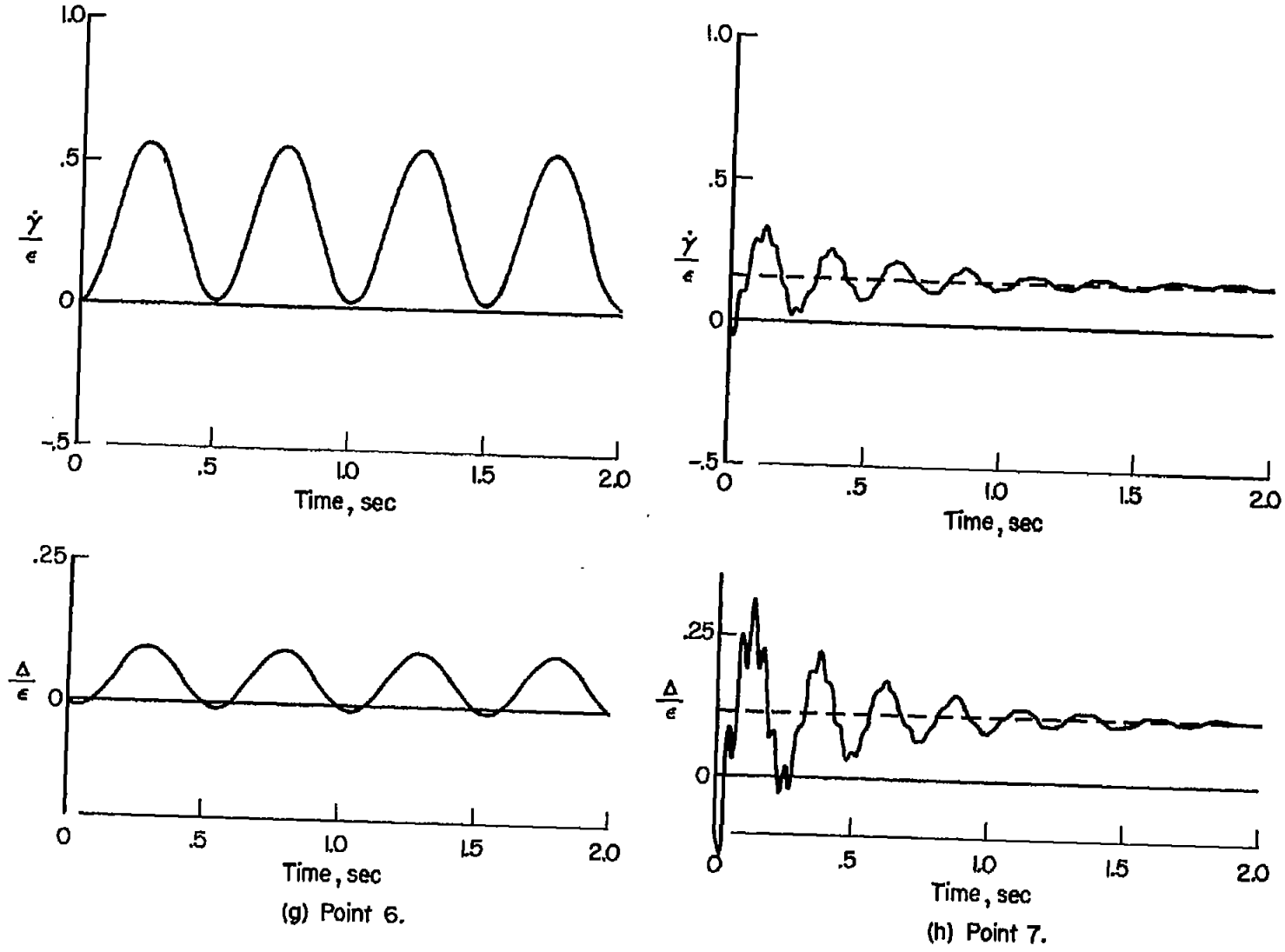

(g) Point 6.

(h) Point 7.

Figure 6.- Concluded.

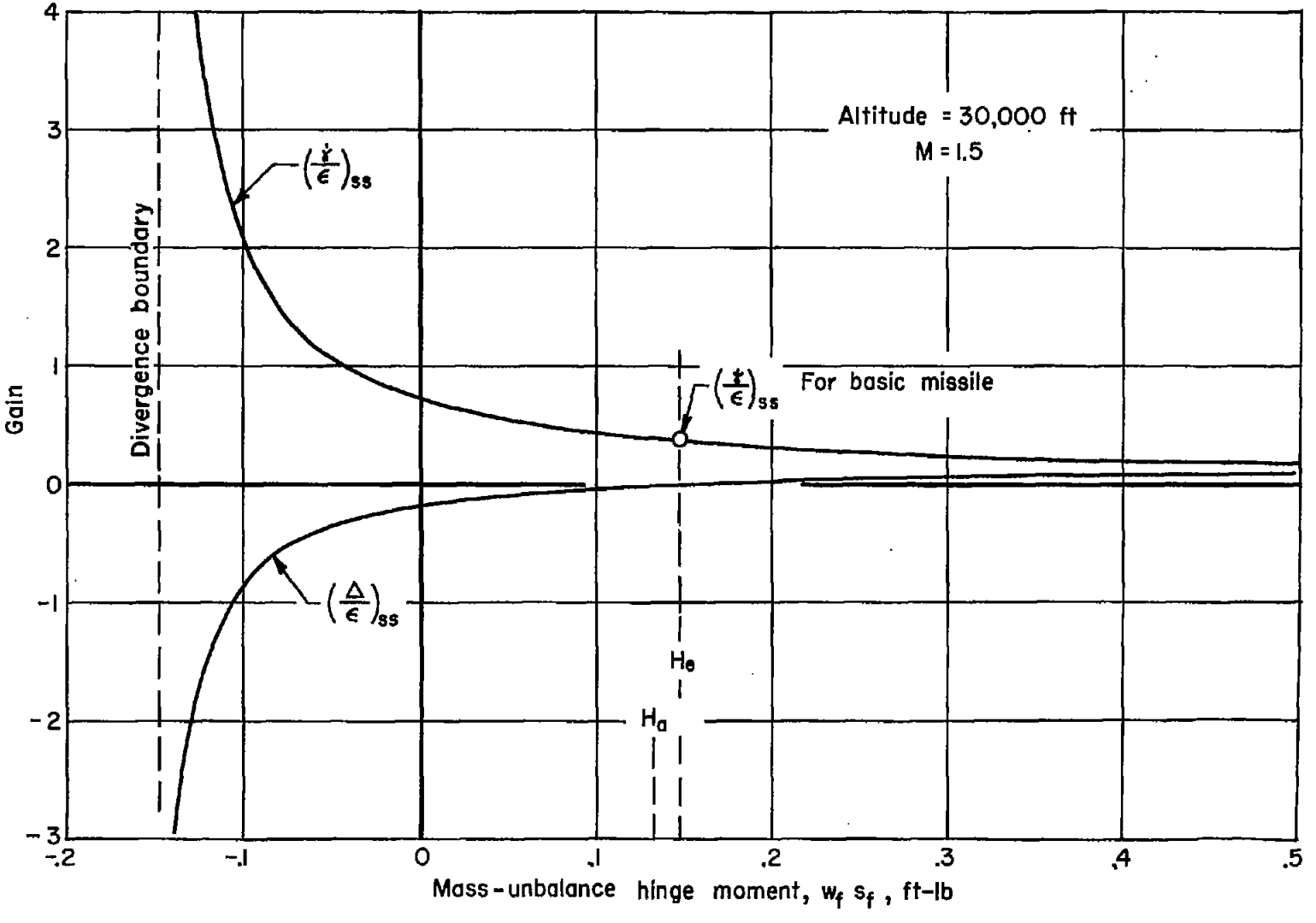

Figure 7.- Turning rate and flap gain as a function of mass-unbalance hinge moment for missile with spring-mounted controls and free-floating flaps.

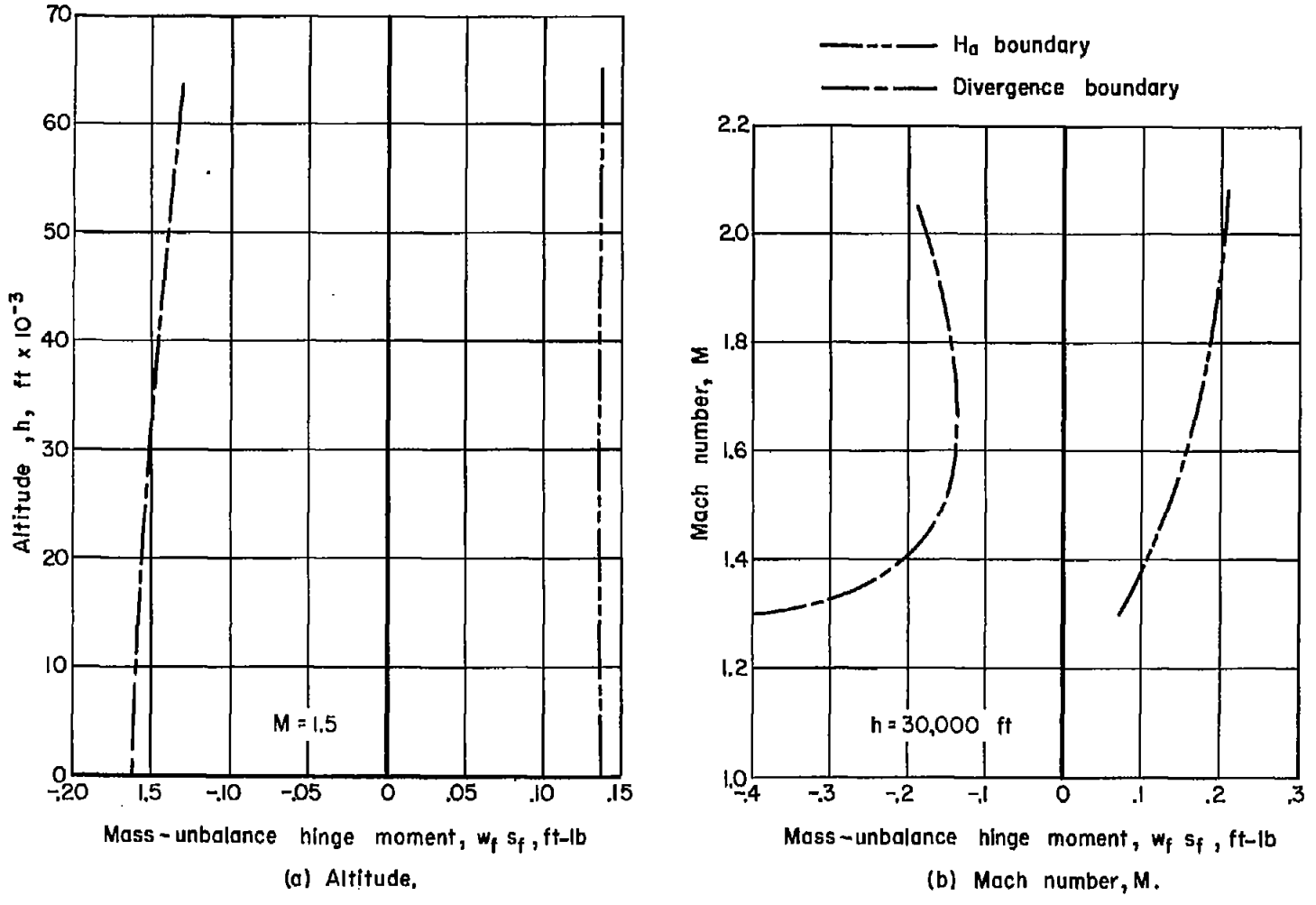

Figure 8.- Effect of various parameters on the divergence and H_a boundaries.

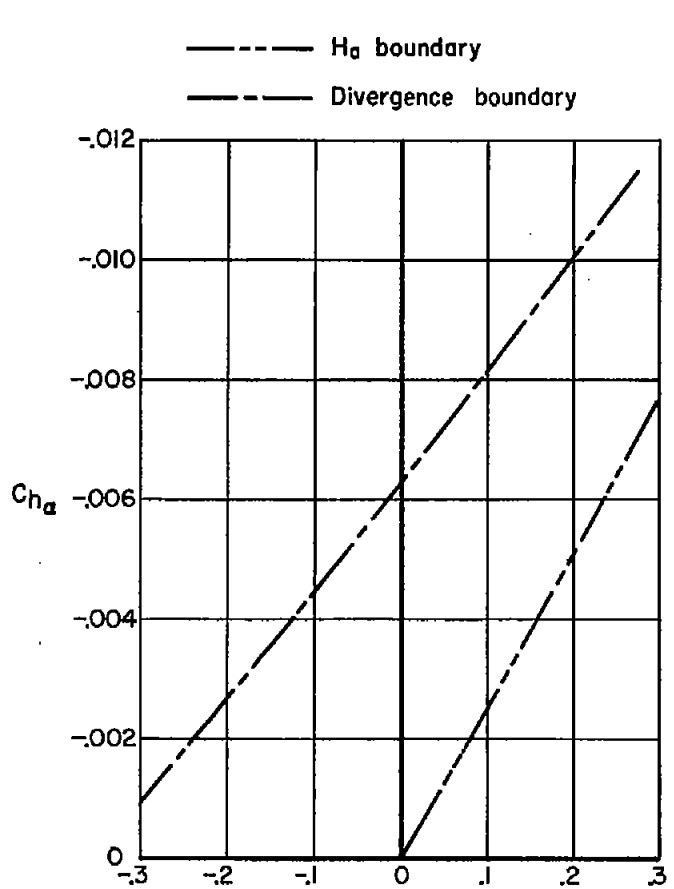

(c) C_{h_α}

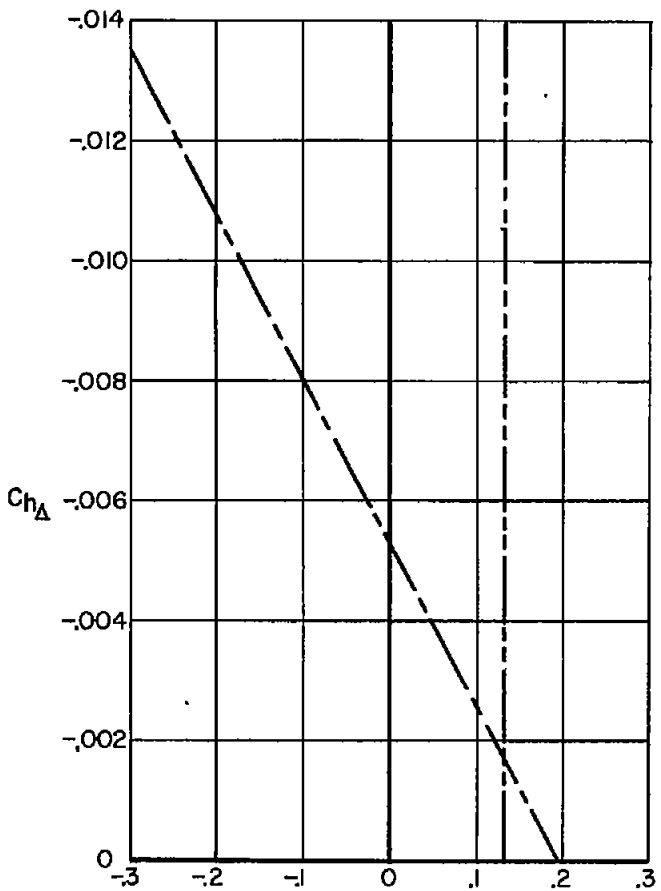

(d) C_{h_Δ}

Figure 8.- Continued.

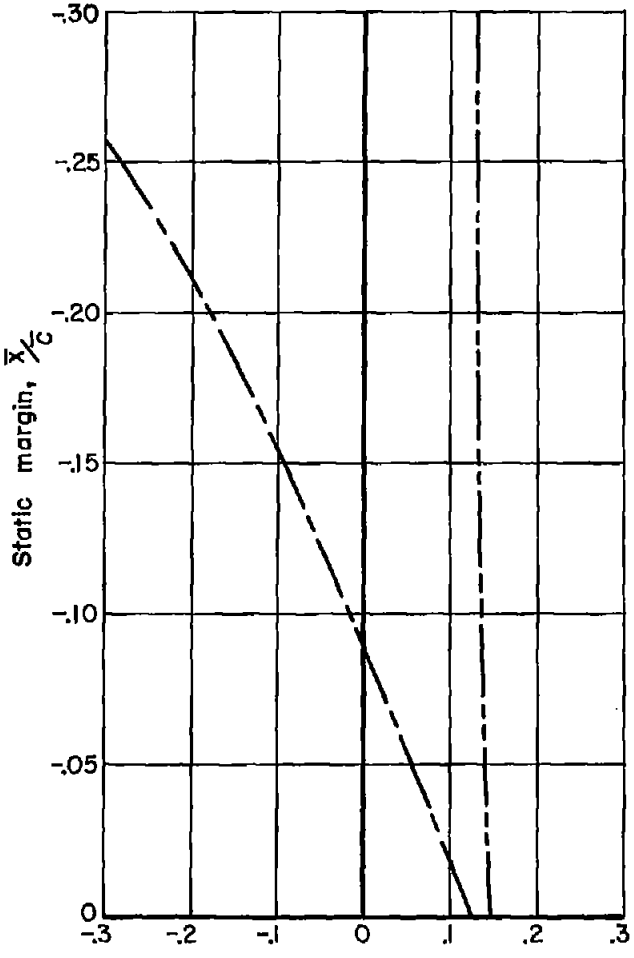

(e) Static margin.

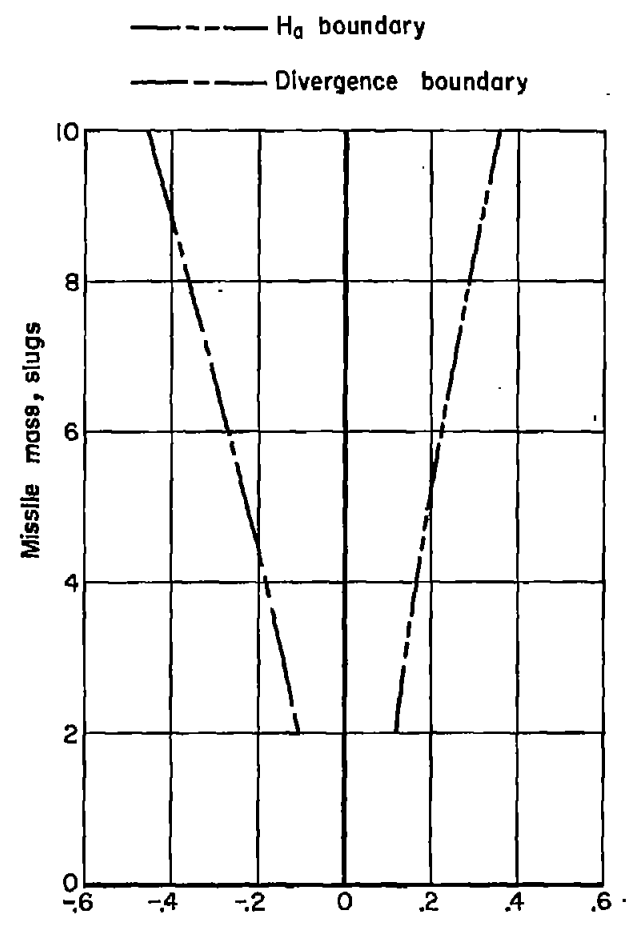

(f) Missile mass.

Figure 8.- Concluded.

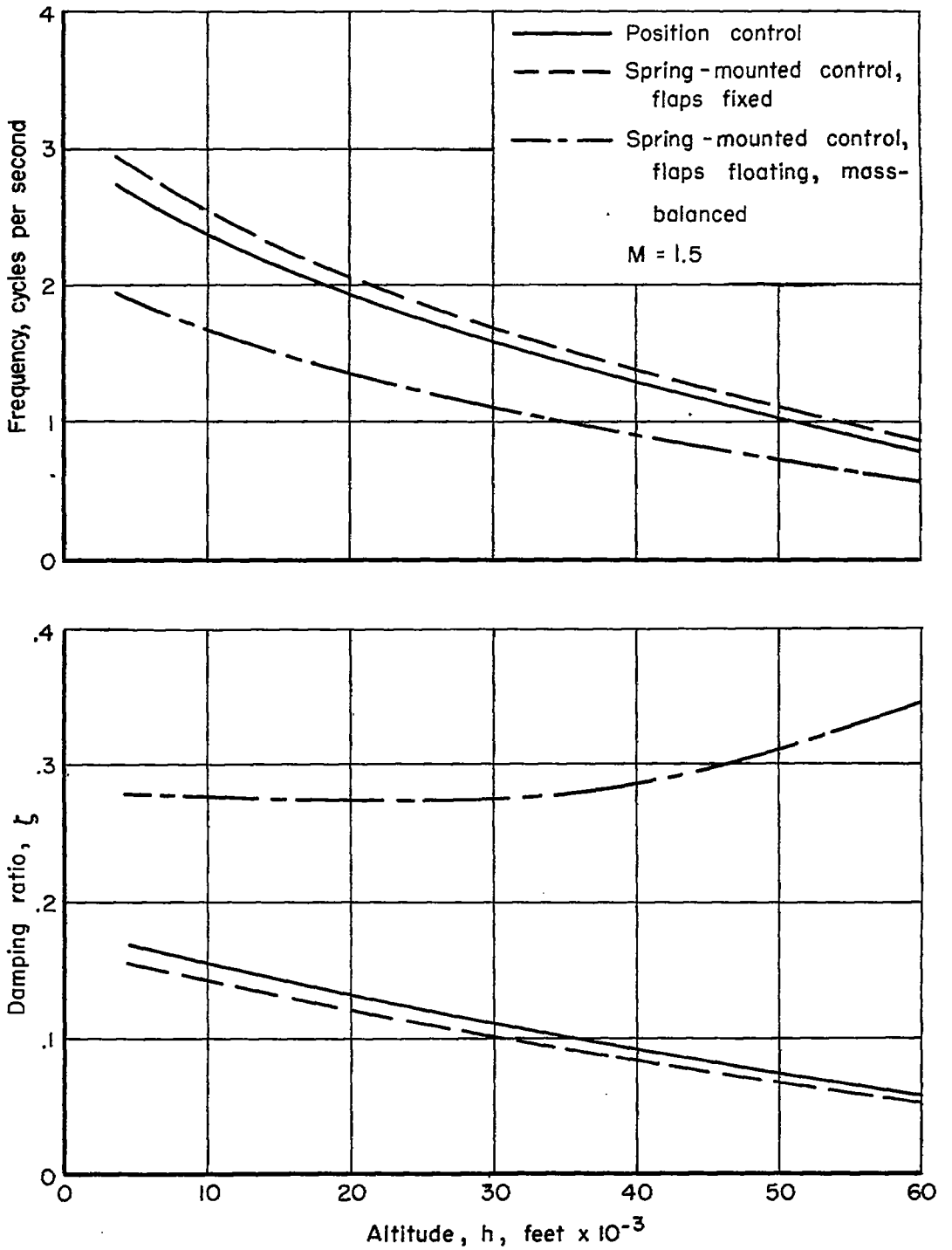

Figure 9.- Variation of frequency and damping ratio with altitude for various control conditions.

[redacted]

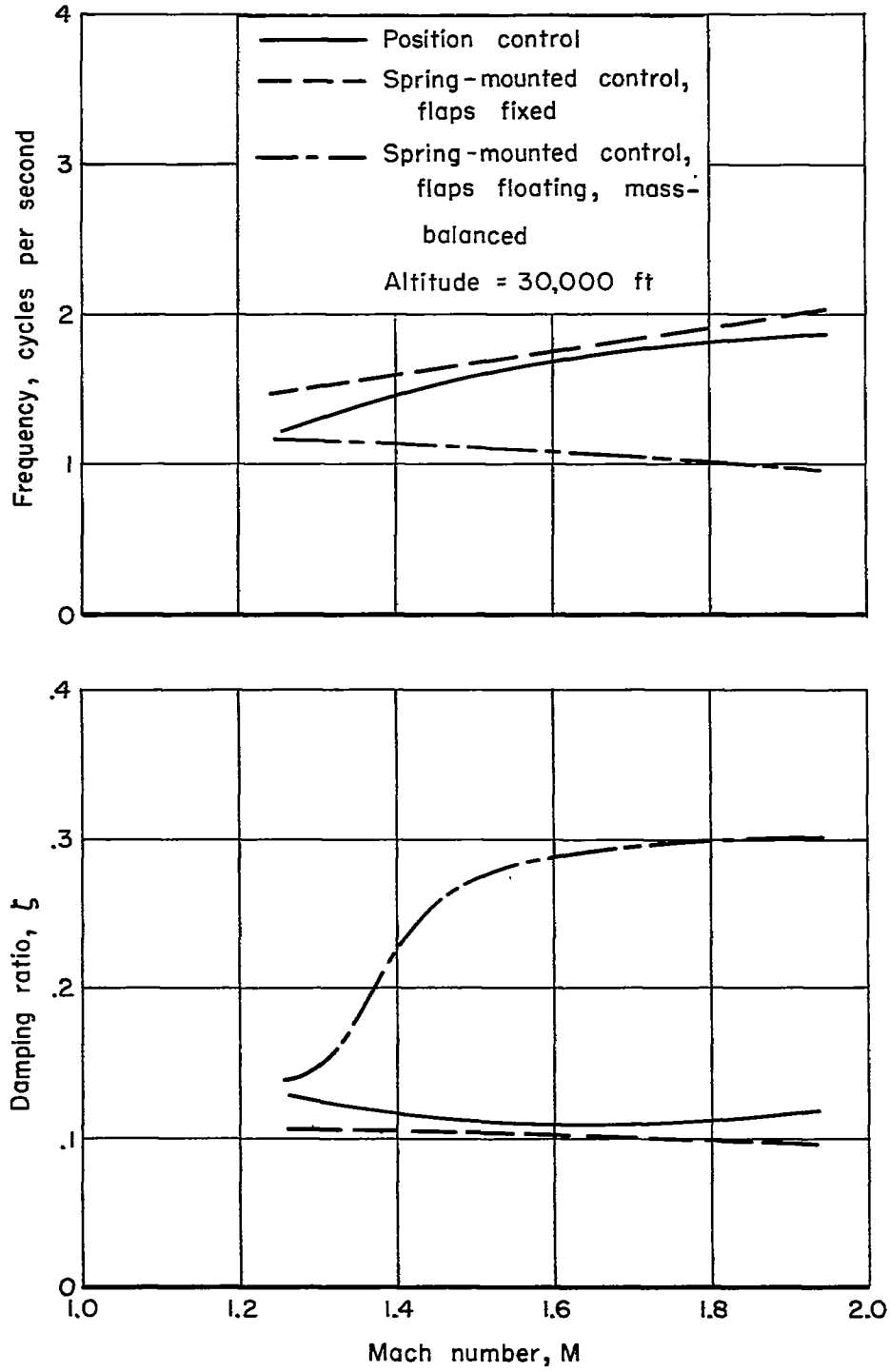

Figure 10.- Variation of frequency and damping ratio with Mach number for various control conditions.

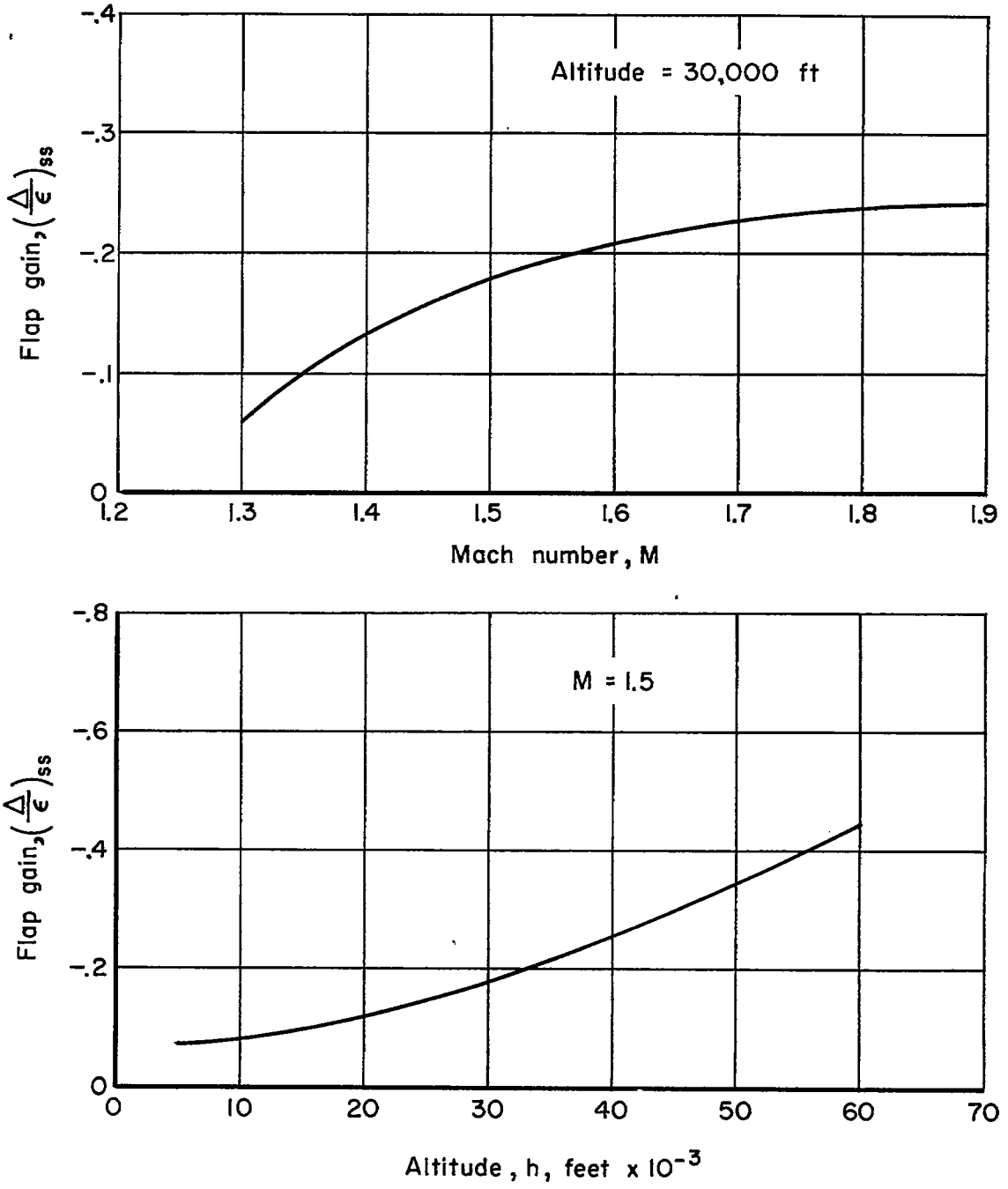

Figure 11.- Variation of flap gain with Mach number and altitude for a missile with spring-mounted controls and mass-balanced, free-floating flaps.

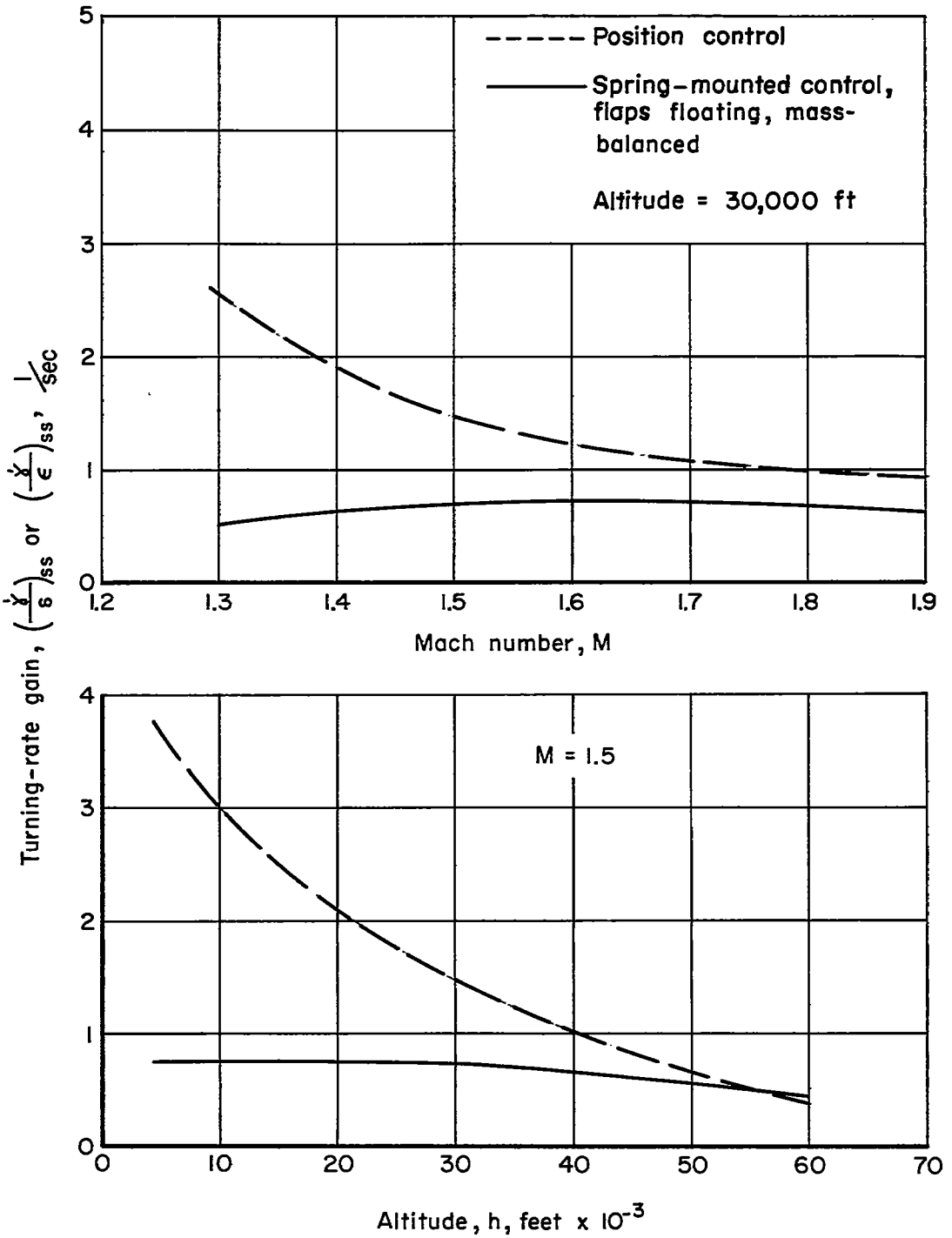

Figure 12.- Improvement of the turning-rate-gain variation through the use of spring-mounted controls and free-floating flaps.

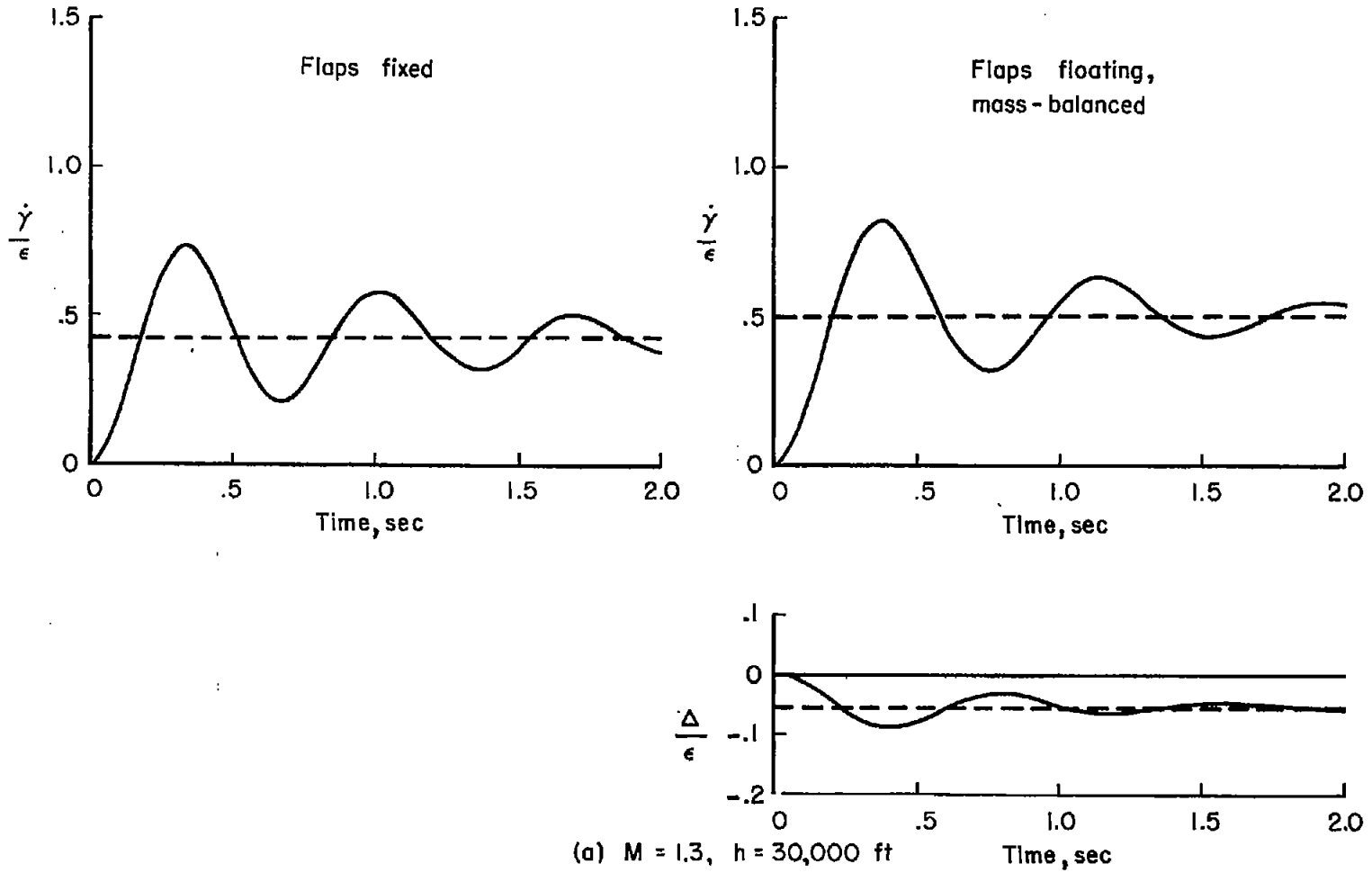

Figure 13.- Comparison of time histories of missile with spring-mounted controls, flaps fixed and floating, for various flight conditions.

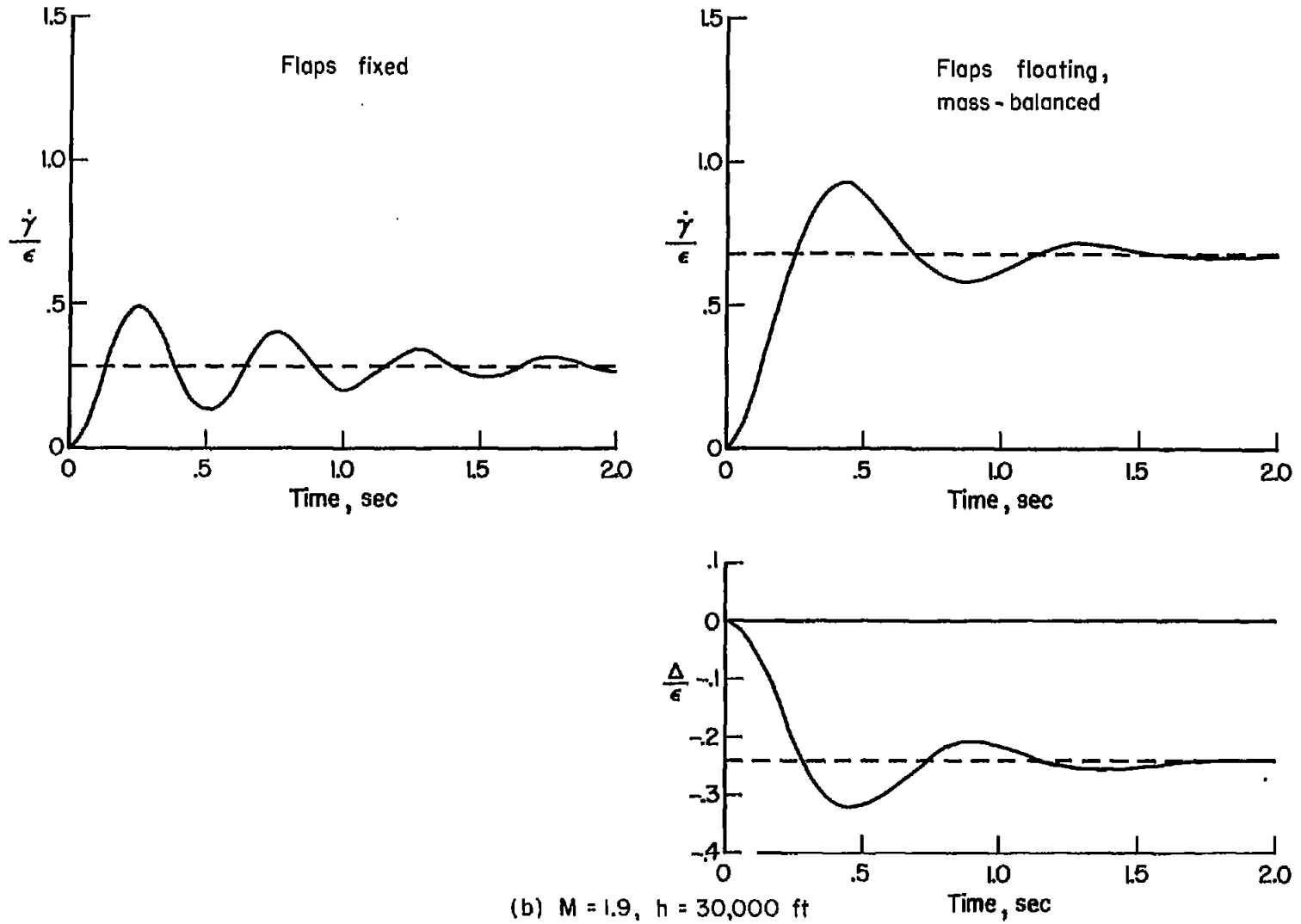

(b) M = 1.9, h = 30,000 ft

Figure 13.- Continued.

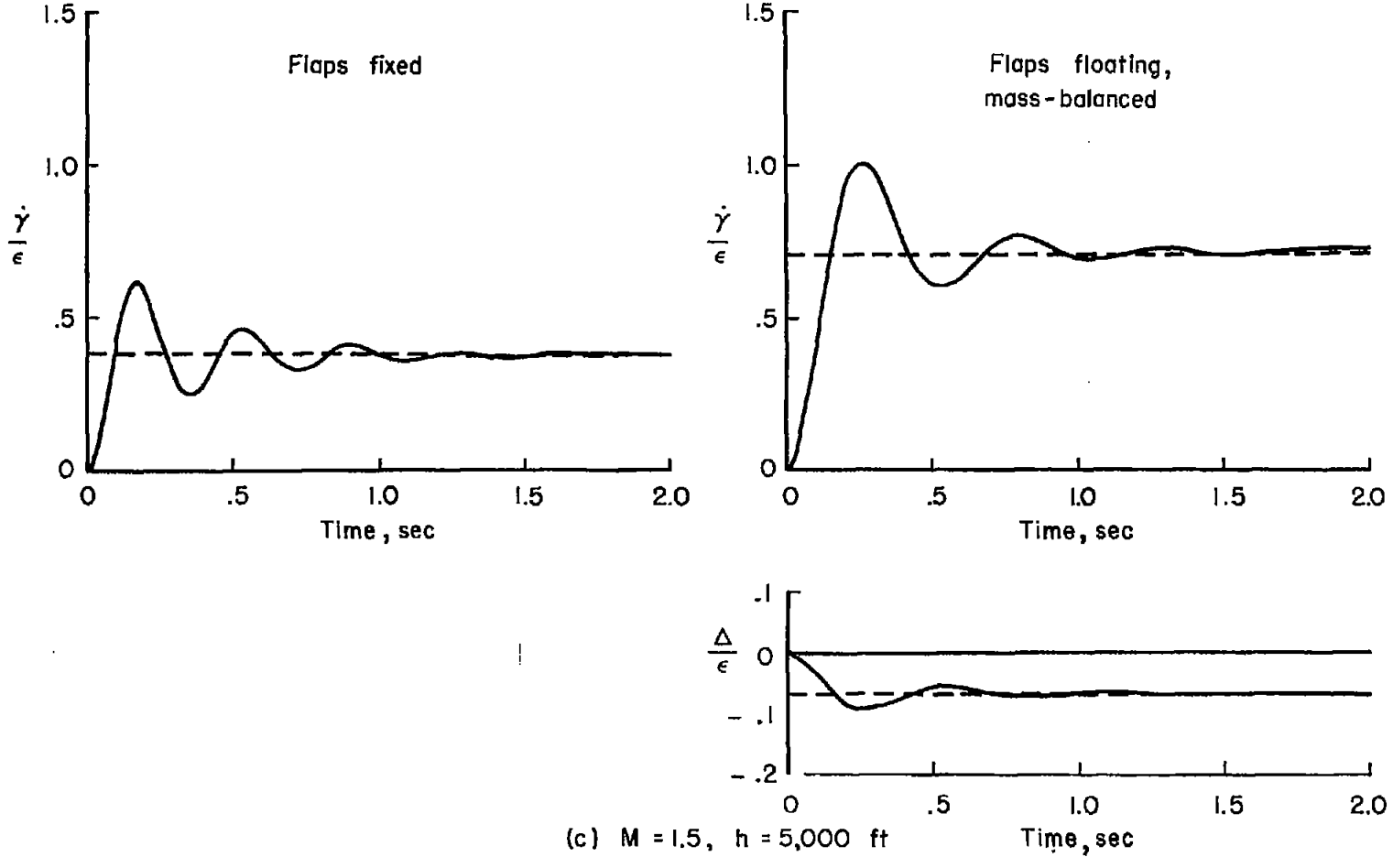

(c) M = 1.5, h = 5,000 ft

Figure 13.- Continued.

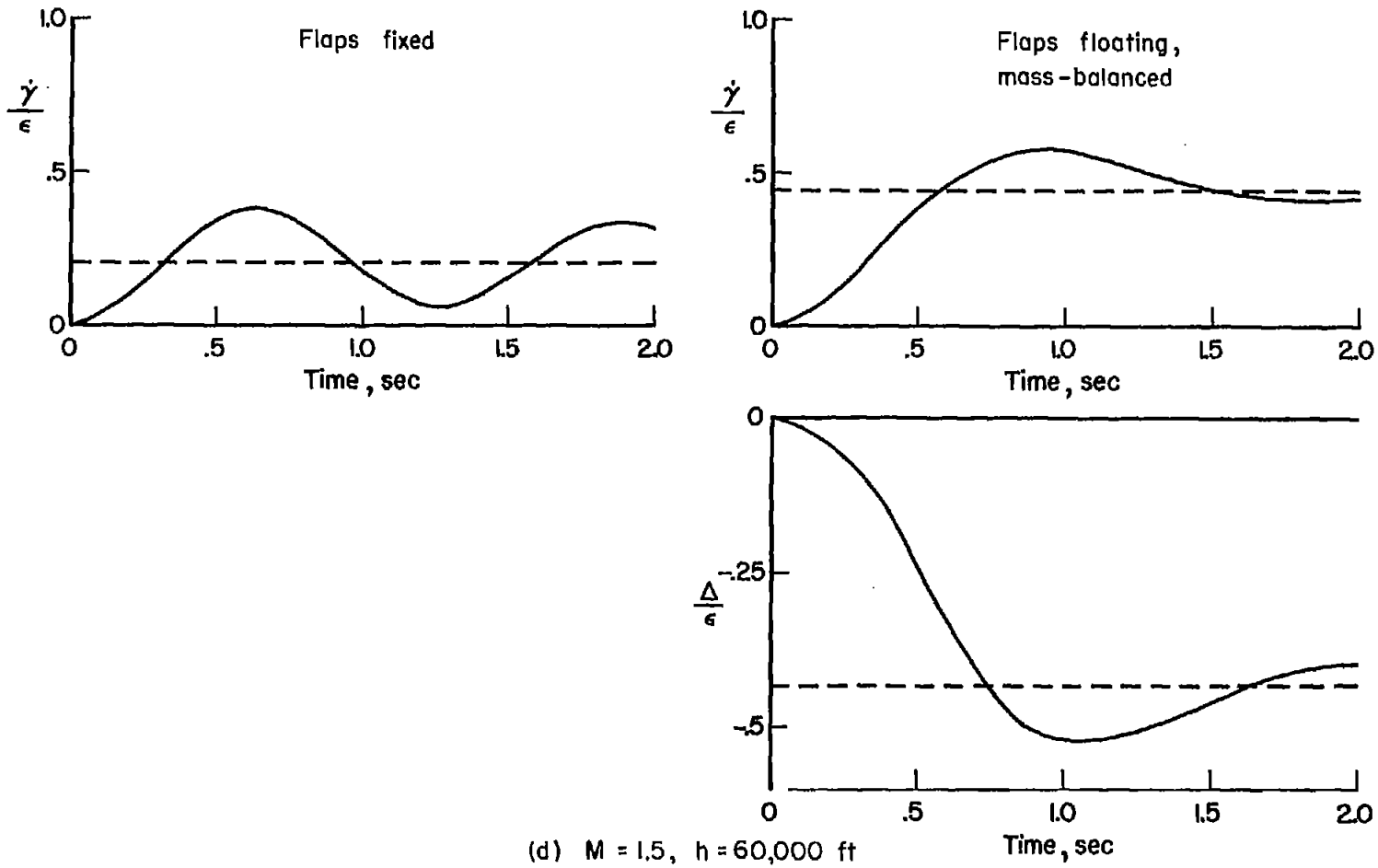

(d) M = 1.5, h = 60,000 ft

Figure 13.- Concluded.

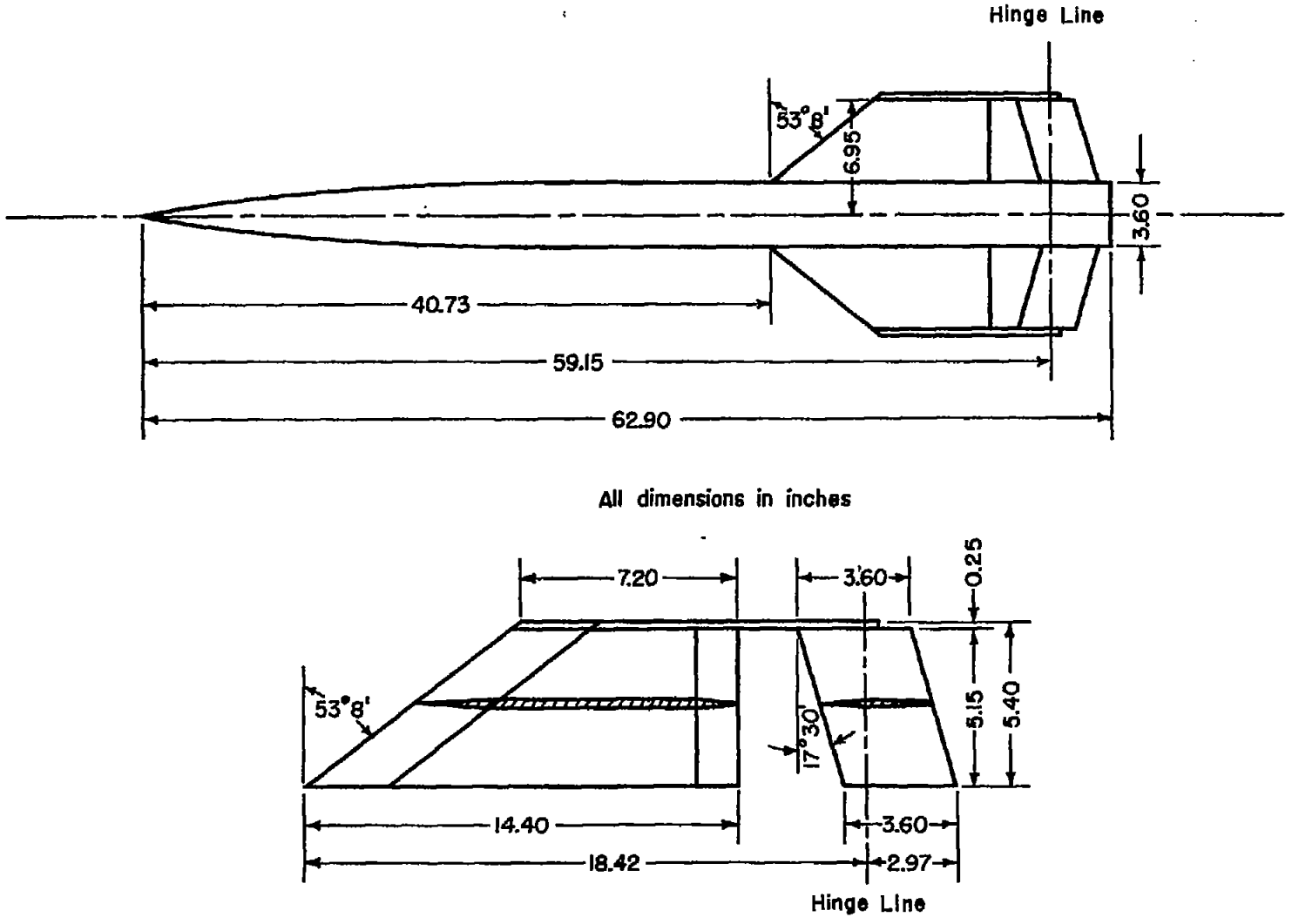

Figure 14.- Geometric characteristics of the model used in the wind-tunnel test.

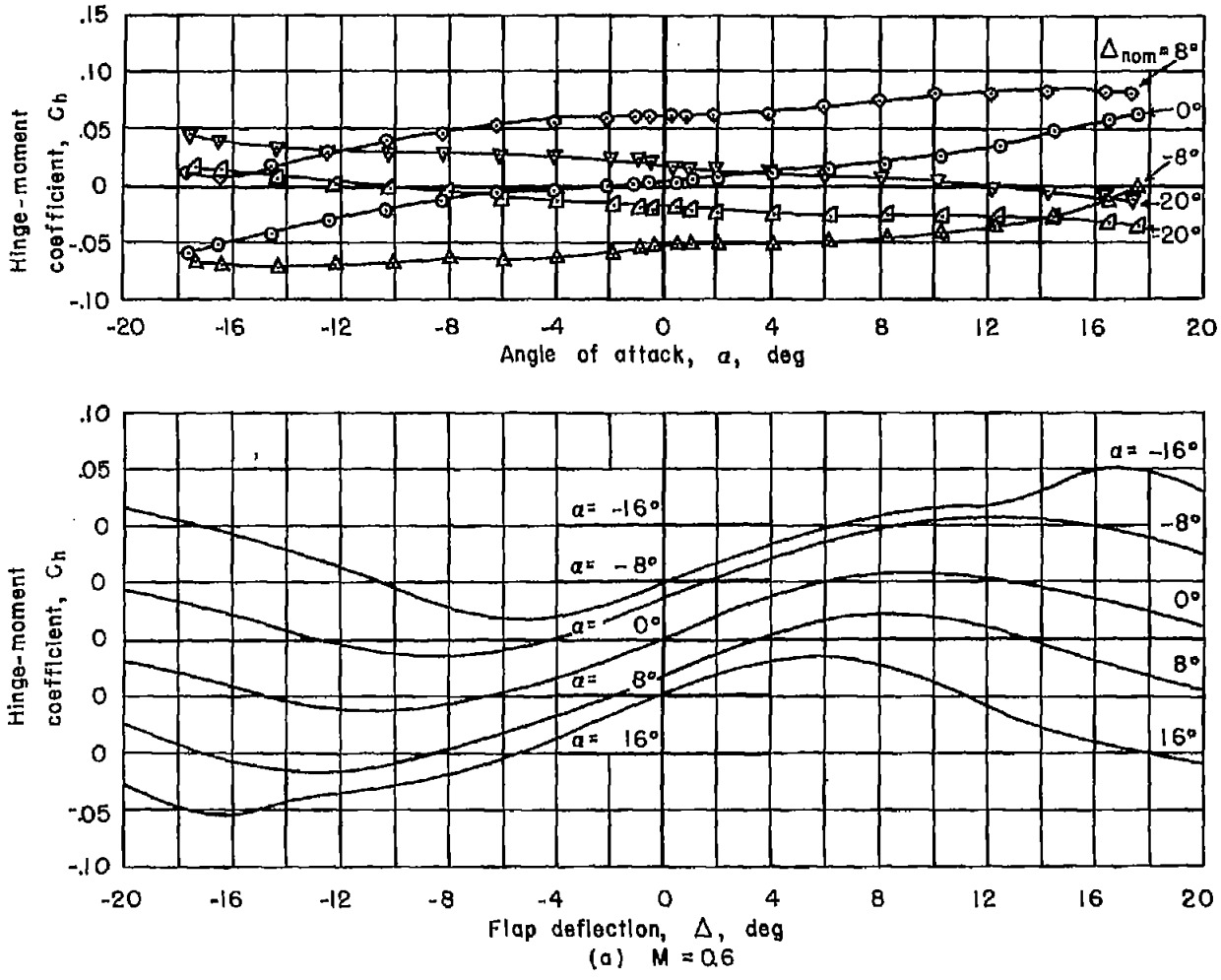

(a) M = 0.6

Figure 15.- Hinge-moment coefficients based on area and chord of flap, $S_f c_f$, for the flap with the half-blunted trailing edge; R = 2.4×10^6.

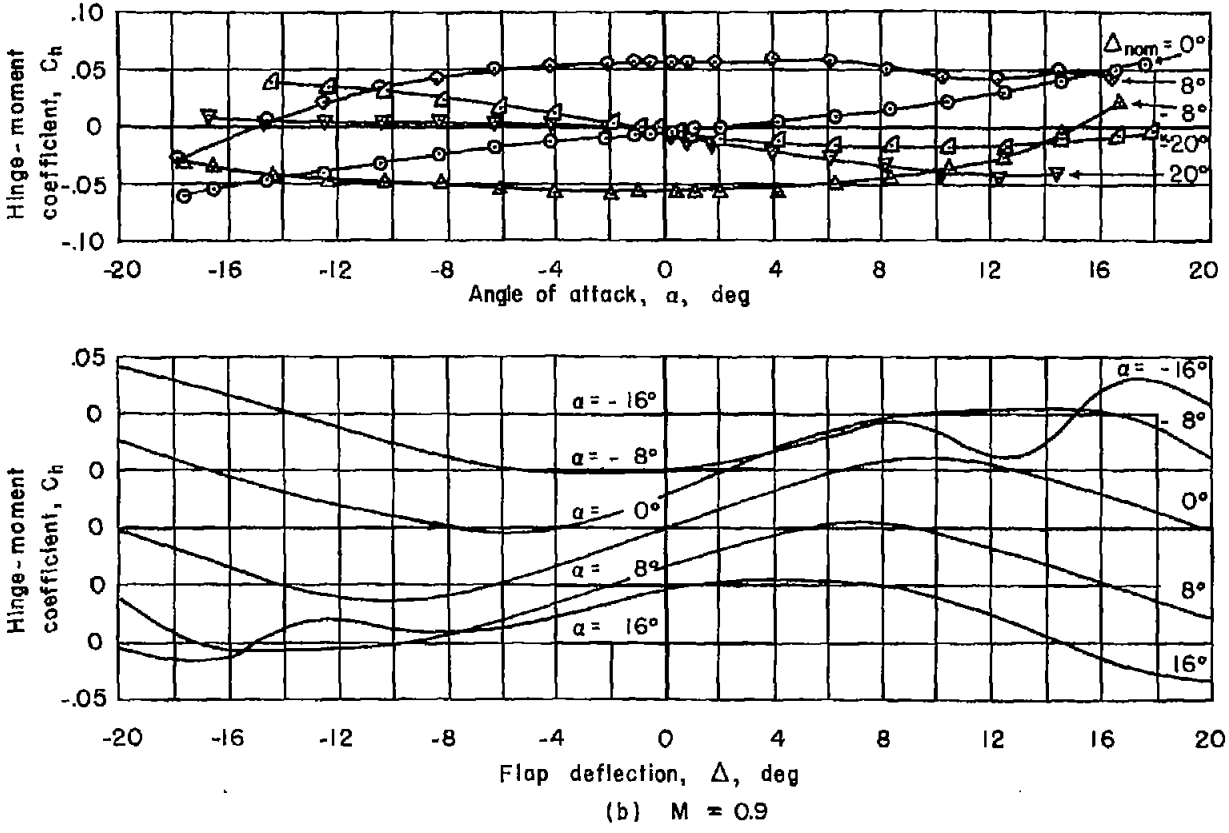

(b) M = 0.9

Figure 15.- Continued.

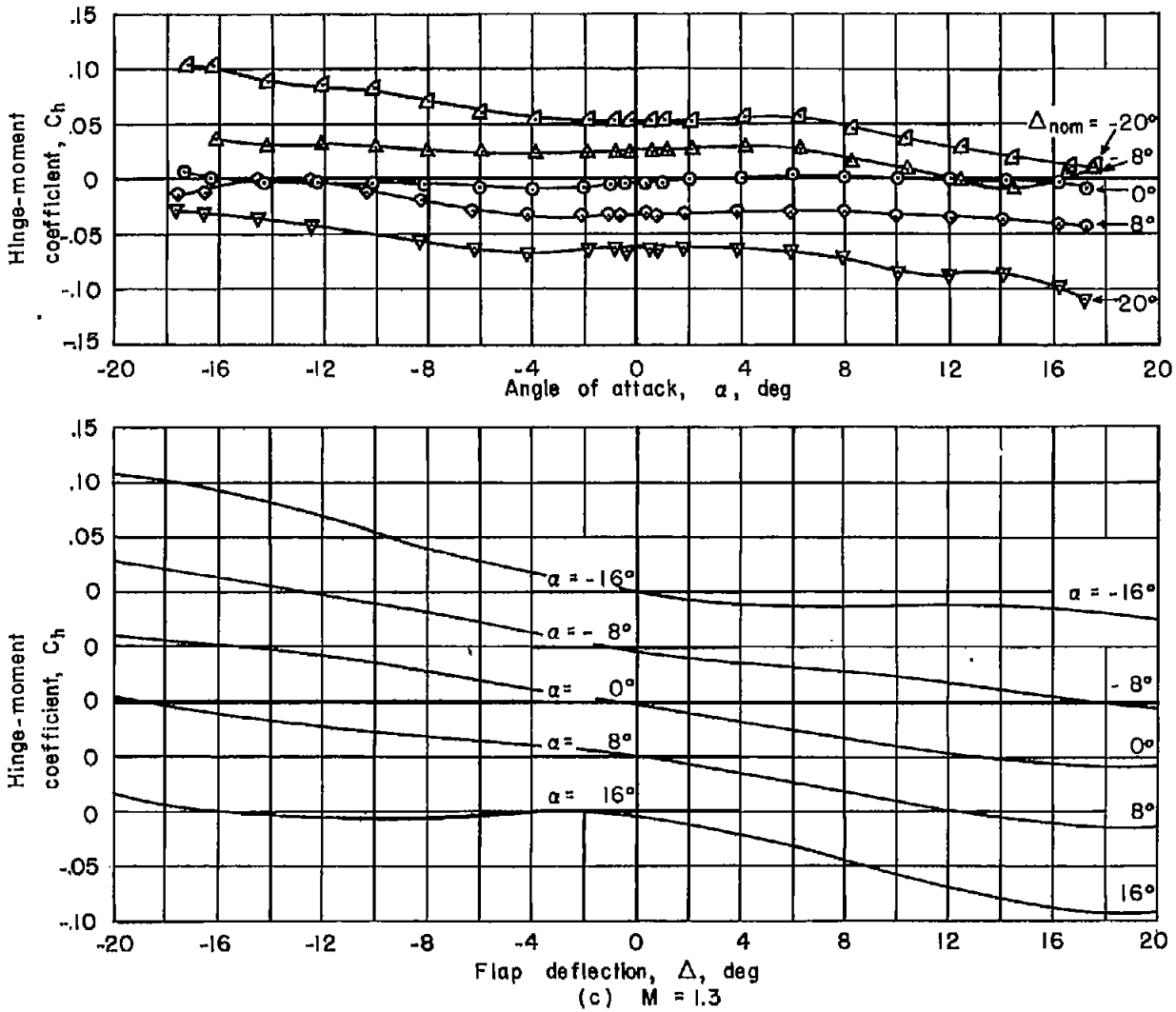

(c) M = 1.3

Figure 15.- Continued.

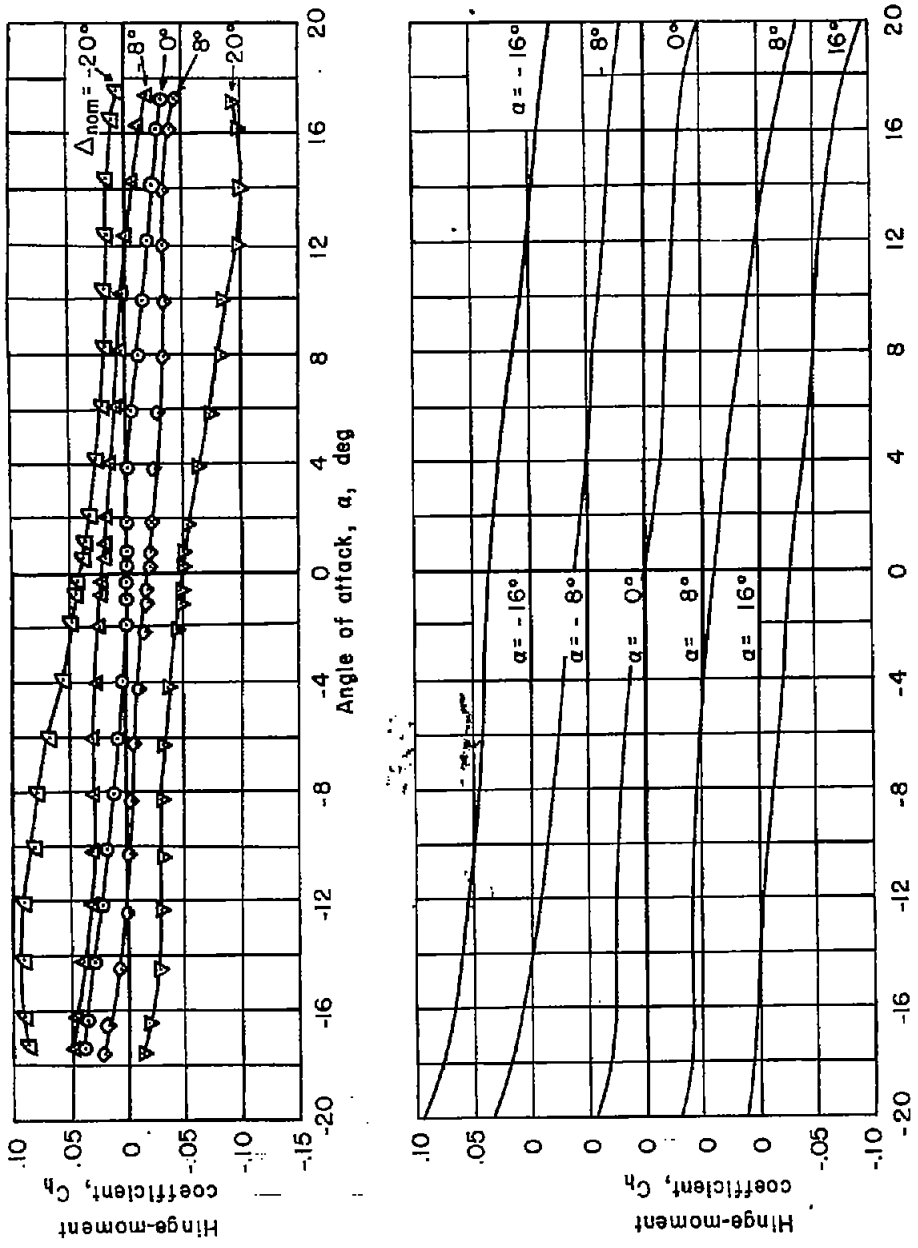

(d) M = 1.9

Figure 15.- Concluded.